Leopard Cats Occupied Human Settlements in China for 3,500 years before the Arrival of Domestic cats in 600-900 CE around the Tang Dynasty

Yu Han[1,2,3]*, Songmei Hu[4,5]*, Ke Liu[1,3], Xiao Xu[1,3], Sean Doherty[6], Alexandra Elizabeth Jamieson[2], Aurelie Manin[2], Sofia Granja Martins[2,7,8], Miaomiao Yang[9], Chong Yu[10], Juan Wang[11], Zhuang Wu[12], Canping Chen[12], Sicheng Han[1,3], Daowei Lu[1,3], Lanhui Peng[1,3], Xianzhu Wu[13], Ziyi Li[14] , Wenquan Fan[15], Quanfa Cai[15], Zongliang Cui[16], Jing Yuan[17], Zihan Li[2], Yang Liu[10], Zhipeng Li[18], Zhendong Liu[18], Qian Ma[2], Jing Shao[9], Zhouyong Sun[9], Fulai Xing[9], Wuzhan Yang[9], Shugang Yang[15], Lianjian Yue[9], Pengcheng Zhang[19], Weilin Wang[20], Huanyuan Zhang[21], Yan Zhuang[1,3], Xin Sun[1,3], Yan Pan[22], Xiaohong Wu[22], Laurent A. F. Frantz[2,23], He Yu[1]†, Joel M. Alves[2,7,8]†, Greger Larson[2]†‡, Shu-Jin Luo[1,3]†‡

*These authors contributed equally to this work.

†Corresponding author. Email: luo.shujin@pku.edu.cn (S.J.L.); greger.larson@arch.ox.ac.uk (G.L.); joel.alves@arch.ox.ac.uk (J.M.A.); yuhe@pku.edu.cn (H.Y.)

‡These authors co-supervised this work.

[1]The State Key Laboratory of Protein and Plant Gene Research, School of Life Sciences; Institute of Ecology, Peking University, Beijing 100871, China

[2]The Palaeogenomics & Bio-Archaeology Research Network, Research Laboratory for Archaeology and History of Art, University of Oxford, Oxford OX1 3QY, UK

[3]Peking-Tsinghua Centre for Life Sciences, Academy for Advanced Interdisciplinary Studies, Peking University, Beijing 100871, China

[4]Joint International Research Laboratory of Environmental and Social Archaeology, Shandong University, Qingdao, Shandong 266237, China

[5]Institute of Cultural Heritage, Shandong University, Qingdao, Shandong 266237, China.

[6]Department of Archaeology, University of Exeter, Exeter EX4 4QE, UK

[7]CIBIO, Centro de Investigação em Biodiversidade e Recursos Genéticos, InBIO Laboratório Associado, Universidade do Porto, Vairão 4485-661, Portugal

[8]BIOPOLIS Program in Genomics, Biodiversity and Land Planning, CIBIO, Vairão 4485-661, Portugal
[9]Shaanxi Academy of Archaeology, Xi'an, Shaanxi 710054, China
[10]School of Sociology and Anthropology, Sun Yat-Sen University, Guangzhou, Guangdong 510275, China
[11]Department for the History of Science and Scientific Archaeology, University of Science and Technology of China, Hefei, Anhui 230026, China
[12]School of History and Culture, Hebei Normal University, Shijiazhuang, Hebei 050024, China
[13]College of History and Social Science, Chongqing Normal University, Chongqing 401331, China
[14]Department of Archaeology, Durham University, Durham DH1 3LE, UK
[15]Henan Provincial Institute of Cultural Heritage and Archaeology, Zhengzhou, Henan 450099, China
[16]Anyang Institute of Cultural Heritage and Archaeology, Anyang, Henan 455000, China
[17]Institute of Archaeological Science, Fudan University, Shanghai 200433, China
[18]Institute of Archaeology, Chinese Academy of Social Sciences, Beijing 100101, China
[19]Yulin Archaeological Exploration Team of Shaanxi Province, Yulin, Shaanxi 719000, China
[20]School of History and Culture, Shanxi University, Taiyuan, Shanxi 030006, China
[21]Environmental Change Institute, School of Geography and the Environment, University of Oxford, OX1 3QY, Oxford, UK
[22]School of Archaeology and Museology, Peking University, Beijing 100871, China
[23]School of Biological and Chemical Sciences, Queen Mary University of London, London E1 4NS, UK

Abstract

The earliest cats in human settlements in China were not domestic cats (*Felis catus*), but native leopard cats (*Prionailurus bengalensis*). To trace when and how domestic cats arrived in East Asia, we analyzed 22 feline bones from 14 sites across China spanning 5,000 years. Nuclear and mitochondrial genomes revealed that leopard cats began occupying anthropogenic scenes around 5,400 years ago and last appeared in 150 CE. Following several centuries' gap of archeological feline remains, the first known domestic cat (706–883 CE) in China was identified in Shaanxi during the Tang Dynasty. Genomic analysis suggested a white or partially white coat and a link to a contemporaneous domestic cat from Kazakhstan, indicating a likely dispersal route via the Silk Road. The two felids once independently occupied ancient anthropogenic environments in China but followed divergent paths and reached different destinations in human-animal interactions.

Keywords: Ancient DNA, ancient China, leopard cats, domestic cats, human settlements

Main Text

The African wildcat (*Felis lybica*) is the ancestor of all modern domestic cats (*F. catus*) (*1–3*). Though the timing and circumstances of cat domestication are uncertain, zooarchaeological evidence demonstrates that the northward dispersal of domestic cats into Europe took place by 3,000 BP (*4*,*5*). Domestic cats were also transported eastwards across Eurasia into the Far East and China, but the route and timing of this dispersal remain unresolved.

A previous study of 5,400-year-old felid remains from the site of Quanhucun in western China concluded that cats had been predating rodents within human settlements, thus implying that domestic cats were present in China by the late Neolithic (*6*). Subsequent morphological (*7*) and ancient mtDNA (*8*) analyses of the same specimens revealed that the remains did not belong to the domestic cat but were instead leopard cats (*Prionailurus bengalensis*), a small wild felid native to continental South, Southeast, and East Asia (*9, 10*). These results thus require a reconsideration of when domestic cats arrived in China,

how long leopard cats persisted in archaeological contexts, and whether the two felids coexisted.

To address these questions, we retrieved whole genome sequences from 22 ancient small felid bones from 14 Chinese archaeological sites dated from c.3,500 BCE to 1,800 CE (Fig. 1A and table S1 and table S2). This sample set represents the vast majority of feline excavations from China thus far. We directly radiocarbon dated six individuals and generated seven nuclear (2.4× - 6.0×) and 22 mitochondrial genomes (12× - 304×) through direct sequencing or targeted sequencing with hybridization capture (Fig. 1). We then analyzed these data in the context of global cat genetic variation, including 63 nuclear and 108 mitochondrial genomes (table S1) previously published from ancient and modern specimens.

Timing of the arrival of domestic cats in China

Among the 22 felid bones from China, 14 individuals spanning >1,000 years from c.730 CE to 1,800 CE were identified as domestic cats (*F. catus*) (Fig. 1 and table S2). These 14 individual cats were identified in seven archeological sites across multiple dynasties, including the Tang (618–907 CE), Song (960–1,279 CE), Yuan (1,279–1,368 CE), Ming (1,368–1,644 CE), and the Qing Dynasty (1,644–1,911 CE). The most ancient domestic cat in our dataset (FS12), identified using both nuclear and mitochondrial genomes, was excavated from Tongwan City (*11*) in Shaanxi, western China, and directly radiocarbon dated to c.730 CE (706–883 cal CE 95%) during the mid-Tang Dynasty (Fig. 1 and table S2). This result supports a relatively recent arrival of domestic cats in eastern Eurasia and undermines the commonly held assumption that domestic cats were present in China as early as the Han Dynasty (206 BCE–220 CE) (*12*).

All 14 Chinese archaeological cats cluster within mtDNA clade IV-B in the phylogenetic tree (Fig. 2 and fig. S3) (*1,2*). Though cats that possess clade IV-B haplotypes are rare in both ancient and modern individuals from western Eurasia (*5*,*13*), this clade includes a contemporaneous domestic cat from Dhzankent of Kazakhstan dated to 775–940 cal CE

(*14*) (table S1), a contemporary African wildcat (FSI48) from the Levant, and 30 out of 38 (78.9%) modern domestic cats from China (*3*) (table S1).

A principal component analysis (PCA) of nuclear genomes highlights three major clusters that correspond to domestic cat and/or African wildcats from western Eurasia, China, Central Asia, and the Levant (Fig. 3A). The PC1 axis separates western Eurasian samples from the rest of the dataset, and the PC2 axis distinguishes all major groups, including Chinese/Central Asian domestic cats, western Eurasian domestic cats, and Levantine African wildcats (Fig. 3A). All ancient and modern domestic cats from China form a cluster that is closely associated with an ancient cat from Dhzankent, Kazakhstan (*14*), which is thus far the earliest domestic cat on the Silk Road (Fig. 3A).

This pattern supports a genomic affinity between domestic cats from China and Central Asia and African wildcats from the Levant. The finding is corroborated by ADMIXTURE analyses, where all these individuals share the same ancestry component at K=6 (Fig. 3C and fig. S4). Our outgroup f_3 analysis is also consistent with these patterns and demonstrates that relative to other ancient Chinese specimens, FS12, the earliest (Fig. 1C and table S2) and westernmost (Fig. 1A) domestic cat sampled in China, shows the strongest genetic association and temporal coincidence with the ancient Dhzankent cat (*14*).

Combined, this evidence suggests that the dispersal of domestic cats towards East Asia occurred via Central Asia before reaching western China. It is possible that this movement was facilitated by trade along the Silk Road since the earliest Chinese domestic cat in our study (FS12) is dated to about 1,200 years ago (706-883 CE) during the Mid-Tang Dynasty, an era in Chinese history when trade linking the East and West along this route was at its peak (*14*,*15*). Since 21.1% (8 of 38 specimens) of contemporary Chinese domestic cats, particularly those from the southern and eastern coastlines, possess mtDNA clade IV-A which is uncommon for cats from northern China (Fig. 2 and table S1), it is possible that cats were also introduced to China via maritime trade routes.

Phenotypic reconstruction of the earliest domestic cat in China

In numerous domestic taxa, shifts in selective pressures associated with living within anthropogenic environments enabled the emergence of phenotypes that distinguish them from their wild counterparts. These include a loss of camouflage and the appearance of novel coat colors and patterns, though the timing of the origin of different variants varies dramatically (*17*). For example, a high frequency of the distinguishing blotched-tabby coat pattern was evident in domestic cats in Europe only after the Middle Ages (*2*). To reconstruct the phenotype of the oldest domestic cat in China (FS12), we generated a 16× coverage of the nuclear genome (table S1) and assessed known genotypes previously identified in domestic cats (tables S7A-E). We characterized 94 variants associated with a wide range of traits, including coat color and pattern (tables S7A to C), tail type (table S7D), and common genetic diseases identified in modern cat breeds (table S7E).

FS12 was a male without any deleterious mutations associated with feline health defects tested in the study. The wild-type alleles present in seven genes suggested that FS12 had short hair (*FGF5*, *HR*, *KRT71*, *LPAR6*, *LIPH*) (*18-21*) (Fig. 4C and table S7C) and a long tail (*HES7*, *T*) (*22*,*23*) (Fig. 4C and table S7D). The variant associated with the recessive pigmentation allele on *ASIP* (*24*) indicated that FS12 did not possess any black hair (Fig. 4C and table S7A). Furthermore, we identified a *FERV1* insertion within the *KIT* gene that is associated with an all or partially white coat common in domestic cats (*25*) (Fig. 4C, fig. S12, and table S7A). Since we excluded the possibility that FS12 carried the blotched-tabby *Taqpep* allele (*26*) (table S7B), it is possible that this cat was either an all-white cat or a mackerel-tabby cat with white patches (Fig. 4C).

The presence of white fur in the earliest Chinese domestic cat is consistent with the observation that in East Asia, modern domestic cats possess a greater proportion of white or white-spotting coloration relative to other regions of the world (*27*). This pattern is also reflected in an iconographic survey in which 85% of the cat images identified in 33 ancient paintings from the Tang Dynasty to the 20th century (827–1,930 CE) showed white coat coloration (table S8).

Assessing gene flow from local wildcat species into ancient Chinese domestic cats

Two Indigenous wildcat species in China, the Chinese mountain cat (*Felis bieti*) and Asiatic wildcat (*F. ornata*), can interbreed with domestic cats and produce fertile offspring (*1,3*). In Europe, analyses of ancient and modern domestic cats and European wildcats (*F. silvestris*) demonstrated that until recently, gene flow between the two taxa was rare (*13*,*28*). In Asia, neither ADMIXTURE (Fig. 3C and fig. S4) nor *D*-statistics (Fig. 3D and fig. S5) revealed evidence for gene flow between the native wildcat species and the ancient domestic cats in China.

This could be because the restricted distribution of the Chinese mountain cat on the eastern part of the Qinghai-Tibetan Plateau does not overlap with the locations where domestic cats were first introduced to China, thus limiting opportunities for interbreeding. Domestic cats likely reached the Qinghai-Tibetan Plateau only within the past centuries and began encountering their alpine relatives. A recent genetic analysis indicated that, as a result of this sympatry, modern domestic cats in this region now possess 1-10% ancestry from Chinese mountain cats (*3*).

Leopard cats occupied human settlements prior to the arrival of domestic cats

Prior to the arrival of domestic cats, all but one of the seven feline remains found in Chinese archaeological sites were identified as leopard cats (*P. bengalensis*). The only exception is an individual that possessed an Asiatic wildcat (*F. ornata*) mtDNA haplotype (Fig. 1 and fig. S2) found at the site of Huoshiliang (FS7, c.1,800 BCE) (*29*). The earliest archaeological leopard cat specimen (FS15) in our dataset is from the site of Quanhucun dated to ~5,400 years ago (*6*,*8*) (Fig. 1 and fig. S6). Six additional feline excavations from six archaeological sites dated between c.3,000 BCE and c.150 CE (spanning from the Chinese Late Neolithic to the terminal Han Dynasty) were all identified as leopard cats using both mtDNA (Fig. 1 and fig. S6) and nuclear DNA analyses (figs. S7-S11). The most recently dated individual was a skeleton (FS19) found within human burials at the site of Zheng and Han City in c.150 CE during the late Han Dynasty (*30*,*31*).

The integration of leopard cats into human culture and society is also reflected in ancient Chinese literature (*32*) and art (Fig. 4A). Decorative paintings on a series of culinary artifacts excavated from the Mawangdui Han Tomb (c.168 BCE) feature one of the earliest known cat depictions in Chinese archaeological history (*33*,*34*). These images portray a spotted feline that more closely resembles a leopard cat than a domestic cat (Figs. 1, 4A and B).

Leopard cats may have been attracted to and begun living within human settlements prior to 3,400 BCE (Quanhucun), at least 4,000 years earlier than the arrival of domestic cats (*6*-*8*) (Fig. 1). A previous stable isotopic analysis suggested that leopard cats predated on rodents within human settlements (*6*), implying that this species may have occupied the same anthropogenic niche that was later filled by domestic cats. This relationship lasted at least 3,500 years given that the most recent leopard cat (FS19) in our dataset was dated to c.200 CE (Fig. 1 and table S2). Following this finding, there is a gap of ~600 years prior to the earliest appearance of a domestic cat (Fig. 1). In fact, over these six centuries, zooarchaeological research in China has thus far failed to identify any small cat remains (*35*). This absence may therefore reflect a real gap during which cats were either absent or extremely rare in human settlements.

The disappearance of leopard cats coincides with a turbulent era in Chinese history after the breakdown of the Han Dynasty and before the Tang Dynasty (Fig. 1). This historical period witnessed a shift toward a colder, dryer climate, dwindling agricultural yields, frequent social conflict, and a demographic contraction that persisted for 400 years (*36*,*37*). These conditions likely contributed to, or were accompanied by, the collapse of the Han Dynasty (*38*), possibly resulting in the decline of agriculture and a contraction of the niche that led to the cohabitation of leopard cats and humans. A study of ancient black rats in Europe demonstrated that, at least in Northern Europe, black rat populations disappeared alongside the demise of the Roman Empire, only to re-emerge from a different source population following the recovery of economic activity (*39*). In each case,

the decline of dynasties on both sides of Eurasia may have led to the disappearance of a commensal animal whose presence was dependent on a suitable anthropogenic niche.

The disappearance of leopard cats was followed six centuries later by the arrival of domestic cats during the rise of the Tang Dynasty (*15*). (Fig. 1). It is possible that the arrival of domestic cats may have prevented the re-establishment of the relationship between leopard cats and humans since both species occupy similar ecological niches. Other contributing factors that prevented a second appearance of leopard cats within human settlements may have included the rise of poultry farming in ancient China after the Han Dynasty (*40*), which could have led to human-leopard cat conflict due to the leopard cat's predation of poultry chicken (*10*,*41*).

Discussion

The zooarchaeological and genetic evidence demonstrates that the earliest commensal felids found within archaeological contexts were leopard cats. They first appeared at least 5,400 years ago and were then present across China for 3,500 years, during which they were incorporated into human burials and depicted in material culture. Following the end of the Han Dynasty in c.200 CE, leopard cats vanished from both zooarchaeological assemblages and artistic depictions. The disappearance of leopard cats may have begun with the socio-economic disruptions associated with dynastic changes, a shift mirrored in the temporary disappearance of black rats in Northern Europe following the end of the Roman Empire (*39*).

Following a six-century period in which no felid has yet been identified within archaeological contexts, domestic cats arrived in China during the Tang Dynasty during the 8th–9th centuries CE (Fig. 1 and table S2). This result first undermines the commonly held assumption that domestic cats were present in China during either the Neolithic (*6*) or Han Dynasty (*12*). Secondly, this evidence demonstrates that cats were introduced to China far more recently than other Eurasian domestic animals, including cattle, sheep, and goats (c.3,000-c.2,000 BCE) (*42*), and horses (c.1,200 BCE) (*43*). In addition, genomic associations with an ancient Central Asian cat suggest that cats were likely

introduced via the Silk Road, thus highlighting the significance of ancient trade routes in facilitating the dispersal of domestic animals.

From a conservation perspective, the introduction of domestic cats has had significant negative consequences for indigenous wildcat species. In Europe, gene flow between the earliest introduced domestic cats and the indigenous European wildcat was minimal (*13*). In the 20th century, however, substantial hybridization between the two taxa has led to the emergence of a hybrid swarm, and the eradication of European wildcats free of domestic cat ancestry at least in Scotland (*28*). Likewise, although we found no evidence of introgression in ancient China between domestic cats and local wildcat species (*F. ornata* and *F. bieti*), contemporary and ongoing admixture between modern domestic cats and *F. bieti* has been reported following the arrival of domestic cats on the Qinghai-Tibetan Plateau (*3*). This pattern raises concerns over the impact of the growing domestic cat population on the genomic integrity of native Chinese wildcats.

By contrast, the leopard cat belongs to *Prionailurus* genus that would not naturally breed with *Felis* species, and human-mediated crossing only occurred in the 1980s, giving rise to the Bengal domestic cat breed (*44*). The evidence presented here hence reveals an intriguing succession of two distinct small felids, each from a separate genus, that independently and consecutively occupied ancient anthropogenic environments in China. Though both were integrated into human cultural expressions in history, they ultimately followed divergent paths in human-animal interactions and reached different destinations.

Acknowledgments

We thank Yuxin Hou, Yeyizhou Fu, and Zhenyan Sui for their help to the project.

Funding: This work was supported in part by the National Key Research and Development Program of China (SQ2022YFF0802300). **Author Contributions:** Y.H., S.H., G.L., and S.J.L. designed the research; Y.H., J.A., K.L., A.E.J., and H.Y. performed the research; A.M., S.G.M., Y.Z., X.S., D.L., S.H., L.P., X.X., and L.A.F.F. assisted in the laboratory work and data analysis; Y.H., M.Y., C.Y., J.W., Z.W., C.C., X.W., Z.L., W.F., Q.C., Z.C., J.Y., Z.L., Y.L., Z.L., Q.M., J.S., Z.S., W.W., F.X., W.Y.,

S.Y., L.Y., H.Z., Z.P.L, X.L., and P.Z. carried out fieldwork and sample collection; C.Y., Y.P., and X.W. conducted radiocarbon dating; Y.H., J.A., S.D., G.L., and S.J.L. wrote the manuscript with comments from all authors. **Competing interests:** None. **Data and materials availability:** The sequencing data generated in this study are available in the NCBI Sequence Read Archive (PRJNA1178732). The NCBI accession numbers of mitochondrial haplotypes are PQ553222 to PQ553243.

References

1. C. A. Driscoll *et al*., The Near Eastern origin of cat domestication. *Science* **317**, 519–523 (2007). doi: 10.1126/science.1139518; Pmid: 17600185
2. C. Ottoni *et al*., The palaeogenetics of cat dispersal in the ancient world. *Nature Ecology & Evolution* **1**, 1–7 (2017). doi: 10.1038/s41559-017-0139
3. H. Yu *et al*., Genomic evidence for the Chinese mountain cat as a wildcat conspecific (*Felis silvestris bieti*) and its introgression to domestic cats. *Science Advances* **7**, eabg0221 (2021). doi: 10.1126/sciadv.abg0221; Pmid: 34162544
4. M. De Martino *et al*., The North African origin of domestic cats and their dispersal into Europe over the last two millennia. *In prep*
5. S. Doherty *et al*., Bioarchaeological approaches reveal waves of domestic cat introductions and the temporal decline of the European wildcat. *In prep*
6. Y. Hu *et al*., Earliest evidence for commensal processes of cat domestication. *Proceedings of the National Academy of Sciences* **111**, 116–120 (2014). doi: 10.1073/pnas.1311439110; Pmid: 24344279
7. J.-D. Vigne *et al*., Earliest "domestic" cats in China identified as leopard cat (*Prionailurus bengalensis*). *PloS One* **11**, e0147295 (2016). doi: 10.1371/journal.pone.0147295; Pmid: 26799955
8. S. Zhu *et al*., Ancient DNA traces a Chinese 5400-year-old cat specimen as leopard cat (*Prionailurus bengalensis*). *Journal of Genetics and Genomics* **49**, 1076-1079 (2022). doi: 10.1016/j.jgg.2022.07.005; Pmid: 35921988
9. S. J. Luo, The hidden Olympic spectator. *Science* **373**, 404 (2021). doi: 10.1126/science.abl3669; Pmid: 34437113
10. K. Nowell, P. Jackson. *Wild Cats: Status Survey and Conservation Action Plan* (IUCN-World Conservation Union, Gland, Switzerland, 1996).
11. X. Weng, B. Zhang, S. Li, Analysis of construction materials of Xiongnu Tongwan city, built 1600 years ago. *Studies in Conservation* **66**, 413–422 (2021). doi: 10.1080/00393630.2020.1853978
12. S. Hu, Z. Liu, J. Zhang, Research report on the faunal remains unearthed from the Southwest Corner of the Wall of Han Chang'an City Site. *Relics and Museology* **5**, 58-60 (2006). doi: 10.3969/j.issn.1000-7954.2006.05.013

13. A. Jamieson *et al*., Limited historical admixture between European wildcats and domestic cats. *Current Biology* 33, 4751–4760 (2023). doi: 10.1016/j.cub.2023.08.031; Pmid: 37935117
14. A. F. Haruda *et al*., The earliest domestic cat on the Silk Road. *Scientific Reports* **10**, 1–12 (2020). doi: 10.1038/s41598-020-67798-6; Pmid: 32647113
15. B. Li, *Communication, Civilization and China: Discovering the Tang Dynasty (618–907)* (Springer, 2020). doi: 10.1007/978-981-15-7808-3
16. F. Wood, *The Silk Road: Two Thousand Years in the Heart of Asia* (University of California Press, 2002). doi: 10.5860/choice.41-6080
17. A. Linderholm, G. Larson, "The role of humans in facilitating and sustaining coat colour variation in domestic animals" in *Seminars in Cell & Developmental Biology,* vol. **24**, pp. 587–593 (2013). doi: 10.1016/j.semcdb.2013.03.015; Pmid: 23567209
18. C. Drögemüller, S. Rüfenacht, B. Wichert, T. Leeb, Mutations within the *FGF5* gene are associated with hair length in cats. *Animal Genetics* **38**, 218–221 (2007). doi: 10.1111/j.1365-2052.2007.01590.x; Pmid: 17433015
19. M. Abitbol *et al*., A *COLQ* Missense mutation in Sphynx and Devon Rex cats with congenital myasthenic syndrome. *PLoS One* **10**, e0137019 (2015). doi: 10.1371/journal.pone.0137019; Pmid: 26327126
20. B. Gandolfi *et al.*, A splice variant in *KRT71* is associated with curly coat phenotype of Selkirk Rex cats. *Scientific Reports* **3**, 2000 (2013). doi: 10.1038/srep02000; Pmid: 23770706
21. A. D. Manakhov, T. V. Andreeva, E. I. Rogaev, The curly coat phenotype of the Ural Rex feline breed is associated with a mutation in the lipase *H* gene. *Animal Genetics* **51**, 584–589 (2020). doi: 10.1111/age.12958; Pmid: 32463158
22. X. Xu *et al*., Whole genome sequencing identifies a missense mutation in *HES7* associated with short tails in Asian domestic cats. *Scientific Reports* **6**, 31583 (2016). doi: 10.1038/srep31583; Pmid: 27560986
23. K. J. Buckingham *et al*., Multiple mutant *T* alleles cause haploinsufficiency of Brachyury and short tails in Manx cats. *Mammalian Genome* **24**, 400–408 (2013). doi: 10.1007/s00335-013-9471-1; Pmid: 23949773
24. E. Eizirik *et al.*, Molecular genetics and evolution of melanism in the cat family. *Current Biology* **13**, 448–453 (2003). doi: 10.1016/s0960-9822(03)00128-3; Pmid: 12620197
25. V. A. David *et al.*, Endogenous retrovirus insertion in the *KIT* oncogene determines white and white spotting in domestic cats. *G3: Genes, Genomes, Genetics* **4**, 1881–1891 (2014). doi: 10.1534/g3.114.013425; Pmid: 25085922
26. C. B. Kaelin *et al*., Specifying and sustaining pigmentation patterns in domestic and wild cats. *Science* **337**, 1536–1541 (2012). doi: 10.1126/science.1220893; Pmid: 22997338

27. L. Peng *et al.*, The genetics and evolution of white spotting coat color in domestic cats (*Felis catus*). *In prep*.
28. J. Howard-McCombe *et al*., Genetic swamping of the critically endangered Scottish wildcat was recent and accelerated by disease. *Current Biology* **33**, 4761–4769 (2023). doi: 10.1016/j.cub.2023.10.026; Pmid: 37935118
29. S. Hu, P. Zhang, M. Yuan, A study on the faunal remains from the Huoshiliang site in Yulin, Shaanxi. *Acta Anthropologica Sinica* **27***,* 58–60 (2008). doi: 10.3969/j.issn.1000-3193.2008.03.005
30. S. Ma, The ancient capital city of Zheng and Han State in Xinzheng. *Cultural Relics of the Central Plains* **2**, 54–55 (1978). doi: CNKI:SUN:ZYWW.0.1978-02-013
31. Henan Provincial Institute of Cultural Heritage and Archaeology, Sacrificial Pits of State Zheng at the Ruined Zheng and Han City. *Chinese Archaeology* **1**, 152–155 (2001). doi: 10.1515/char.2001.1.1.152
32. G. Ban, *Han Shu Huo Qu Bing Zhuan*. *Original Work Published in the 1th Century. [The Biography of Huo Qubing in The Book of Han]*.
33. H. Yang, A preliminary study of the Felis design on lacquer objects from the Han Tombs at Mawangdui. *Journal of Hunan Provincial Museum* **1**, 17-18, 312-331 (2016).
34. W. Hung, Art in a ritual context: rethinking Mawangdui. *Early China* **17**, 111–144 (1992). doi: 10.1017/s0362502800003692
35. Y. Jing, *Zooarchaeology of China* (Press of Cultural Relics, Beijing, 2015). doi: CNKI:SUN: WENW.0.2015-09-008
36. Q. Pei, D. D. Zhang, Long-term relationship between climate change and nomadic migration in historical China. *Ecology and Society* **19**, 68 (2014). doi: 10.5751/es-06528-190268
37. D. D. Zhang *et al*., The pulse of imperial China: a quantitative analysis of long-term geopolitical and climatic cycles. *Global Ecology and Biogeography* **24**, 87–96 (2015). doi: 10.1111/geb.12247
38. W. K. Wicky, *The Collapse of China's Later Han Dynasty, 25–220 CE: The Northwest Borderlands and the Edge of Empire* (Routledge, 2018). doi: 10.4324/9781315532332
39. H. Yu *et al.*, Palaeogenomic analysis of black rat (*Rattus rattus*) reveals multiple European introductions associated with human economic history. *Nature Communications* **13**, 1–13 (2022). doi: 10.1038/s41467-022-30009-z; Pmid: 35504912
40. S. Jia, *Qi Min Yao Shu. Original Work Published in the 6th Century. [An Essential Ancient Chinese Text on Agriculture and Horticulture, Documenting Early Practices and Technologies]*.

41. H. Fatima, *et al.*, Spatial distribution and dietary niche breadth of leopard cats (*Prionailurus bengalensis*) inhabiting Margalla Hills National Park, Pakistan. *Zoological Studies* **60**, 34 (2021). doi:10.6620/ZS.2021.60-34. Pmid: 34963787
42. L. Ren *et al*., Direct dating of the earliest domesticated cattle and caprines in northwestern China reveals the history of pastoralism in the Gansu-Qinghai region. *Journal of Archaeological Science* **144**, 105627 (2022). doi: 10.1016/j.jas.2022.105627
43. J. Yuan, H. Jian-Lin, R. Blench, "Livestock in ancient China: An archaeozoological perspective" in *Past Human Migrations in East Asia* (Routledge, 2008), pp. 116–136. doi: 10.4324/9780203926789
44. C. B. Kaelin *et al*., Ancestry dynamics and trait selection in a designer cat breed. *Current Biology* **34**, 1506–1518 (2024). doi: 10.1016/j.cub.2024.02.075; Pmid: 38531359

Figure Legends

Figure 1. Sampling location, species identification, and age of small feline specimens from ancient China. (A) Archaeological sites of small felid specimen sampling in China. The colors of the dots correspond to the species of small felid found at the sites. The IDs of small felids excavated at each site are displayed in parentheses after the site names. The Zheng and Han City is the only site where both leopard cats and domestic cats were found. **(B)** A maximum likelihood (ML) phylogenetic tree constructed based on mitogenomes of ancient feline samples from China. All 22 cat samples in archaeological contexts are included in this analysis in addition to mitogenomes from *F. catus* (NC_001700.1), *F. ornata* (FSI204, FSIP0006), *P. bengalensis* (NC_016189.1, NC_028301.1), and the tiger (NC_010642.1) as an outgroup. **(C)** The temporal distribution of small felids from archeological sites in this study, with the horizontal time scale showing the historical periods of China. The dots represent specimens excavated from the corresponding period and are color-coded according to their species identification.

Figure 2. The geographical distribution of the mtDNA haplogroups of Eurasian domestic cats. A maximum likelihood (ML) phylogenetic tree is reconstructed based on mitogenomes from 14 ancient domestic cats in China and other cats from Eurasia. A simplified diagram of the phylogenetic tree is shown in the lower left corner of the figure. Each small icon corresponds to one specimen, and icons within the same box represent samples from the same location. The color of the icon corresponds to the mtDNA clade it belongs to, as shown in the simplified tree in the bottom left corner. The mtDNA clade coding system follows the previous description (*1*). Red triangles represent newly generated ancient samples in this study, black triangles represent published ancient samples, and circles represent published modern samples, as indicated in the upper right corner.

Figure 3. Nuclear genome analysis of ancient domestic cats in China. Four ancient Chinese domestic cats (FS1, FS2, FS12, FS21) with whole-genome sequencing data are included in the analysis. **(A)** The result of a Principal Component Analysis (PCA). Data from modern samples are used to construct an initial PCA followed by a subsequent projection of ancient samples. **(B)** The result of outgroup f_3-statistics statistics. The shared drifts of different pairs of individuals from ancient domestic cats and other populations are tested. The sand cat (*F. margarita*) is used as an outgroup. The color gradient, ranging from yellow to red, signifies the magnitude of f_3 values. **(C)** Genetic clustering of domestic cats and wildcats inferred by ADMIXTURE (K=6). Each individual is represented by a vertical bar, which is partitioned into K colored segments and represents the individual affiliation to each cluster. See supplementary fig. S9. for clustering results for K from 2 to 4. **(D)** *D-statistics* test for gene flow between ancient Chinese domestic cats and *F. bieti* or *F. ornata,* with the analysis setup as *D* (Outgroup, bieti/ornata, PopX, Ancient Chinese domestic cats). The sand cat is used as an outgroup and PopX is labeled on the Y-axis. Results with significant *Z* values are outlined in black, while those with non-significant *Z*-values in red.

Figure 4. Phenotypic reconstruction of the earliest domestic cat in China and an artistic depiction of a leopard cat-like figure from ancient China. (A) Painting of one of the earliest known cat figures on a decorative artifact excavated from the Mawangdui Han Tomb (c.168 BCE), whose distinct spotted coat closely resembles that of a leopard cat (Source: Hunan Museum Collection Database, https://www.hnmuseum.com/zh-hans/zuixin_tuijie). **(B)** A wild leopard cat from Beijing (Credit: School of Life Sciences, Peking University), highlighting the similarity between its spotted coat and the artistic depiction of a cat on the archeological artifact. **(C)** Phenotypic reconstruction, based on whole genome sequencing at 16× coverage, of FS12, the earliest domestic cat discovered in China (706–883 cal CE) from the Tang Dynasty. Genomic inference suggests FS12 was either an all-white cat (left) or a partially white cat with a mackerel tabby pattern (right). The background is an artistic illustration of ancient Tongwan City, Shaanxi, where FS12 was excavated (Image credit: Lanhui Peng).

SUPPLEMENTARY MATERIALS

Supplementary Results and Discussion

- Population structure of ancient leopard cats from the Middle Yellow River Basin
- Phenotypic reconstruction of the earliest domestic cat of China

Supplementary Materials and Methods

- Archaeological sites description
- Biological specimens
- Radiocarbon dating
- Ancient DNA laboratory procedures
- Genomic data processing
- Assembly and analysis of cat images in ancient artwork from China

Supplementary Figure Legends

Fig. S1. Plots of mapDamage analysis showing damage patterns of 22 ancient Chinese cat specimens used in this study. The 5' and 3' ends of all samples exhibit a clear deamination pattern signature for ancient DNA.

Fig. S2. A maximum likelihood (ML) phylogenetic tree constructed based on the mitochondrial genomes of 22 ancient felid samples collected from China. A TN93+I+G model is implemented with 1,000 bootstrap replicates and a tiger genome (NC_010642.1) is used as an outgroup. The numbers on branches represent the statistical support values based on 1,000 bootstrap replicates. A refined version of the tree is in Fig. 1B.

Fig. S3. A maximum likelihood (ML) phylogenetic tree based on mitogenomes of ancient and modern domestic cats worldwide, including 14 ancient domestic cats from China. A TN93+I+G model is implemented with 1,000 bootstrap replicates. The

missing data rate for Chinese samples is less than 2% each sample and the sequencing depth is greater than 30´. The missing data rate for European or Central Asian samples is generally less than 10% and the sequencing depth is greater than 10´. Notes with significant statistical support (≥ 70%) based on 1,000 bootstrap replicates are labeled with red dots.

Fig. S4. ADMIXTURE analysis for ancient and modern domestic cats and wildcats from Eurasia. **(A)** ADMIXTURE clustering results based on the number of assumed ancestral populations (*K*) from 2 to 6. **(B)** Cross-validation (CV) errors for each number of assumed ancestral populations (*K*) from 1 to 7.

Fig. S5. The result of outgroup f3-statistics illustrates the affinity between ancient domestic cats from China and other domestic cat populations. The error bars in the four stacked blocks, from bottom to top, correspond to the f3 values between FS1/FS2/ FS12/FS21 and other cat populations (labeled on the right). The color gradient, ranging from light to dark blue, shows an increased magnitude of the absolute value of Z. This figure, compared to Fig. 3B, highlights the relationship between ancient domestic cats and modern domestic cats.

Fig. S6. A maximum likelihood (ML) phylogenetic tree based on leopard cat mitochondrial genomes. The tree is reconstructed based on ancient leopard cats from the middle Yellow River Basin of China (n=7) and modern leopard cats from the Russian Far East (n=4), Indochina (n=6), Malay Peninsula (n=6), and Sundaland (n=4). Two fishing cats (*P. viverrinus*) and a flat-headed cat (*P. planiceps*) are included in the analysis. The tiger reference genome (NC_010642.1) is used as an outgroup. The sample names of ancient leopard cats from the Yellow River Basin are marked in red.

Fig. S7. A maximum likelihood (ML) phylogenetic tree based on ancient and modern leopard cats. The tree is reconstructed based on autosomal SNPs from ancient specimens from China (n=3) and modern samples from the Russian Far East (n=2), Indochina (n=6), Malay Peninsula (n=4), and Sundaland (n=3). A fishing cat (*P. viverrinus*) is included in the analysis. Two domestic cats are used as outgroups. Numbers at each node represent the statistical support values based on 200 bootstrap replicates.

Fig. S8. Principal component analysis (PCA) of leopard cats. PCA is first conducted based on autosomal SNPs from high-quality genome data from modern leopard cats. Data from ancient leopard cats are then projected onto it. Three ancient leopard cats from China and 15 modern leopard cats from range wide, including the Russian Far East (n=2), Indochina (n=6), Malay Peninsula (n=4), and Sundaland (n=3), are included in the analysis.

Fig. S9. ADMIXTURE analysis of leopard cats. (**A**) Clustering results based on the number of assumed ancestral populations (*K*) from 2 to 4. A total of 18 specimens are used in the analysis including ancient leopard cats from China (n=3) and modern leopard cats from the Russian Far East (n=2), Indochina (n=6), Malay (n=4), and Sundaland

(n=3). A fishing cat was used as an outgroup. (**B**) Cross-validation (CV) errors for each number of assumed ancestral populations (*K*) from 1 to 8.

Fig. S10. Outgroup f3-statistics analysis of leopard cats. A heatmap of the outgroup f_3-statistics analysis. Two domestic cats are used as outgroups. The shared drifts of different pairs of individuals of leopard cat or fishing cat are tested. The color gradient, ranging from light to dark green, shows the increased magnitude of f3 values. The sample names from different populations were labeled with different colors. Ancient Chinese leopard cats (n=2) were marked in red; Russian Far East (n=2) in orange; Indochina (n=6) in light blue; Malay (n=4) in green; Sunda (n=3) in brownish yellow; and fishing cat (n=1) in dark blue.

Fig. S11. D-statistics analysis of leopard cats. The population combinations were set as (Outgroup, *P. bengalensis*_X, Russian Far East, ancient China) (labeled on the top of each block). Two domestic cats were used as outgroups. Leopard cats from Indochina, Malay Peninsula, Sundaland, and a fishing cat are individually placed in P.bengal_X to evaluate the signals of gene flow between the target ancient Chinese leopard cat and a modern leopard cat from P.bengal_X, relative to a Russian Far East leopard cat. The vertical axis shows the ID of leopard cats in P.bengal_X (on the left) and their population assignments (on the right). The horizontal axis shows the *D* scores. The color gradient, ranging from light to dark green, indicates an increased magnitude of |Z| values.

Fig. S12. Mapping patterns of the sequencing data to the domestic cat's *KIT* gene with *FERV1* insertion. (A) Alignment of FS12's *KIT* gene with *FERV1* insertion. **(B)** Alignment of a wild-type domestic cat *KIT* gene without *FERV1* insertion. **(C)** Alignment of a domestic cat homozygous of *FERV1* insertion. **(D)** Alignment of a domestic cat heterozygous of *FERV1* insertion.

Supplementary Tables

Table S1. (A) Information of the ancient samples from this study. **(B)** Information of ancient samples from other studies. **(C)** Information of modern *Felis* samples from other resources. **(D)** Information of Leopard cat and fishing cat samples from other studies.

Table S2. Radiocarbon dating of small cat specimens from archeological sites of China.

Table S3. Pairwise outgroup f_3-statistics of ancient and modern leopard cats (Data of Fig. S10).

Table S4. *D*-statistics of leopard cats from modern Asia and ancient China (Data of Fig. S11).

Table S5. Pairwise f_3-statistics of the genetic relationships between various populations of ancient or modern *Felis* species (Data of Fig. 3B).

Table S6. *D*-statistics test for gene flow between ancient Chinese domestic cats (FS1, FS2, FS12, FS21) and wildcats (*F. lybica*, *F. silvestris*, *F. bieti*, *F. ornata*) with the analysis set up as D (Outgroup, wildcatsX, Pop2, ancient_China) (Data of Fig. 3D).

Table S7. (A) Genotypes and inferred phenotypes of FS12 associated with coat colors. **(B)** Genotypes and inferred phenotypes of FS12 associated with coat patterns. **(C)** Genotypes and inferred phenotypes of FS12 associated hair morphology. **(D)** Genotypes and inferred phenotypes of FS12 associated with tail length and morphology. **(E)** Genotypes and inferred phenotypes of FS12 associated with genetic diseases.

Table S8. Information of ancient paintings from China involving images of domestic cats within the time frame of this study from the Tang Dynasty to modern time (827-1930 CE).

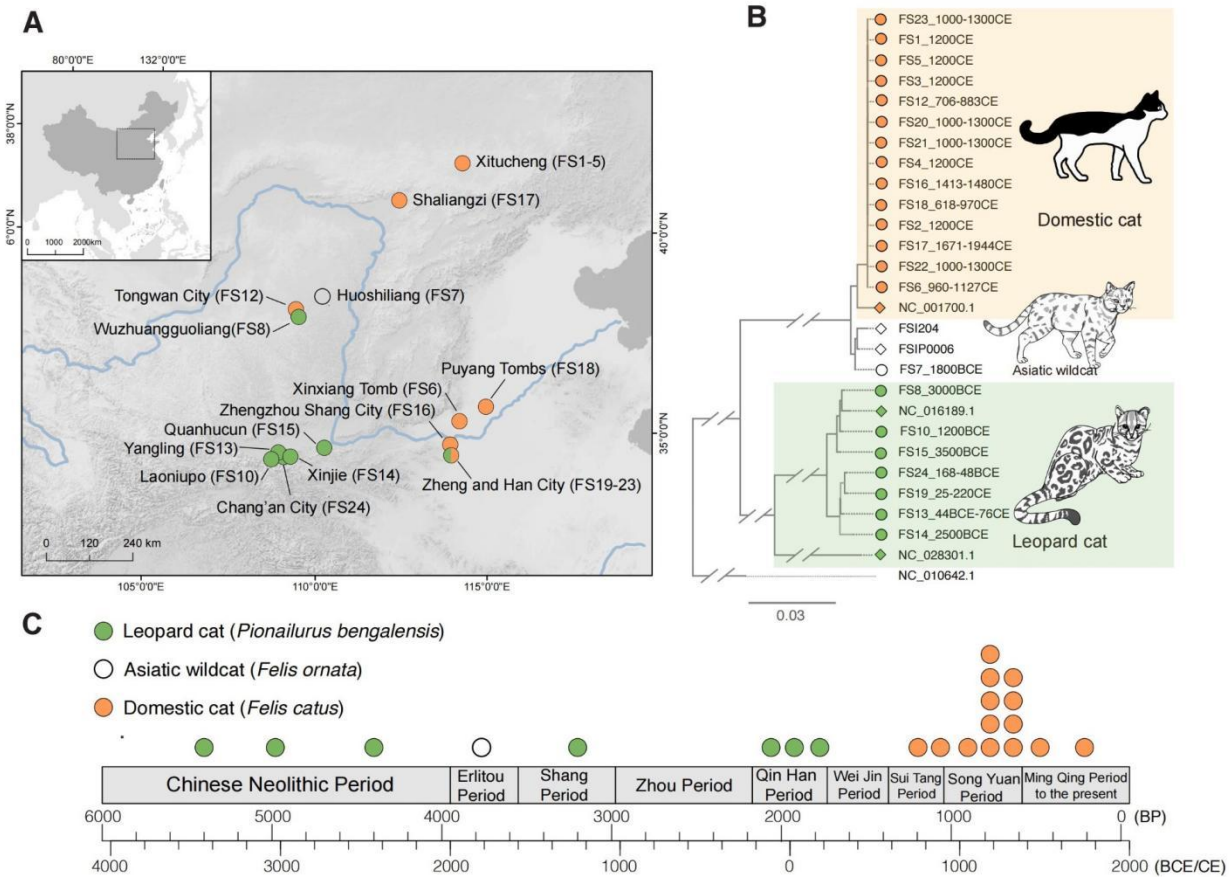

Fig 1. Sampling location, species identification, and age of small feline specimens from ancient China

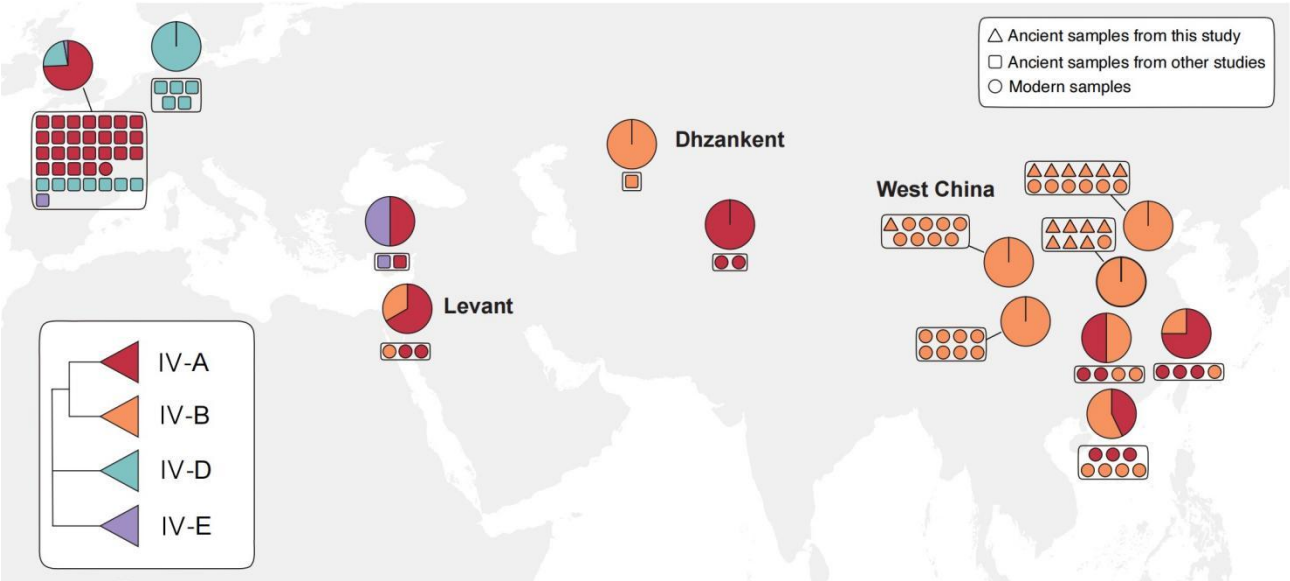

Fig 2. The geographical distribution of the mtDNA haplogroups of Eurasian domestic cats

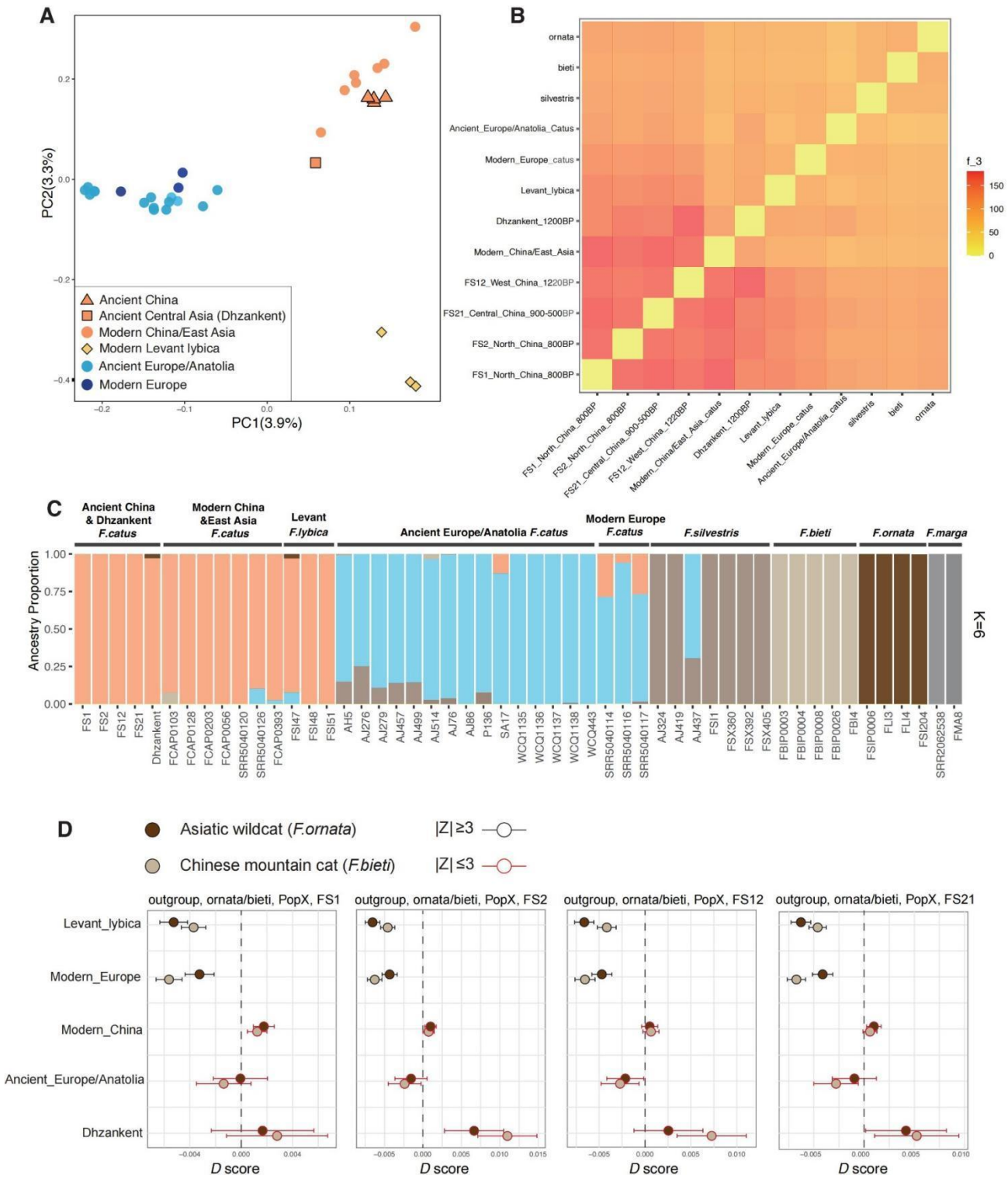

Fig 3. Nuclear genome analysis of ancient domestic cats in China

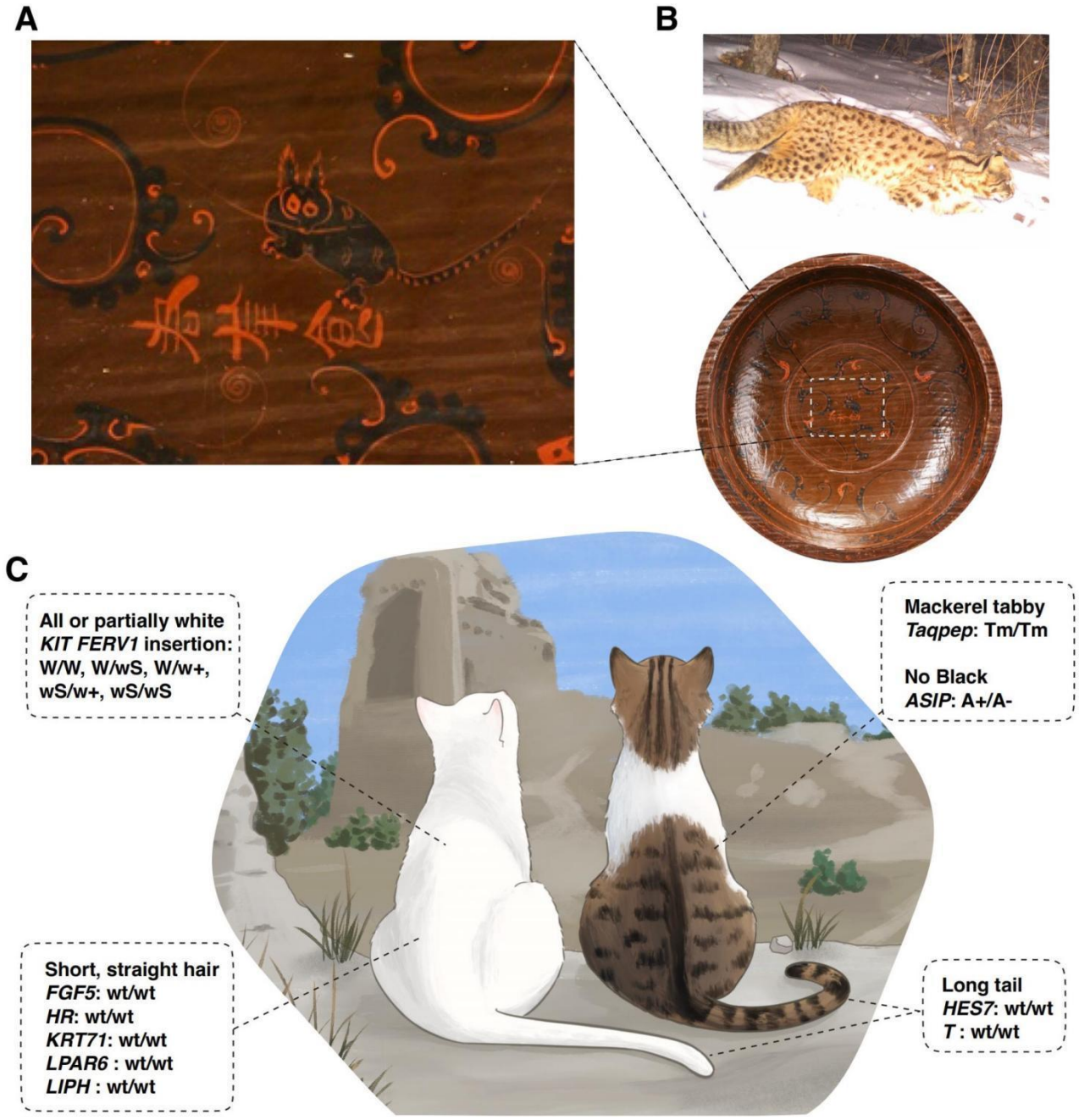

Fig 4. Phenotypic reconstruction of the earliest domestic cat in China and an artistic depiction of a leopard cat-like figure from ancient China

Supplementary Materials for

Leopard Cats Occupied Human Settlements in China for 3,500 years before the Arrival of Domestic cats in 600-900 CE around the Tang Dynasty

Yu Han[1,2,3]*, Songmei Hu[4,5]*, Ke Liu[1,3], Xiao Xu[1,3], Sean Doherty[6], Alexandra Elizabeth Jamieson[2], Aurelie Manin[2], Sofia Granja Martins[2,7,8], Miaomiao Yang[9], Chong Yu[10], Juan Wang[11], Zhuang Wu[12], Canping Chen[12], Sicheng Han[1,3], Daowei Lu[1,3], Lanhui Peng[1,3], Xianzhu Wu[13], Ziyi Li[14] , Wenquan Fan[15], Quanfa Cai[15], Zongliang Cui[16], Jing Yuan[17], Zihan Li[2], Yang Liu[10], Zhipeng Li[18], Zhendong Liu[18], Qian Ma[2], Jing Shao[9], Zhouyong Sun[9], Fulai Xing[9], Wuzhan Yang[9], Shugang Yang[15], Lianjian Yue[9], Pengcheng Zhang[19], Weilin Wang[20], Huanyuan Zhang[21], Yan Zhuang[1,3], Xin Sun[1,3], Yan Pan[22], Xiaohong Wu[22], Laurent A. F. Frantz[1,23], He Yu[1]†, Joel M. Alves[2,7,8]†, Greger Larson[2]†‡, Shu-Jin Luo[1,3]†‡

*These authors contributed equally to this work.
†To whom correspondence and requests for materials should be addressed. Email: luo.shujin@pku.edu.cn (S.J.L.); greger.larson@arch.ox.ac.uk (G.L.); joel.alves@arch.ox.ac.uk (J.M.A.); yuhe@pku.edu.cn (H.Y.)
‡These authors co-supervised this work.

This PDF file includes:

Supplementary Results and Discussion
- Population structure of ancient leopard cats from the Middle Yellow River Basin
- Phenotypic reconstruction of the earliest domestic cat of China

Supplementary Materials and Methods
- Archaeological sites description
- Biological specimens
- Radiocarbon dating
- Ancient DNA laboratory procedures
- Genomic data processing
- Assembly and analysis of cat images in ancient artwork from China

Supplementary References

Figs. S1 to S21
Table S1 to S8

Supplementary Results and Discussions

Population structure of ancient leopard cats from the Middle Yellow River Basin

The leopard cat has a widespread distribution in Asia and appears to be more tolerant of deforestation and human disturbance than most other Asian wild felids (*1–5*), and it often is found in plantations and near villages, showing an affinity to human settlements (*6–8*). Previous studies demonstrated that the leopard cat can be divided into two deeply diverging lineages to the level of speciation. or the mainland leopard cat (*P. bengalensis*) and Sunda leopard cat (*P. javanensis*). The mainland lineage contains leopard cats ranging from the Russian Far East to Indochina, while the Sunda leopard cat includes populations from Malay Peninsula and Sundaland. Research on the population structure of leopard cats in the middle reaches of the Yellow River was limited (*5*).

To better understand the population dynamics of ancient leopard cats in this region, we analyzed a dataset consisting of 30 mitochondrial genomes. This included seven newly sequenced ancient samples from the Middle Yellow River Basin and contemporary samples in various regions Russian Far East (n=3), Indochina (n=6), Malay (n=6) and Sundaland (n=3) (table S1D). Additionally, mitochondrial genomes from two fishing cats and a flat-headed cat were included for comparison. For the nuclear DNA analysis, we examined 18 genomes, including three ancient samples from China and 15 modern leopard cats: two from the Russian Far East, six from Indochina, four from Malay, and three from Sundaland. Comparative analysis also included nuclear genomes from a fishing cat and two domestic cats. After SNP calling and filtering, we identified 20,436,894 SNPs in our nuclear genome dataset (table S1).

An ML (Maximum Likelihood) tree was constructed to elucidate the maternal genetic relationships among ancient leopard cats and other populations, as detailed in fig. S6. The analysis divided the leopard cats into two principal clades: Mainland and Insular. Within the Mainland clade, two sub-clades emerged, primarily comprising individuals from the Russian Far East and Indochina, respectively. Notably, our ancient samples from China, though from the same geographical area, were distributed across these sub-clades. FS13, FS14, FS19, and FS24 were grouped with the sub-clade dominated by Indochina individuals, whereas FS8, FS10, and FS15 were aligned with the sub-clade associated with the Russian Far East. This distribution indicates that the ancient leopard cats from the Middle Yellow River Basin shared mtDNA with both Indochina and the Russian Far East, suggesting a complex and interconnected maternal structure in this region during ancient times.

The phylogenetic tree constructed from autosomal SNPs, with robust statistical support for each branch (bootstrap ≥99%), clearly segregates the leopard cat populations into four primary groups: Sundaland, Malay, Indochina, and Russian Far East (fig. S7). Notably, our three ancient samples, FS8, FS15, and FS19, form a monophyletic group closely aligned with the Russian Far East population. This pattern suggests a close relationship between the leopard cats from the Middle Yellow River Basin and those from the Russian Far East.

PCA (fig. S8) demonstrated that the ancient samples form a distinct clade closely associated with both the Russian Far East and Indochina populations along the PC1. Along the PC2, these ancient samples are positioned intermediately between the Russian Far East and Indochina populations, as shown in Figure S8. In the ADMIXTURE analysis (fig. S9), from K=2 to K=4, the ancient samples consistently show a predominant genetic affinity with the Russian Far East population. This relationship is further supported by the outgroup f_3-statistics (fig. S10; table S3), which indicate that the Russian Far East population shares a more extended evolutionary history with the ancient leopard cats.

Our analyses also point to potential gene flows between the populations of Indochina and the Middle Yellow River Basin. As revealed by the phylogenetic analysis, sample FS19, which clusters with the Indochina clade in the tree constructed using mtDNA, generally aligned with the Russian Far East population in the nuclear DNA analysis (figs. S6-S7). However, in the PCA (fig. S8), ancient Chinese leopard cats were distributing between Russian Far East and Indochina populations. This inconsistency suggested potential genetic exchanges.

To confirm this, we applied D-statistics analysis. For the combination (domestic cats, Indochina, Russian Far East, ancient China), the D values consistently yielded positive results coupled with significant Z values ($|Z| > 3$) (fig. S11; table S4). Since our samples from the Middle Yellow River Basin, this results likely suggests that gene flow occurred between ancient population from the Middle Yellow River Basin and the ancestral population of Indochina leopard cats in history.

Combined, these results suggested a significant genetic linkage between the leopard cats from the Middle Yellow River Basin and those from the Russian Far East, indicating they were more closely related genetically than with other contemporary populations. This close relationship may reflect historical gene flow or a shared ancestral population between these regions.

Phenotypic reconstruction of the earliest domestic cat of China

A domestic cat remain FS12 was found among the Tang Dynasty's remains of the Tongwan City in northwest China and directly radiocarbon dated to 706 - 883 CE. It is thus far the earliest domestic cat discovered in China. Comparison of the ratio of the X chromosome to the autosomal chromosomes (approximately 0.5) indicated it as a male individual. FS12 was sequenced to a genome coverage of 16× to infer its phenotypes, including coat color (table S7A), pigmentation pattern (table S7B), fur type (table S7C), tail type (table S7D), and potential genetic diseases (table S7E).

Genomic analysis indicated that FS12 has an all-white or partially white pelage. White coloration in domestic cats is attributed to a feline endogenous retrovirus (*FERV1*) insertion within the *KIT* (*proto-oncogene, receptor tyrosine kinase*) gene's intron 1. The repercussions of this insertion can lead to body surface depigmentation **(*9*)**. While

distinguishing between homozygosity (fig. S12A and C) and heterozygosity (fig. S12A and D) for the *FERV1* insertion within the *KIT* gene is challenging, the distinct alignment patterns observed when compared to the wildtype (fig. S12A and B) suggest that FS12 likely carries either a heterozygous or homozygous *FERV1* insertion (*61*). This genetic configuration is associated with white coloration, indicating that FS12 may exhibit either pure white or white-spotted coat color (Fig. 4C).

Our analysis indicated that FS12 does not possessed black fur, another coat color for domestic cats. This trait stems from a homozygous two-nucleotide deletion (Felis_catus_9.0 GCA_000181335.4, ChrA3:25086566-25086567del) in the *ASIP* gene (*10*). FS12's heterozygous genotype negates black coloration. We also examined other coloration loci with well-documented genetic mechanisms in FS12, finding that all of these loci are homozygous for the wildtype alleles, which prevents the expression of those specific colors (*11–16*). The genomic regions associated with the Mocha (Felis_catus_9.0 GCA_000181335.4, ChrD1:45898609-45898771dup) (*17*) and Dilution (Felis_catus_9.0 GCA_000181335.4, ChrC1:219396820del) (*18*) colorations are absent in FS12, leaving the status of these color patterns inconclusive (table S7A and fig. 4C).. Considering that the Mocha and Dilution colorations are primarily found in Western cat breeds, it is unlikely that FS12 exhibits these two colors.

We assessed the genetic variants associated with the blotched (*19*) and ticked tabby to elucidate FS12's pigmentation pattern (*20*) (table S7B). Since no mutation associated with the blotched or ticked variant was identified, we infer FS12 to be a wild-type mackerel tabby, akin to that of *Chinese Lihua* or *Dragon Li* cats (fig. S4C; table S7B).

While it is known that FS12 displays white coloration, the current information is inadequate to ascertain the precise extent of the white coverage (*9*). If FS12 possessed a all-white coat, the tabby pattern would not appear due to the all-white coat variant's epistatic effect. On the other side, FS12 could show a partially white fur with patches of wild-type mackerel tabby pattern. Either coat color morph, an all-white cat or a mackerel tabby cat with white patches, is possible for FS12 (Fig. 4C).

To investigate the hair length morphology, we examined the genetic variants responsible for short hair, long hair, curly hair, hairlessness, and Lykoi-style hair (table S7C) and revealed no variant in FS12 that would result in these specific coat types (*21–27*). Although the two mutations in *HR* gene associated with the Lykoi pattern were not available for analysis (*24*), considering that the Lykoi pattern is found in modern Western commercial breeds, it is unlikely to be present in an ancient individual from China. Therefore, we exclude this variation. Based on these findings, we inferred that FS12 has straight and short hair as a wild type (Fig. 4C).

The tail morphology and associated mutations are detailed in table S7D. Since FS12 carries wild-type alleles at all loci (*28*, *29*), it is apparent that it has a full-length, normal tail (Fig. 4C).

We assessed 52 deleterious variants associated with 37 genetic diseases found in modern cats. Detailed information about these can be found in table S7E. No defect variant was found in FS12 (*24*, *30–69*).

In summary, phenotypic reconstruction based on 16× coverage of whole genome sequencing data suggests FS12 the earliest domestic cat found in China thus far as an all-white cat or partially white cat with mackerel tabby pattern. It has short hair and a long tail (Fig. 4C; table S7). In addition, no genetic defect commonly found in modern domestic cat breeds are detected in FS12 (table S7E).

We further explored the appearance of cat color in historical artwork with a specific focus on two prominent pelage morphs, the black and white (*70*). We collected 33 historically significant feline-themed paintings spanning from the Tang Dynasty to modern times (827 - 1930 CE) (table S8). Iconographic analysis revealed that 68% of these paintings illustrated cats with black coloration and a staggering 85% portrayed white cats (table S8). Artwork often reflects societal preference, and the high prevalence of white cats in historical Chinese paintings are consistent with an ancient proclivity for white animals in East Asian culture. Phenotypic reconstruction based on genome data and artistic reflection of cat images from ancient artwork jointly confirmed that a preference towards white color may exist historically in China. This preference in feline aesthetics, merging genetics with art, provides a fascinating glimpse into the cultural and biological expression in East Asia. Further research will be essential to illuminate these insights.

Supplementary Materials and Methods

Archaeological sites description

Tongwan City Site (Contact: Songmei Hu)
Tongwan City was founded in northwestern China in 413 CE by Helian Bobo, the founder of the Daxia Kingdom. Due to its strategic lofelidion in the heart of the Ordos region, it gradually became a crucial hub for both commercial and military activities within the Inner Asian realm. Its importance was further emphasized by its position along the Silk Road. After the dissolution of Daxia, Tongwancheng continued to be inhabited and used by subsequent periods (*71*). In the present study, a domestic felid sample (FS12) retrieved from an excavation site within the city was subjected to radiocarbon dating. The results indicated that this sample can be dated to 706 - 883 cal CE within the era of the Tang Dynasty.

Puyang Tombs (Contact: Juan Wang)
The Puyang is in the Puyang City, Henan Province. The excavation of the site has revealed several burials. Faunal remains identified in these tombs included a variety of species, including the domestic cattle, horse, felid, hare, canid, badger, deer, Chinese zokor, and pheasant. One sample (FS18) from the Tomb M10 was analyzed in this study. This individual was believed to as early as the late Tang Dynasty to the Five Dynasties and Ten Kingdoms (618 - 970 CE) (*72*).

Xitucheng City Site (Contact: Zhuang Wu)
The Xitucheng City Site, situated in the westernmost part of Xitucheng Village within Erhao Bu Township, Kangbao County, Zhangjiakou City, Hebei Province, occupies a strategic location. Archaeological evidence suggests that this city site dates back to the Jin Dynasty (1,115 - 1,234 CE), making it approximately 800 years old (*73*, *74*). Five domestic felid samples from the site (labeled FS1, FS2, FS3, FS4, and FS5) have been analyzed in this study.

Xinxiang Song Tomb (Contact: Xianzhu Wu)
The tomb is located within the construction project of the new campus of Henan Institute of Technology. Excavation revealed that the site served as a family burial ground during the Northern Song Dynasty, spanning from 960 - 1,127 CE. The four tombs discovered shared a similar architectural style, all mimicking wooden structures with brick chambers. Each tomb consisted of three distinct sections: a burial shaft, an entrance, and a burial chamber. The burial shafts were oriented towards the south, and the stratigraphic accumulation of the burial ground was relatively simplistic. In Tomb 2012XJZM4, apart from the discovery of burial goods such as porcelain and copper coins, a collection of animal bones was also found, including those of a domestic felid. The felid was buried adjacent to the head of the tomb occupant (*75*). This sample has been used in this study labeled as FS6.

Zheng and Han City Site (Contact: Ziyi Li)
Zheng and Han City is in the heartland of Central China. Throughout the Spring and Autumn and Warring States periods (770 – 221 BCE), it served as the capital for both the Zheng and Han states successively (Ma, 1978). The felid bones used in this study did not originate from the Spring and Autumn or Warring States periods but were excavated from remains dating to the Han Dynasty and later. Specifically, the FS19 sample was unearthed from a tomb dating to the late Eastern Han period (25 - 220 CE) and radiocarbon dated to 200 - 380 cal CE, while samples FS20, FS21, FS22, and FS23 were derived from pits dating between the Song and Yuan Periods (960-1,368 CE).

Zhengzhou Shang City Site (Contact: Juan Wang)
The Zhengzhou Shang City Site is located within Henan Province in Central China and served as the capital city during the Shang Dynasty (*76*, *77*). This region has maintained its usage as a residential area, consistently utilized throughout successive eras. The current study involves a felid bone excavated from a pit radiocarbon dated to the Ming Dynasty (1,413 - 1,480 cal CE) within this site. This sample has been analyzed in this study and is labeled as FS16.

Shaliangzi City Site (Contact: Chong Yu)
The Shaliangzi City Site, located in Inner Mongolia's Hohhot City, encompasses an area of roughly 110,000 square meters. At its center, archaeologists have discovered and excavated a large, single-structure rammed-earth platform dating back to the Han Dynasty. Artifacts recovered from the site primarily consist of architectural materials such as flat tiles, tube tiles, eave tiles, and square bricks with geometric patterns (*78*). A felid skeleton (FS17) was found under the foundation of the granary. Although the main

body of the foundation was identified as a creation of the Han Dynasty, radiocarbon dating indicated that the felid sample was originated in the Qing Dynasty (1,671 - 1,944 CE).

Quanhucun Site (Contact: Songmei Hu)
The Quanhucun Site is in the village of the same name within Hua County, Shaanxi Province, in Central China. Archaeological remains at the site can be attributed to the Middle to Late Yangshao Culture (4,000 - 2,700 BCE). Agricultural practices of the Yangshao culture encompassed the cultivation of foxtail millet and common millet, and domestication of animals such as pigs and dogs. Studies identified that leopard felids were having a commensal relationship with humans in the site(*6–8*). This research incorporated one felid sample (FS15) that can be dated to approximately 5,400 years ago unearthed from the Quanhucun site (*6–8*).

Wuzhuangguoliang Site (Contact: Songmei Hu)
The Wuzhuang Guoliang archaeological site is situated in the Jingbian County, Shaanxi Province, northwestern China. Occupying about 600,000 square meters, the site spanned across five mountain ridges. The site contains cultural remains ranging from the Neolithic Age to the Warring States period (~3,000 - 221 BCE) (*7*, *79*). One felid sample (FS8) dated back to the Neolithic Period was analyzed in this research.

Huoshiliang Site (Contact: Songmei Hu)
The Huoshiliang Site, situated in the desert interior of Yulin City, Shaanxi Province, northwestern China, spans about 100,000 square meters. A significant number of animal bones were also unearthed. Preliminary analysis identified that the primary cultural content of the Huoshiliang site ranges from the late Longshan period of Chinese Neolithic Age to the Erlitou Period (~1,800 BCE) (*80*). One felid sample (FS7) unearthed from the site was included in this study.

Xinjie Site (Contact: Songmei Hu)
The Xinjie site is a settlement located on the loess plateau on the eastern bank of the Ba River, in the Wei River basin of Shaanxi Province, China. The site encompassed the period from the late Yangshao period to the Longshan period during the Chinese Neolithic Age (~3,500 - 1,800 BCE), with most of the remains belonging to the late Yangshao period. The site extends approximately 600 meters east to west and about 500 meters north to south, covering a total area of approximately 300,000 square meters. A felid sample (FS14) from the Longshan context was included in this study.

Laoniupo Site (Contact: Songmei Hu)
The site of Laoniupo is located at the eastern suburb of Xi'an City, Shaanxi Province, China. It was occupied by many archaeological cultures spanning from the Neolithic period to the Shang Dynasty (~5,000 - 1,200 BCE) (*81*). One sample (FS10) from the Shang remains of the site was included in this study.

Han Chang'an City Site (Contact: Songmei Hu)

The Han Chang'an City is in Weiyang District, Xi'an City, Shaanxi Province, China. It was the capital city of the Western Han Dynasty built and expanded by Emperor Gaozu of Han and his successors on the foundation of the Qin Dynasty's Xingle Palace. In 2002, the Han Chang'an City Working Group from the Institute of Archaeology, Chinese Academy of Social Sciences, conducted an excavation at the southwest corner site of the Han Chang'an City wall (*82*). During the excavation, a tibia of felid (FS24) was discovered. This sample has been analyzed and radiocarbon dated to 44 cal BCE - 76 cal CE in this research, further confirming its assignment to the Han Dynasty.

Yangling Mausoleum (Contact: Songmei Hu)
The Yangling Mausoleum is the joint burial tomb of Emperor Jing of the Western Han Dynasty, Liu Qi, and his queen (157-126 BCE). It is situated in Xianyang City, Shaanxi Province, China. This mausoleum is the easternmost of the emperor tombs located on the Xianyang Plain of the Western Han Dynasty *(*83*)*. During excavations, a felid skeleton (FS13) was discovered in the external burial pit on the east side of the tomb mound within the mausoleum garden and analyzed in this study. Radiocarbon dating confirmed that the age of the sample is 168 - 48 cal BCE falling into the range of the Western Han Dynasty.

Biological specimens

All the specimens newly assembled for this study were obtained from archaeological excavations in collaboration with respective excavators or zooarchaeologists. Each sample has clear records of the archaeological remain or stratigraphic layers from which it was retrieved. This ensures the accuracy of the archaeological context of the samples.

In total, 22 ancient felid bones excavated from 14 archaeological sites dated from ~3,500 BCE to 1,800 CE were collected (table S1 and Sites Description in Supplementary Materials). From which, 3 nuclear genomes (FS8, FS15, FS19) (3.3× - 6×) and 7 mitochondrial genomes (11.5× - 91×) belong to leopard cats (*P. bengalensis*); 4 nuclear genomes (2.4×-3.5×), 14 mitochondrial genomes (34.7× - 304×) of domestic cats (*Felis catus*) and a mitochondrial genome (16.9×) of Asiatic wild cat (*F. ornata*) or Chinese mountain cat (*F. bieti*) were generated. To obtain phenotypic information of the earliest domestic cats so far found in China. We further deep sequenced FS12 and increased its depth of nuclear genome from 3.5× to16× (table S1A).

In addition to ancient samples newly analyzed in this research, mitochondrial genomes of 42 ancient domestic cats from the British Isle (n=34), Demark (n=5), Near East (n=2) (provided by School of Archaeology, University of Oxford) (*84*), Central Asia (n=1) (*85*) (table S1B), 38 modern domestic cats from China (provided by School of Life Sciences, Peking University) are analyzed jointly in this research. A VCF files containing a total of 43 ancient and modern *Felis* samples (provided by School of Archaeology, University of Oxford and School of Life Sciences, Peking University) (*84*, *86*) were also jointly analyzed with new ancient Chinese samples. The VCF file includes modern Chinese domestic cats (n=5), modern East Asia domestic cats (n=2), ancient Central Aisa domestic cat (n=1), modern Levantine African wildcats (*F. lybica*) (n=3), ancient or

historical western Eurasia domestic cats (n=15), modern western Eurasia domestic cats (n=3), ancient European wildcats (*F. silvestris*) (n=3), modern European wildcats (n=4), modern Asiatic wildcats (*F. ornata*) (n=4), modern Chinese mountain cats (*F. bieti*) (n=5) , and modern Sand cats (*F. margarita*) (n=2) (table S1C).

In addition to *Felis* species, modern mitochondrial genomes of 18 leopard cats (*P. bengalensis*) from the Russian Far East (RFE, n=3), Indochina (n=6), Malay (n=6) and Sundaland (n=3) and a fishing cat (*P. viverrinus*) were jointly analyzed with ancient leopard cats. Together with 3 nuclear genomes of ancient Chinese leopard cats, modern nuclear genomes of 15 leopard cats from RFE (n=2), Indochina (n=6), Malay Peninsula (n=4), Sundaland (n=3). Together with this dataset one fishing cat and two domestic cats are also combined and analyzed with the ancient leopard cats from China. All leopard cats and fishing cat data were originally generated and provided by School of Life Sciences, Peking University.

Radiocarbon dating

Six samples were submitted for accelerator mass spectrometry (AMS) dating. Three samples (FS16, FS17, and FS19) were dated at *Beta Analytic* in the United States and the remaining samples (FS12, FS13, and FS24) were processed at the School of Archaeology, Peking University, China. All radiocarbon dates reported were calibrated using the INTCAL20 calibration curve (*87*).

Ancient DNA laboratory procedures

DNA extraction was performed in the dedicated ancient DNA laboratory at the School of Life Sciences, Peking University. All sterilized centrifuge tubes and other plastic consumables used in the following procedures were sterilized using a UV crosslinker with high-intensity UV radiation for 15 minutes. In this study, we utilized the Dabney method for ancient sample DNA extraction and optimized it further.

Sample preparation
Bone samples, weighing between 100 - 250 mg, were prepared using a Dremel multi-tool drill. The bone surface was carefully removed with a circular cutting disk to eliminate any exogenous DNA. To minimize the risk of cross-contamination, the drill was cleaned with a 10% bleach solution, and the spindle and disposable disk were replaced after processing each sample. The benchtop was also cleaned with 10% bleach and 75% ethanol between each sample, and gloves were changed frequently. Negative controls were employed as blanks for each batch of tested samples at every stage of the laboratory procedures, from extraction to capture. The bones were pulverized using a hammer. Any equipment that had come in contact with the samples was thoroughly cleaned between sample processing using 10% bleach and 75% ethanol.

DNA Extraction
All samples were processed using Dabney method (*88*) with slight modification by adding a pre-treatment step . Initially, samples were pre-treated to remove external DNA contamination, which included pre-digestion (*89*). For this step, 1 mL of pre-digestion

premix containing EDTA and proteinase K (see Table A.1) was added to the sample tube. The sample tube was then placed in a four-dimensional rotary mixer located inside a constant temperature oven and incubated at 37°C for 10 minutes with rotation; this was followed by centrifugation at 12,000 rpm for 1 minute and subsequent removal of the supernatant.

Following pre-treatment, samples underwent extended digestion using a digestion premix containing EDTA and proteinase K to release internal DNA. DNA extraction was then completed using the MinElute PCR Purification Kit according to the manufacturer's instructions. The specific steps were as follows: 4 mL of digestion premix was added to the 5 mL centrifuge tube containing the pre-treated sample, and the sample was incubated overnight at 55°C with rotation (16 - 24 hours). The next day, MinElute spin columns, sterile plastic funnels, and 50 mL sterile centrifuge tubes were assembled. 10 times the volume of the digestion fluid of weakly acidic PB buffer was added to another batch of 5 mL sterile centrifuge tubes. The tube containing the digestion fluid was centrifuged at 12,000 rpm for 1 minute, and the supernatant was transferred to a 50 mL centrifuge tube and thoroughly mixed with the binding buffer. The mixture of digestion fluid and binding buffer was then transferred in batches to the assembly tube using a sterile 5 mL pipette and centrifuged at 400 g at 4°C until the mixture had completely passed through the MinElute spin column. After the transfer was complete, the MinElute spin column was removed from the assembly tube and placed in a collection tube and centrifuged at 12,000 rpm at 4°C for 1 minute. Then 700 μL of PE buffer was added to the MinElute spin column, centrifuged at 8,000 g for 1 minute, and the waste liquid was discarded. This step was repeated once. A dry spin at 12,000 rpm for 1 minute was performed; the MinElute spin column was then transferred to a 1.5 mL DNA LoBind tube, 50 μL of EB buffer was added to the filter membrane of the MinElute spin column and incubated at 37°C for 10 minutes. The eluate was collected by centrifuging at 12,000 rpm for 1 minute, the MinElute spin column was discarded, and the DNA extract was stored at 4°C.

Library construction

This study employed the Blunt-End Single-Tube double-stranded library building method (BEST protocol) (*90*). The BEST protocol involves three main steps: end repair, adaptor ligation, and fill-in. First, 16 μL of DNA extract is added to a 0.2 mL PCR tube and diluted with 16 μL of EB buffer. Then, 8 μL of end repair premix is added, mixed thoroughly, and subjected to a PCR program of 30 minutes at 20 °C followed by 30 minutes at 65°C. For adaptor ligation, the appropriate concentration and volume of adaptor for each sample is calculated based on the concentration of the DNA eluate, with volumes not exceeding 2 μL; if less is needed, EB buffer is used to make up the volume. Then, 8 μL of ligation enzyme premix is added, mixed thoroughly, and subjected to a PCR program of 30 minutes at 20°C followed by 10 minutes at 65°C. For the fill-in step, 10 μL of fill-in premix is added and the mixture is incubated in a PCR machine for 15 minutes at 65°C followed by 15 minutes at 80°C. The DNA is then purified according to the SPRI bead protocol, eluted in 34 μL of EB buffer, and collected in a 1.5 mL DNA LoBind tube, stored at 4°C.

qPCR

For quantification and amplification of the DNA library, 1 μL of DNA library liquid and 19 μL of qPCR premix are taken in a new 0.2 mL PCR tube and subjected to a qPCR program. Based on the qPCR amplification curve, suitable indexing PCR cycle numbers are selected for each sample; 15 μL of DNA library liquid and 35 μL of Indexing PCR premix are mixed and subjected to the Indexing PCR program. The amplified DNA library is purified using SPRI beads, eluted in 40 μL of EB buffer, and collected in a 1.5 mL DNA LoBind tube. The concentration of the amplified DNA library liquid is determined using the Qubit 4.0 fluorometer as per the manufacturer's instructions.

Library amplification

Libraries was subsequently amplified and externally indexed (*91*)using standard Illumina P5 and P7 primers with double indexes in a 50 μL PCR reaction, consisting of 15 μL of library, 25 μL Gold Taq 360 Master Mix, 5 μL Reaction Enhancer, 3 μL H_2O, 1 μL of P5 primer, and 1 μL of P7 primer (10nM). Thermocycling conditions included an initial denaturation step of 2 minutes at 95°C, followed by cycles of 15 seconds denaturation at 95°C, 30 seconds annealing at 60°C, and 30 seconds extension at 72°C for the specified number of cycles for each sample. A final extension step of 7 minutes at 72°C was conducted. The amplified libraries were purified using SPRI beads (*Beckman Coulter*), and quality control was performed on a Fragment Analyzer (*Spectro Scientific*) prior to sequencing.

Sample screening

All samples underwent screening sequencing on *NovaSeq* 6000 instrument (*92*) at Novogene, China. Approximately 3 Gb of raw data were obtained for each sample. Following the screening sequencing, the ratio of nucleotides mapped to the domestic cat whole nuclear reference genome (Felis_catus_9.0 GCA_000181335.4) (endogenous DNA) and the number of reads mapped to the mitochondrial genome (NC_001700.1) were calculated. For leopard cat samples we estimated endogenous DNA content by calculating the ratio of nucleotides that mapped to the leopard cat reference genome (Genome assembly Fcat_Pben_1.1_paternal_pri GCF_016509475.1) or the number of reads mapped to the leopard cat reference mitochondrial genome (NC_028301.1). We then determined further sequencing strategies based on these results.

Whole genome resequencing

Samples representing the spatial and temporal contexts or possessing more than 10% endogenous DNA in screening were selected for deeper sequencing. In total, four domestic cats (FS1, FS2, FS12, FS21) and three leopard cats (FS8, FS15, FS19) are deep sequenced. All samples were sequenced on a *NovaSeq* 6000 instrument at Novogene, Beijing. We obtained approximately 100 Gb of data each for FS1, FS2, FS12, and FS22. FS8, FS15, FS19 are processed in a whole lane. To reveal the phenotypic information of FS12, the most ancient domestic cats so far found in China, we further sequenced this sample in a single lane of *NovaSeq* 6000 instrument at Novogene, Beijing, and obtained an additional approximately 900 Gb data.

Mitochondrial genome sequencing
An additional 4 Gb of sequencing data were obtained to acquire full mitochondrial genomes for samples that did not qualify for whole nuclear genome sequencing but had more than 2,000 reads mapped to the mitochondrial reference genome (NC_001700.1). Samples FS3, FS4, FS5, and FS17 were processed using this strategy and were sequenced on an Illumina *NovaSeq* 6000 instrument at Novogene, China.

Ancient mitochondrial DNA capture sequencing
In-solution targeted capture of the cat mitochondrial genome was conducted on 14 domestic cat samples (FS6, FS7 FS8, FS10, FS13, FS14, FS15, FS16, FS17, FS18, FS19, FS20, FS21, FS22, FS23) using the *myBaits* (*Arbor Biosciences*) Hybridization Capture for Targeted Next-Generation Sequencing protocol (*93*), with a hybridization temperature of 55°C and a hybridization time of 48 hours.

The domestic cat mitochondrial reference genome (NC_001700.1) was employed to synthesize baits for capture. Due to the degraded nature of ancient DNA (*94*, *95*), the amount of endogenous DNA per sample is considerably lower than that of modern samples, resulting in the potential for probes in a single capture reaction to be significantly overwhelmed for each sample. To achieve optimal cost-effectiveness, more than one sample was pooled per reaction. Consequently, three reactions, each containing 2-3 ancient libraries pooled equimolarly, were prepared. The libraries combined in a single pool had distinct indexes. The three reactions were then sequenced on an Illumina *NovaSeq* 6000 instrument at Novogene, China.

Genomic data processing

Raw data processing

Raw sequencing data were processed by trimming adapters with default setting and merges completely overlapping paired-end reads into a single sequence (--collapse) using AdapterRemoval v2.3.0 (*96*). Subsequently, Cutadapt v3.5 (*97*) was employed to remove 5 bases from both the 5' and 3' ends (-u 5 -u -5) of the reads to minimize the impact of deamination (*94*, *95*). The same software was also utilized to trim low-quality reads shorter than 25 bp (--minimum-length 25) and containing over 10% Ns (--max-n 0.1).

Mitochondrial genome data mapping and filtering

Leopard cats. The filtered data of leopard cats were mapped to the leopard cat mitochondrial reference genome (NC_028301.1) using the “aln” function in BWA v0.1.17 (*98*) with specifying the maximum allowed mismatch ratio to be 0.01(-n 0.01), allowing for up to two gap openings (insertions or deletions) in a read (-o 2), and a seed length to be 1024 (-l 1024). SAMtools v.1.14 (*99*) were used to sort the bam files with “sort” function, and to filter out PCR duplicates by “markdup” function with a parameter “-r” added. Unmapped reads and reads with a mapping quality less than 30 were removed by the parameters “-F 4”, and “-q 30” of the “view” function in SAMtools.

Domestic cats. The filtered data of domestic cats were then mapped to the leopard cat mitochondrial reference genome (NC_001700.1) using the "aln" function in BWA v0.1.17 (H. Li, 2013) with specifying the maximum allowed mismatch ratio to be 0.01(-n 0.01), allowing for up to two gap openings (insertions or deletions) in a read (-o 2), and a seed length to be 1024 (-l 1024). SAMtools v.1.14 (*99*) were used to sort the bam files with "sort" function, and to filter out PCR duplicates by "markdup" function with a parameter "-r" added. Unmapped reads and reads with a mapping quality less than 30 were removed by the parameters "-F 4", and "-q 30" of the "view" function in SAMtools.

HTSbox (https://github.com/lh3/htsbox) was used to call consensus mitochondrial sequences with the default settings. Control regions of the consensus sequences were then excluded manually, and the remaining sequences were then aligned to each other using MUSCLE v.5 (*100*) with default setting.

Nuclear genome data mapping

Leopard cat. The filtered data of leopard cats was then mapped to the leopard cat whole nuclear reference genome (Genome assembly Fcat_Pben_1.1_paternal_pri GCF_016509475.1) using the "aln" function in BWA v0.1.17 (*98*) with specifying the maximum allowed mismatch ratio to be 0.01(-n 0.01), allowing for up to two gap openings (insertions or deletions) in a read (-o 2), and a seed length to be 1024 (-l 1024). SAMtools v.1.14 (*99*) were used to sort the bam files with "sort" function, and to filter out PCR duplicates by "markdup" function with a parameter "-r" added. Unmapped reads and the reads with a mapping quality less than 30 were removed by the parameters "-F 4", and "-q 30" of the "view" function in SAMtools.

Domestic cat. Filtered data of domestic cats were mapped to the domestic cat nuclear reference genomes (Felis_catus_9.0 GCA_000181335.4) using the "aln" function in BWA v0.1.17 (*98*) with specifying the maximum allowed mismatch ratio to be 0.01(-n 0.01), allowing for up to two gap openings (insertions or deletions) in a read (-o 2), and a seed length to be 1024 (-l 1024). SAMtools v.1.14 (*99*) were used to sort the bam files with "sort" function, and to filter out PCR duplicates by "markdup" function with a parameter "-r" added. Unmapped reads and the reads with a mapping quality less than 30 were removed by the parameters "-F 4", and "-q 30" of the "view" function in SAMtools.

Validation of ancient data

To evaluate the authenticity of the ancient DNA samples, we employed the mapDamage v2.0 (*101*, *102*). During the initial processing of our data, we trim the first and last 5 base pairs (bp) from each read to avoid the effects of deamination. However, this practice contradicts the principle behind using mapDamage (*101*, *102*), which is designed to show signals of ancient DNA damage. Therefore, for each sample, we also prepare a version with the ends untrimmed, and we use this version for analysis with mapDamage. The mapDamage analysis revealed clear and distinct signals of deamination on the 5' and 3' ends of all 22 ancient Chinese samples. The observed C-to-T or A-to-G misincorporations were consistent with known patterns of ancient DNA damage,

providing strong evidence for the authenticity of the ancient DNA in these samples (Fig. S1).

SNP variant calling

Leopard cat. The genomic data of three ancient leopard cats, 15 modern leopard cats from Russian Far East (n=2), Indochina (n=6), Malay (n=4), and Sundaland (n=3), and one fishing cat, in addition to two domestic cats as outgroup, were used to generate SNPs. The SNPs were identified using GATK v.4.2 (*103–105*). Subsequently, the variants were filtered. Bcftools v 1.15.1 (*99*) "filter" was used to filter out all transition-type single nucleotide variants, retaining only transversion-type single nucleotide variants to avoid analytical errors caused by cytosine deamination. The variant sites were further filtered using Plink v1.90b6.26 software (*106*), including keeping biallelic SNPs only (--biallelic-only) setting a minimum allele frequency with '--maf 0.01', a missing genotype rate with '--geno 0.2', and filtering for linkage disequilibrium (LD) by pruning with a window of 10kb, step of 2 SNPs, and an R^2 threshold of 0.5 with '--indep-pairwise 10K 2 0.5'. Only the autosomal were kept for downstream analysis. After filtering, we obtained the SNP dataset covering 18 autosomes of leopard cats. Through all these steps, a total of 20,436,894 SNPs were called and used for downstream analysis.

Domestic cat. SNPs of 4 ancient Chinese domestic cats were called with GATK v.4.2 (*103–105*). Subsequently, the variants were filtered following the methods as described in Jamieson et al 2023. Specifically, BEDtools v.2.30.0 (*107*) was employed to exclude all non-neutral loci. Bcftools v 1.15.1 (*99*) "filter" was used to filter out all transition-type single nucleotide variants, retaining only transversion-type single nucleotide variants to avoid analytical errors caused by cytosine deamination. The variant sites were further filtered using Plink software v1.90b6.26, including keeping biallelic SNPs only (--biallelic-only) setting a minimum allele frequency with '--maf 0.01', a missing genotype rate with '--geno 0.2', and filtering for linkage disequilibrium (LD) by pruning with a window of 10kb, step of 2 SNPs, and an R^2 threshold of 0.5 with '--indep-pairwise 10K 2 0.5'. After filtering, we obtained the SNP dataset covering 825,403 SNPs in 18 autosomes of domestic cats.

VCF files containing a total of 43 ancient and modern *Felis* samples (*84*, *86*) was then merged with our ancient data. We eventually get a VCF file containing ancient Chinese domestic cats (n=4) modern Chinese domestic cats (n=5), modern East Asia domestic cats (n=2), ancient Central Aisa domestic cat (n=1), modern Levantine African wildcats (*F. lybica*) (n=3), ancient or historical Western Eurasian domestic cats (n=15), modern western Eurasia domestic cats (n=3), ancient European wildcats (*F. silvestris*) (n=3), modern European wildcats (n=4), modern Asiatic wildcats (*F. ornata*) (n=4), modern Chinese mountain cats (*F. bieti*) (n=5), modern sand cats (*F. margarita*) (n=2). Through these steps, a total of 825,403SNPs were generated for downstream analysis.

Species identification through phylogenetic clustering

A maximum likelihood phylogenetic tree (ML) was performed using IQ-tree v2.3.6 (*108*, *109*) to identify the species of the samples. This analysis included all 22 ancient samples,

and modern mitochondrial genomes of domestic cats, wild cats, and leopard cats, with the tiger (NC_010642.1) chosen as the outgroup. We implemented the Tamura-Nei 93 (TN93) nucleotide substitution model (*110*), incorporating both a gamma distribution (G) and a proportion of invariant sites (I) (-m TN93+I+G) following previously published procedure (*86*). The bootstrap replicates were set to be 1,000 (-B 1000). The trees were visualized using FigTree v1.4.4 (http://tree.bio.ed.ac.uk/software/figtree/) and iTOL v5 an online tool for tree visualization (*111*, *112*).

Population genetic and phylogenetic analyses of leopard cats

A Maximum likelihood phylogenetic tree was constructed using IQ-tree v2.3.6 (*108*, *109*). The tree included 7 ancient samples and 20 modern leopard cats, comprising four individuals from Russian Far East, 6 individuals from Indochina, 4 individuals from Sundaland, and 6 from Malay. In addition to leopard cats, 2 fishing cats, and a flat-headed () cat were used for comparison. A tiger (NC_010642.1) was used as outgroup. The tree construction using TN93+I+G model (-m TN93+I+G) with 1000 bootstrap replicates (-B 1000). The trees were visualized using FigTree v1.4.4 (http://tree.bio.ed.ac.uk/software/figtree/).

For whole-genome data, we used the vcf2aln software (*113*) to convert the VCF format variation information files of ancient and modern samples into aligned FASTA sequence files to fit the requirement of input file format of IQ-tree v2.3.6 software (*108*, *109*). We set the parameter "-s" to ignore missing site information and "-O" to print only one haplotype for diploid data. A ML (maximum likelihood) phylogenetic tree was constructed based on the 20 million SNPs with IQ-tree. The bootstrap was set to 200 replicates (-B 200). The best model was automatically found by the IQ-tree software by adding “-m MF” A total of 3 ancient leopard cats, 18 samples, including 2 Chinese domestic cats and 15 modern leopard cats from Russian Far East (n=2), Indochina (n=6), Malay (n=4), Sundaland (n=3), and a fishing cat were included in the analysis. Domestic cat was used as outgroup. The trees were visualized using FigTree v1.4.4 (http://tree.bio.ed.ac.uk/software/figtree/).

Principal component analysis (PCA) was performed using SmartPCA v16000 in EIGANSTRAT v7.2.1 (*114*, *115*) with a total of 18 samples, including 3 ancient Chinese leopard cats and 15 modern leopard cats from Russian Far East (n=2), Indochina (n=6), Malay (n=4), and Sundaland (n=3), along with a fishing cat. Due to the large amount of missing data in ancient samples that could impact PCA results, the PCA was first constructed using high-quality modern data. The ancient leopard cats were then projected onto it by applying the "LsqProject: Yes" function.

ADMIXTURE analysis was performed using ADMIXTURE 1.3.0 (*116*) on over 20 million SNPs derived from a total of 18 samples, which included 3 ancient Chinese leopard cats, 12 modern leopard cats from Russian Far East (n=2), Indochina (n=6), Malay (n=4), Sundaland (n=3), and a fishing cat. We performed the analysis with K value from 1 to 8. Three duplications (CV=3) for each K value. The convergence threshold was set to 0.0001 (-c 0.0001). The results were visualized using an R script.

Outgroup f_3-statistics were conducted through the qp3Pop method in EIGENSTRAT v7.2.1 (*115*, *117*) to test the gene flow between Indochina population and ancient leopard cats from China. Over 20 million SNPs from a total of 20 samples, including 3 ancient Chinese leopard cats, 15 modern leopard cats from Russian Far East (n=2), Indochina (n=6), Malay (n=4), and Sundaland (n=3), a fishing cat, and two domestic cats, were used. Domestic cat was used as the outgroup.

D-statistics analysis was conducted using *qpDstat* method in EIGENSTRAT v7.2.1 (*115*, *117*). The same dataset as the outgroup f_3-statistics was used. The population combinations were set as *D* (Outgroup, P.bengal_X, Russian Far East, ancient China) mainly to test the potential gene flow between the leopard cats in ancient China and Indochina . Domesttic cats were used as the outgroup. Leopard cats from Indochina, Malay and Sundaland are then individually placed in P.bengle_X.

Population genetic and phylogenetic analyses of domestic cats

Maximum Likelihood (ML) phylogenetic analysis of whole mitochondrial genomes was used 14 ancient Chinese domestic cats, 42 ancient or historical domestic cats from western Eurasia, 1 ancient Domestic cat from central Asia, 50 modern domestic cats from China, 2 modern domestic cats from Central Asia, 3 modern African wildcats from the Levant, and 1 modern domestic cat from Western Eurasia. The phylogenetic analysis was performed using IQ-tree v2.3.6 software (*108*, *109*), implementing TN93+I+G model (-m TN93+I+G) with 1,000 replicates (-B 1000). The trees were visualized using FigTree v1.4.4 (http://tree.bio.ed.ac.uk/software/figtree/). Phylogeographical assignment of mtDNA haplotype is conducted as previously described (*84*, *118*).

Using 825,403 SNPS, PCA were performed with SmartPCA in EIGENSTRAT v7.2.1 (*114*, *115*). To elucidate high-resolution geographic patterns among different domestic cat populations; therefore, European wildcats, Asiatic wild cats and Chinese mountain cats were excluded from the analysis. As African wild cats are the progenitors of domestic cats, they were retained. In total, 4 ancient Chinese domestic cats, 5 modern Chinese domestic cats, 2 modern East Asia domestic cats, 1 ancient Central Asia domestic cat, 3 modern Levantine African wildcats, 15 ancient or historical Western Eurasia domestic cats, 3 modern western Eurasia domestic cats were included in this analysis. Since ancient samples may contain a considerable amount of missing data, potentially impacting PCA results, the "LsqProject: Yes" function was adopted to project all ancient data onto the PCA initially defined by high-quality modern data. The results were visualized with a R

ADMIXTURE analysis employed 825,403 SNPS. The assay was conducted using ADMIXTURE 1.3.0 (*116*). We performed the analysis with K value from 2 to 7. Three duplications (CV=3) for each K value and selected K = 6 based on the cross-validation (CV) error. The convergence threshold was set to 0.0001 (-c 0.0001). The results were visualized using an R script. This analysis has included 4 ancient Chinese domestic cats, 5 modern Chinese domestic cats, 2 modern East Asia domestic cats, 1 ancient Central

Aisa domestic cat, 3 modern Levantine African wildcats, 15 ancient or historical Western Eurasia domestic cats, 3 modern western Eurasia domestic cats, 3 ancient European wildcats, 4 modern European wildcats, 4 modern Asiatic wildcats, 5 modern Chinese mountain cats, and 2 modern Sand cats. The results were visualized with a R

Outgroup f_3-statistics in EIGENSTRAT v7.2.1(*115*, *117*) was utilized to inform the genetic affinity among different populations of domestic cats. Sand cat (*F. margarita*) was selected as the outgroup.

Subsequently, qp*D*stat in EIGENSTRAT v7.2.1 (*115*, *117*) was employed to further explore potential admixtures between ancient Chinese individuals and Asiatic wildcats or Chinese mountain cats (*D*(Outgroup, , ancient European domestic cat, ancient Chinese domestic cat)), where sand cat was used as outgroup. This analysis has included 4 ancient Chinese domestic cats, 5 modern Chinese domestic cats, 2 modern East Asia domestic cats, 1 ancient Central Asia domestic cat, 3 modern Levantine African wildcats, 15 ancient or historical Western Eurasia domestic cats, 3 modern western Eurasia domestic cats, 3 ancient European wildcats, 4 modern European wildcats, 4 modern Asiatic wildcats, 5 modern Chinese mountain cats, and 2 modern Sand cats.

Phenotypic inference of the earliest domestic cat of China

Whole genome sequencing of FS12 for a 16x genome coverage was obtained and mapped to the domestic cat nuclear reference genome (Felis_catus_9.0 GCA_000181335.4) and filtered using the same methods as mentioned above using BWA v0.1.17 (*98*) and SAMtools v.1.14 (*99*). The resulted BAM file for FS12 is then used for downstream analysis for phenotypic inference.

In determining the sex of the specimen FS12, we ascertained the sequencing depths of its X chromosome and autosomes using SAMtools v.1.14 (*99*), followed by calculating the ratio of sequencing depth between the two. A ratio near 1 suggests a female individual, whereas a ratio approximating 0.5 indicates a male.

We procured the reference sets for phenotype-related variants of domestic cats from the database *Online Mendelian Inheritance in Animals* (OMIA) (*119*) (https://omia.org/home/). Incorporated within these variants are 61 single nucleotide polymorphisms (SNPs) and 31 deletions or insertions (Indels), associated with thirteen coat colors, five coat forms, three pigmentation patterns, two tail type variations, and 37 genetic diseases (Table S7). Next, from the generated alignment files, we extracted the specific genomic locus related to a particular phenotype, as well as the 200bp regions before and after this locus, using SAMtools v.1.14 (*99*) with the command "view -h -b". Afterwards, we used BCFtools v 1.15.1 (*99*) with the command "mpileup -B -C50 -q 30 -Q 30" to obtain high-quality genotype data for the corresponding regions. Only loci with a sequencing depth greater than 10x were considered reliable.

With respect to mutations in the *KIT* gene responsible for white pigmentation (*9*) given that the domestic cat reference genome (Felis_catus_9.0 GCA_000181335.4) lacks the

retroviral (*FERV1*) insertion, aligning FS12 to this reference posed a challenge in discerning its genuine genotype. To solve the problem, we manually constructed an reference genome, integrating the retroviral (*FERV1*) fragment into the domestic cat's *KIT* gene (refer to KIT_FERV1_10K). The raw data of FS12 was subsequently aligned to the KIT_FERV1_10K with the same methods as mentioned above using BWA. The outcome is then visualized using IGV v2.16.2. For comparative purposes, we also sourced individuals exhibiting homozygosity, heterozygosity for the *KIT* white-related mutation, and wildtype individuals. Using BWA v0.1.17 mem (*120*) and SAMtools v1.14 (*99*), these specimens were aligned against KIT_FERV1_10K. The results are visualized with the same method as FS12. The alignment pattern of FS12 is then compared to the wildtype, homozygosity and heterozygosity individuals to determine the genotype of its own.

Assembly and analysis of cat images in ancient artwork from China

Artwork from a certain historical period may to some extent reflect the aesthetic view and preference from contemporaneous society. We examined the coat color of domestic cats displayed in ancient paintings from China to evaluate the anthropogenic preference of specific cat's coat color, with a particular focus on the white cat.
Historical paintings were assembled from published archaeological reports and the digital repository Artlib (http://www.artlib.cn). The dataset includes 91 domestic cats from 33 pieces of paintings, covering a historical period from the Tang Dynasty to modern time (827 - 1933 CE). Coat color of the cats was discerned through visual assessment. A primary focus was to discern cats with black and white color and to calculate the proportion of cats bearing these specific coat color.

Supplementary References

1. P. W. Bateman, P. A. Fleming, Big city life: carnivores in urban environments. *Journal of Zoology* **287**, 1–23 (2012). doi: 10.1111/j.1469-7998.2011.00887.x
2. T.-Y. Choi, H.-S. Kwon, D.-G. Woo, C.-H. Park, Habitat selection and management of the leopard cat (*Prionailurus bengalensis*) in a rural area of Korea. *Korean Journal of Environment and Ecology* **26**, 322–332 (2012). doi: 10.3390/su7044668
3. W. Shehzad, T. Riaz, M. A. Nawaz, C. Miquel, C. Poillot, S. A. Shah, F. Pompanon, E. Coissac, P. Taberlet, Carnivore diet analysis based on next-generation sequencing: Application to the leopard cat (*Prionailurus bengalensis*) in Pakistan. *Molecular Ecology* **21**, 1951–1965 (2012). doi: 10.1111/j.1365-294X.2011.05424.x; Pmid: 22250784
4. S.-J. Luo, The hidden Olympic spectator. *Science* **373**, 404–404 (2021). doi: 10.1126/science.abl3669; Pmid: 34437113
5. S.-J. Luo, Y. Zhang, W. E. Johnson, L. Miao, P. Martelli, A. Antunes, J. L. Smith, S. J. O'Brien, Sympatric Asian felid phylogeography reveals a major Indochinese–Sundalandic divergence. *Molecular ecology* **23**, 2072–2092 (2014). doi: 10.1111/mec.12716; Pmid: 24629132

6. Y. Hu, S. Hu, W. Wang, X. Wu, F. B. Marshall, X. Chen, L. Hou, C. Wang, Earliest evidence for commensal processes of cat domestication. *Proceedings of the National Academy of Sciences* **111**, 116–120 (2014). doi: 10.1073/pnas.1311439110; Pmid: 24344279
7. J.-D. Vigne, A. Evin, T. Cucchi, L. Dai, C. Yu, S. Hu, N. Soulages, W. Wang, Z. Sun, J. Gao, Earliest "domestic" cats in China identified as leopard cat (*Prionailurus bengalensis*). *PloS One* **11**, e0147295 (2016). doi: 10.1371/journal.pone.0147295; Pmid: 26799955
8. S. Zhu, Z. Chen, S. Hu, W. Wang, P. Cao, F. Liu, Q. Dai, X. Feng, R. Yang, W. Ping, Ancient DNA traces a Chinese 5400-year-old cat specimen as leopard cat (Prionailurus bengalensis). *Journal of Genetics and Genomics*, S1673-8527 (2022). doi: 10.1016/j.jgg.2022.07.005; Pmid: 35921988
9. V. A. David, M. Menotti-Raymond, A. C. Wallace, M. Roelke, J. Kehler, R. Leighty, E. Eizirik, S. S. Hannah, G. Nelson, A. A. Schäffer, Endogenous retrovirus insertion in the KIT oncogene determines white and white spotting in domestic cats. *G3: Genes, Genomes, Genetics* **4**, 1881–1891 (2014). doi: 10.1534/g3.114.013425; Pmid: 25085922
10. E. Eizirik, N. Yuhki, W. E. Johnson, M. Menotti-Raymond, S. S. Hannah, S. J. O'Brien, Molecular genetics and evolution of melanism in the cat family. *Curr Biol* **13**, 448–453 (2003). doi: 10.1016/s0960-9822(03)00128-3; Pmid: 12620197
11. M. Peterschmitt, F. Grain, B. Arnaud, G. Deléage, V. Lambert, Mutation in the *melanocortin 1 receptor* is associated with amber colour in the Norwegian Forest Cat. *Anim Genet* **40**, 547–552 (2009). doi: 10.1111/j.1365-2052.2009.01864.x; Pmid: 19422360
12. N. A. Gustafson, B. Gandolfi, L. A. Lyons, Not another type of potato: *MC1R* and the russet coloration of Burmese cats. *Anim Genet* **48**, 116–120 (2017). doi: 10.1111/age.12505; Pmid: 27671997
13. M. Abitbol, V. Gache, Copal, a new *MC1R* allele in the domestic cat. *Anim Genet* **50**, 553–554 (2019). doi: 10.1111/age.12829; Pmid: 31361350
14. L. A. Lyons, D. L. Imes, H. C. Rah, R. A. Grahn, Tyrosinase mutations associated with Siamese and Burmese patterns in the domestic cat (*Felis catus*). *Anim Genet* **36**, 119–126 (2005). doi: 10.1111/j.1365-2052.2005.01253.x; Pmid: 15771720
15. D. L. Imes, L. A. Geary, R. A. Grahn, L. A. Lyons, Albinism in the domestic cat (Felis catus) is associated with a tyrosinase (*TYR*) mutation. *Anim Genet* **37**, 175–178 (2006). doi: 10.1111/j.1365-2052.2005.01409.x; Pmid: 16573534
16. M. Abitbol, P. Bossé, B. Grimard, L. Martignat, L. Tiret, Allelic heterogeneity of albinism in the domestic cat. *Anim Genet* **48**, 127–128 (2017). doi: 10.1111/age.12503; Pmid: 27634063
17. Y. Yu, R. A. Grahn, L. A. Lyons, Mocha tyrosinase variant: a new flavour of cat coat coloration. *Anim Genet* **50**, 182–186 (2019). doi: 10.1111/age.12765; Pmid: 30716167
18. Y. Ishida, V. A. David, E. Eizirik, A. A. Schäffer, B. A. Neelam, M. E. Roelke, S. S. Hannah, S. J. O'Brien, M. Menotti-Raymond, A homozygous single-base deletion in *MLPH* causes the dilute coat color phenotype in the domestic cat. *Genomics* **88**, 698–705 (2006). doi: 10.1016/j.ygeno.2006.06.006; Pmid: 16860533

19. C. B. Kaelin, X. Xu, L. Z. Hong, V. A. David, K. A. McGowan, A. Schmidt-Küntzel, M. E. Roelke, J. Pino, J. Pontius, G. M. Cooper, H. Manuel, W. F. Swanson, L. Marker, C. K. Harper, A. van Dyk, B. Yue, J. C. Mullikin, W. C. Warren, E. Eizirik, L. Kos, S. J. O'Brien, G. S. Barsh, M. Menotti-Raymond, Specifying and sustaining pigmentation patterns in domestic and wild cats. *Science* **337**, 1536–1541 (2012). doi: 10.1126/science.1220893; Pmid: 22997338
20. L. A. Lyons, R. M. Buckley, R. J. Harvey, 99 Lives Cat Genome Consortium, Mining the 99 Lives Cat Genome Sequencing Consortium database implicates genes and variants for the Ticked locus in domestic cats (*Felis catus*). *Anim Genet* **52**, 321–332 (2021). doi: 10.1111/age.13059; Pmid: 33780570
21. C. Drögemüller, S. Rüfenacht, B. Wichert, T. Leeb, Mutations within the *FGF5* gene are associated with hair length in cats. *Anim Genet* **38**, 218–221 (2007). doi: 10.1111/j.1365-2052.2007.01590.x; Pmid: 17433015
22. J. S. Kehler, V. A. David, A. A. Schäffer, K. Bajema, E. Eizirik, D. K. Ryugo, S. S. Hannah, S. J. O'Brien, M. Menotti-Raymond, Four independent mutations in the feline *fibroblast growth factor 5* gene determine the long-haired phenotype in domestic cats. *J Hered* **98**, 555–566 (2007). doi: 10.1093/jhered/esm072; Pmid: 17767004
23. G. D. Shaffer, B. C. Ballif, K. Meurs, L. G. Shaffer, H. Flores-Smith, Identification of a novel missense mutation in the *fibroblast growth factor 5* gene associated with longhair in the Maine Coon Cat. *Hum Genet* **140**, 1517–1523 (2021). doi: 10.1007/s00439-021-02373-1; Pmid: 34599367
24. R. M. Buckley, B. Gandolfi, E. K. Creighton, C. A. Pyne, D. M. Bouhan, M. L. LeRoy, D. A. Senter, J. R. Gobble, M. Abitbol, L. A. Lyons, 99 Lives Consortium, Werewolf, There Wolf: Variants in Hairless Associated with Hypotrichia and Roaning in the Lykoi Cat Breed. *Genes (Basel)* **11**, 682 (2020). doi: 10.3390/genes11060682; Pmid: 32580512
25. B. Gandolfi, C. A. Outerbridge, L. G. Beresford, J. A. Myers, M. Pimentel, H. Alhaddad, J. C. Grahn, R. A. Grahn, L. A. Lyons, The naked truth: Sphynx and Devon Rex cat breed mutations in *KRT71*. *Mamm Genome* **21**, 509–515 (2010). doi: 10.1007/s00335-010-9290-6; Pmid: 20953787
26. B. Gandolfi, H. Alhaddad, V. K. Affolter, J. Brockman, J. Haggstrom, S. E. K. Joslin, A. L. Koehne, J. C. Mullikin, C. A. Outerbridge, W. C. Warren, L. A. Lyons, To the Root of the Curl: A Signature of a Recent Selective Sweep Identifies a Mutation that Defines the Cornish Rex Cat Breed. *PLoS One* **8**, e67105 (2013). doi: 10.1371/journal.pone.0067105; Pmid: 23826204
27. A. D. Manakhov, T. V. Andreeva, E. I. Rogaev, The curly coat phenotype of the Ural Rex feline breed is associated with a mutation in the lipase *H* gene. *Anim Genet* **51**, 584–589 (2020). doi: 10.1111/age.12958; Pmid: 32463158
28. K. J. Buckingham, M. J. McMillin, M. M. Brassil, K. M. Shively, K. M. Magnaye, A. Cortes, A. S. Weinmann, L. A. Lyons, M. J. Bamshad, Multiple mutant *T* alleles cause haploinsufficiency of Brachyury and short tails in Manx cats. *Mamm Genome* **24**, 400–408 (2013). doi: 10.1007/s00335-013-9471-1; Pmid: 23949773
29. X. X. Xu Xiao, S. X. Sun Xin, H. X. Hu XueSong, Z. Y. Zhuang Yan, L. Y. Liu YueChen, M. H. Meng Hao, M. L. Miao Lin, Y. H. Yu He, L. S. Luo ShuJin, Whole genome sequencing identifies a missense mutation in *HES7* associated with

short tails in Asian domestic cats. (2016). doi: 10.1038/srep31583; Pmid: 27560986
30. D. E. Bender, M. T. Kloos, J. U. Pontius, M. E. Hinsdale, D. A. Bellinger, Molecular characterization of cat *factor XII* gene and identification of a mutation causing *factor XII* deficiency in a domestic shorthair cat colony. *Vet Pathol* **52**, 312–320 (2015). doi: 10.1177/0300985814532821; Pmid: 24793828
31. H. Maruyama, H. Hosoe, K. Nagamatsu, R. Kano, H. Kamata, A novel missense mutation in the *factor XII* gene in a litter of cats with *factor XII* deficiency. *J Vet Med Sci* **79**, 822–826 (2017). doi: 10.1292/jvms.16-0602; Pmid: 28392508
32. K. M. Meurs, M. M. Norgard, M. M. Ederer, K. P. Hendrix, M. D. Kittleson, A substitution mutation in the myosin binding protein C gene in ragdoll hypertrophic cardiomyopathy. *Genomics* **90**, 261–264 (2007). doi: 10.1016/j.ygeno.2007.04.007; Pmid: 17521870
33. L. A. Lyons, D. S. Biller, C. A. Erdman, M. J. Lipinski, A. E. Young, B. A. Roe, B. Qin, R. A. Grahn, Feline polycystic kidney disease mutation identified in *PKD1*. *J Am Soc Nephrol* **15**, 2548–2555 (2004). doi: 10.1097/01.ASN.0000141776.38527.BB; Pmid: 15466259
34. F. Shitamori, A. Nonogaki, T. Motegi, Y. Matsumoto, M. Sakamoto, Y. Tanizawa, Y. Nakamura, T. Yonezawa, Y. Momoi, S. Maeda, Large-scale epidemiological study on feline autosomal dominant polycystic kidney disease and identification of novel *PKD1* gene variants. *J Feline Med Surg* **25**, 1098612X231185393 (2023). doi: 10.1177/1098612X231185393; Pmid: 37489504
35. A. C. Crawley, G. Yogalingam, V. J. Muller, J. J. Hopwood, Two mutations within a feline mucopolysaccharidosis type VI colony cause three different clinical phenotypes. *J Clin Invest* **101**, 109–119 (1998). doi: 10.1172/JCI935; Pmid: 9421472
36. G. Yogalingam, T. Litjens, J. Bielicki, A. C. Crawley, V. Muller, D. S. Anson, J. J. Hopwood, Feline mucopolysaccharidosis type VI. Characterization of recombinant N-acetylgalactosamine 4-sulfatase and identification of a mutation causing the disease. *J Biol Chem* **271**, 27259–27265 (1996). doi: 10.1074/jbc.271.44.27259; Pmid: 8910299
37. S. Clavero, Y. Ahuja, D. F. Bishop, B. Kwait, M. E. Haskins, U. Giger, R. J. Desnick, Diagnosis of feline acute intermittent porphyria presenting with erythrodontia requires molecular analyses. *Vet J* **198**, 720–722 (2013). doi: 10.1016/j.tvjl.2013.10.008; Pmid: 24239138
38. D. Aberdein, J. S. Munday, B. Gandolfi, K. E. Dittmer, R. Malik, D. J. Garrick, L. A. Lyons, 99 Lives Consortium, A FAS-ligand variant associated with autoimmune lymphoproliferative syndrome in cats. *Mamm Genome* **28**, 47–55 (2017). doi: 10.1007/s00335-016-9668-1; Pmid: 27770190
39. L. A. Lyons, E. K. Creighton, H. Alhaddad, H. C. Beale, R. A. Grahn, H. Rah, D. J. Maggs, C. R. Helps, B. Gandolfi, Whole genome sequencing in cats, identifies new models for blindness in *AIPL1* and somite segmentation in *HES7. BMC Genomics* **17**, 265 (2016). doi: 10.1186/s12864-016-2595-4; Pmid: 27030474
40. S. L. Owens, M. E. Downey, B. M. Pressler, A. J. Birkenheuer, D. W. Chandler, J. C. Scott-Moncrieff, Congenital adrenal hyperplasia associated with mutation in an

11β-hydroxylase-like gene in a cat. *J Vet Intern Med* **26**, 1221–1226 (2012). doi: 10.1111/j.1939-1676.2012.00971.x; Pmid: 22827537

41. S. Clavero, D. F. Bishop, U. Giger, M. E. Haskins, R. J. Desnick, Feline congenital erythropoietic porphyria: two homozygous *UROS* missense mutations cause the enzyme deficiency and porphyrin accumulation. *Mol Med* **16**, 381–388 (2010). doi: 10.2119/molmed.2010.00038; Pmid: 20485863
42. M. Abitbol, P. Bossé, A. Thomas, L. Tiret, A deletion in *FOXN1* is associated with a syndrome characterized by congenital hypotrichosis and short life expectancy in Birman cats. *PLoS One* **10**, e0120668 (2015). doi: 10.1371/journal.pone.0120668; Pmid: 25781316
43. K. Mizukami, K. Raj, U. Giger, Feline cystinuria caused by a missense mutation in the *SLC3A1* gene. *J Vet Intern Med* **29**, 120–125 (2015). doi: 10.1111/jvim.12501
44. K. Mizukami, K. Raj, C. Osborne, U. Giger, Cystinuria Associated with Different *SLC7A9* Gene Variants in the Cat. *PLoS One* **11**, e0159247 (2016). doi: 10.1371/journal.pone.0159247; Pmid: 27404572
45. H.-S. Chang, T. Shibata, S. Arai, C. Zhang, A. Yabuki, S. Mitani, T. Higo, K. Sunagawa, K. Mizukami, O. Yamato, Dihydropyrimidinase deficiency: the first feline case of dihydropyrimidinuria with clinical and molecular findings. *JIMD Rep* **6**, 21–26 (2012). doi: 10.1007/8904_2012_139; Pmid: 23430934
46. B. Gandolfi, S. Alamri, W. G. Darby, B. Adhikari, J. C. Lattimer, R. Malik, C. M. Wade, L. A. Lyons, J. Cheng, J. F. Bateman, P. McIntyre, S. R. Lamandé, B. Haase, A dominant **TRPV4** variant underlies osteochondrodysplasia in Scottish fold cats. *Osteoarthritis Cartilage* **24**, 1441–1450 (2016). doi: 10.1016/j.joca.2016.03.019; Pmid: 27063440
47. B. Gandolfi, T. J. Gruffydd-Jones, R. Malik, A. Cortes, B. R. Jones, C. R. Helps, E. M. Prinzenberg, G. Erhardt, L. A. Lyons, First WNK4-hypokalemia animal model identified by genome-wide association in Burmese cats. *PLoS One* **7**, e53173 (2012). doi: 10.1371/journal.pone.0053173; Pmid: 23285264
48. S. Wakitani, S. Torisu, T. Yoshino, K. Hattanda, O. Yamato, R. Tasaki, H. Fujita, K. Nishino, Multiple Acyl-CoA Dehydrogenation Deficiency (*Glutaric Aciduria Type II*) with a Novel Mutation of Electron Transfer Flavoprotein-Dehydrogenase in a Cat. *JIMD Rep* **13**, 43–51 (2014). doi: 10.1007/8904_2013_268; Pmid: 24142280
49. J. C. Fyfe, R. L. Kurzhals, M. G. Hawkins, P. Wang, N. Yuhki, U. Giger, T. J. Van Winkle, M. E. Haskins, D. F. Patterson, P. S. Henthorn, A complex rearrangement in *GBE1* causes both perinatal hypoglycemic collapse and late-juvenile-onset neuromuscular degeneration in glycogen storage disease type IV of Norwegian forest cats. *Mol Genet Metab* **90**, 383–392 (2007). doi: 10.1016/j.ymgme.2006.12.003; Pmid: 17257876
50. D. R. Martin, B. A. Rigat, P. Foureman, G. S. Varadarajan, M. Hwang, B. K. Krum, B. F. Smith, J. W. Callahan, D. J. Mahuran, H. J. Baker, Molecular consequences of the pathogenic mutation in feline *GM1* gangliosidosis. *Mol Genet Metab* **94**, 212–221 (2008). doi: 10.1016/j.ymgme.2008.02.004; Pmid: 18353697
51. D. R. Martin, B. K. Krum, G. S. Varadarajan, T. L. Hathcock, B. F. Smith, H. J. Baker, An inversion of 25 base pairs causes feline *GM2* gangliosidosis variant. *Exp Neurol* **187**, 30–37 (2004). doi: 10.1016/j.expneurol.2004.01.008; Pmid: 15081585

52. Y. Kanae, D. Endoh, O. Yamato, D. Hayashi, S. Matsunaga, H. Ogawa, Y. Maede, M. Hayashi, Nonsense mutation of feline beta-hexosaminidase beta-subunit (HEXB) gene causing Sandhoff disease in a family of Japanese domestic cats. *Res Vet Sci* **82**, 54–60 (2007). doi: 10.1016/j.rvsc.2006.05.007; Pmid: 16872651
53. M. Goree, J. L. Catalfamo, S. Aber, M. K. Boudreaux, Characterization of the mutations causing *hemophilia B* in 2 domestic cats. *J Vet Intern Med* **19**, 200–204 (2005). doi: 10.1892/0891-6640(2005)19<200:cotmch>2.0.co;2; Pmid: 15822564
54. K. M. Meurs, X. Sanchez, R. M. David, N. E. Bowles, J. A. Towbin, P. J. Reiser, J. A. Kittleson, M. J. Munro, K. Dryburgh, K. A. Macdonald, M. D. Kittleson, A cardiac myosin binding protein C mutation in the Maine Coon cat with familial hypertrophic cardiomyopathy. *Hum Mol Genet* **14**, 3587–3593 (2005). doi: 10.1093/hmg/ddi386; Pmid: 16236761
55. D. G. Ginzinger, M. E. Lewis, Y. Ma, B. R. Jones, G. Liu, S. D. Jones, A mutation in the lipoprotein lipase gene is the molecular basis of chylomicronemia in a colony of domestic cats. *J Clin Invest* **97**, 1257–1266 (1996). doi: 10.1172/JCI118541; Pmid: 8636438
56. K. L. Mealey, N. S. Burke, Identification of a nonsense mutation in feline ABCB1. *J Vet Pharmacol Ther* **38**, 429–433 (2015). doi: 10.1111/jvp.12212; Pmid: 25660379 107. X. He, C. M. Li, C. M. Simonaro, Q. Wan, M. E. Haskins, R. J. Desnick, E. H. Schuchman, Identification and characterization of the molecular lesion causing mucopolysaccharidosis type I in cats. *Mol Genet Metab* **67**, 106–112 (1999). doi: 10.1006/mgme.1999.2860; Pmid: 10356309
57. X. He, C. M. Li, C. M. Simonaro, Q. Wan, M. E. Haskins, R. J. Desnick, E. H. Schuchman, Identification and characterization of the molecular lesion causing mucopolysaccharidosis type I in cats. *Mol Genet Metab* **67**, 106–112 (1999). doi: 10.1006/mgme.1999.2860; Pmid: 10356309
58. J. C. Fyfe, R. L. Kurzhals, M. E. Lassaline, P. S. Henthorn, P. R. Alur, P. Wang, J. H. Wolfe, U. Giger, M. E. Haskins, D. F. Patterson, H. Sun, S. Jain, N. Yuhki, Molecular basis of feline beta-glucuronidase deficiency: an animal model of mucopolysaccharidosis VII. *Genomics* **58**, 121–128 (1999). doi: 10.1006/geno.1999.5825; Pmid: 10366443
59. P. Wang, J. Sorenson, S. Strickland, C. Mingus, M. E. Haskins, U. Giger, Mucopolysaccharidosis VII in a Cat Caused by 2 Adjacent Missense Mutations in the *GUSB* Gene. *J Vet Intern Med* **29**, 1022–1028 (2015). doi: 10.1111/jvim.13569; Pmid: 26118695
60. B. Gandolfi, R. J. Daniel, D. P. O'Brien, L. T. Guo, M. D. Youngs, S. B. Leach, B. R. Jones, G. D. Shelton, L. A. Lyons, A novel mutation in *CLCN1* associated with feline myotonia congenita. *PLoS One* **9**, e109926 (2014). doi: 10.1371/journal.pone.0109926; Pmid: 25356766 111. M. Menotti-Raymond, V. A. David, A. A. Schäffer, R. Stephens, D. Wells, R. Kumar-Singh, S. J. O'Brien, K. Narfström, Mutation in *CEP290* discovered for cat model of human retinal degeneration. *J Hered* **98**, 211–220 (2007). doi: 10.1093/jhered/esm019; Pmid: 17507457
61. M. Menotti-Raymond, V. A. David, A. A. Schäffer, R. Stephens, D. Wells, R. Kumar-Singh, S. J. O'Brien, K. Narfström, Mutation in *CEP290* discovered for cat

model of human retinal degeneration. *J Hered* **98**, 211–220 (2007). doi: 10.1093/jhered/esm019; Pmid: 17507457

62. B. Cogné, X. Latypova, L. D. S. Senaratne, L. Martin, D. C. Koboldt, G. Kellaris, L. Fievet, G. Le Meur, D. Caldari, D. Debray, M. Nizon, E. Frengen, S. J. Bowne, 99 Lives Consortium, E. L. Cadena, S. P. Daiger, K. M. Bujakowska, E. A. Pierce, M. Gorin, N. Katsanis, S. Bézieau, S. M. Petersen-Jones, L. M. Occelli, L. A. Lyons, L. Legeai-Mallet, L. S. Sullivan, E. E. Davis, B. Isidor, Mutations in the Kinesin-2 Motor *KIF3B* Cause an Autosomal-Dominant Ciliopathy. *Am J Hum Genet* **106**, 893–904 (2020). doi: 10.1016/j.ajhg.2020.04.005; Pmid: 32386558
63. R. A. Grahn, J. C. Grahn, M. C. Penedo, C. R. Helps, L. A. Lyons, Erythrocyte pyruvate kinase deficiency mutation identified in multiple breeds of domestic cats. *BMC Vet Res* **8**, 207 (2012). doi: 10.1186/1746-6148-8-207; Pmid: 23110753
64. K. L. Somers, M. A. Royals, E. D. Carstea, M. A. Rafi, D. A. Wenger, M. A. Thrall, Mutation analysis of feline Niemann-Pick C1 disease. *Mol Genet Metab* **79**, 99–103 (2003). doi: 10.1016/s1096-7192(03)00074-x; Pmid: 12809639
65. D. A. Mauler, B. Gandolfi, C. R. Reinero, D. P. O'Brien, J. L. Spooner, L. A. Lyons, and 99 Lives Consortium, Precision Medicine in Cats: Novel Niemann-Pick Type C1 Diagnosed by Whole-Genome Sequencing. *J Vet Intern Med* **31**, 539–544 (2017). doi: 10.1111/jvim.14599; Pmid: 28233346
66. S. Zampieri, E. Bianchi, C. Cantile, R. Saleri, B. Bembi, A. Dardis, Characterization of a spontaneous novel mutation in the *NPC2* gene in a cat affected by Niemann Pick type C disease. *PLoS One* **9**, e112503 (2014). doi: 10.1371/journal.pone.0112503; Pmid: 25396745
67. J. C. Fyfe, M. Menotti-Raymond, V. A. David, L. Brichta, A. A. Schäffer, R. Agarwala, W. J. Murphy, W. J. Wedemeyer, B. L. Gregory, B. G. Buzzell, M. C. Drummond, B. Wirth, S. J. O'Brien, An approximately 140-kb deletion associated with feline spinal muscular atrophy implies an essential *LIX1* function for motor neuron survival. *Genome Res* **16**, 1084–1090 (2006). doi: 10.1101/gr.5268806; Pmid: 16899656
68. V. Geisen, K. Weber, K. Hartmann, Vitamin D-dependent hereditary rickets type I in a cat. *J Vet Intern Med* **23**, 196–199 (2009). doi: 10.1111/j.1939-1676.2008.00220.x; Pmid: 19138382
69. L. A. Lettice, A. E. Hill, P. S. Devenney, R. E. Hill, Point mutations in a distant sonic hedgehog cis-regulator generate a variable regulatory output responsible for preaxial polydactyly. *Hum Mol Genet* **17**, 978–985 (2008). doi: 10.1093/hmg/ddm370; Pmid: 18156157
70. L. Peng, The genetics and evolution of white spotting coat color in domestic cats (*Felis catus*). *In prep*.
71. X. Weng, B. Zhang, S. Li, Analysis of Construction aterials of Xiongnu Tongwan city, built 1600 years ago. *Studies in Conservation* **66**, 413–422 (2021). doi: 10.1080/00393630.2020.1853978
72. Y. Li, F. Zhang, J. Liu, C. Liu, Z. Cui, Preliminary Report on the Excavation of the Han and Tang Tombs of the Jianyeshihefu, Puyang, Hernan Provience. *Huaxia Archaeology*, 7 (2022). doi:10.16143/j.cnki.1001-9928.2022.03.008

73. C. Chen, W. Zhang, K. Liu, The Archaeological Survey of the Xitucheng Site, Kangbao, Hebei Province. *Steppe Cultural Relics*, 63–77 (2014). doi: 10.16327/j.cnki.cn15-1361/k.2014.01.008
74. Z. Wu, C. Chen, Y. Han, Z. Liu, Q. Li, Research on the faunal remains of the Xitucheng City Site, Kangbao, Hebei Provience. *Cultural Relics in Southern China*, 126–133 (2020). doi: 10.3969/j.issn.1004-6275.2020.02.016
75. K. Zhao, X. Wu, H. Li, Q. Guo, Z. Wang, Research on the domestic cat remains in the Xinxiang Song Tomb Henan Province. *Quaternary Sciences*, 391–398 (2020). doi: 10.11928/j.issn.1001-7410.2020.02.09
76. J. An, The Shang City at Zhengzhou and Related Problems. *Early China* **9**, 3–4 (1986). doi: 10.1017/s0362502800002893
77. P. Chen, P. Lu, S. Yang, M. Storozum, R. Yang, Y. Tian, H. Wang, Q. Wu, J. Xu, X. Wang, The Impact of Ancient Landscape Changes on the City Arrangement of the Early Shang Dynasty Capital Zhengzhou, Central China. *Frontiers in Earth Science* **9**, 656193 (2021). doi: 10.3389/feart.2021.656193
78. School of History and Culture,IMNU, Inner Mongolia Institute of Cultural Heritage and Archaeology, Yuquan Institute of Cultural Heritage, Preliminary report on the excavation of Shaliangzi City Site, Yuquan District, Inner Mongolia. *Steppe Cultural Relics*, 12–19 (2019). doi: 10.16327/j.cnki.cn15-1361/k.2019.02.002
79. S. Hu, Z. Sun, The faunal remains of the Wuzhuangguoliang site and its palaeoenvironment analyses. *Archaeol Cult Relics* **6**, 72–84 (2005). doi: 10.3969/j.issn.1000-7830.2005.06.015
80. S. Hu, P. Zhang, M. Yuan, A study on the faunal remains from the Huoshiliang site in Yulin, Shaanxi. *Acta Anthropologica Sinic*, 58–60 (2008). doi: 10.3969/j.issn.1000-3193.2008.03.005
81. K. Chen, S. Liu, Y. Li, J. Mei, A. Shao, L. Yue, Evidence of arsenical copper smelting in Bronze Age China: A study of metallurgical slag from the Laoniupo site, central Shaanxi. *Journal of Archaeological Science* **82**, 31–39 (2017). doi: 10.1016/j.jas.2017.04.006
82. S. Hu, Z. Liu, J. Zhang, Research report on the faunal remains unearthed from the Southwest Corner of the Wall of Han Chang'an City Site. *Relics and Museology*, 58–60 (2006). doi: 10.3969/j.issn.1000-7954.2006.05.013
83. N. F. Jiao, Preliminary study on outer burial pits of Han Yangling Mausoleum. *Cult Relics* **7**, 51–57 (2006). doi: CNKI:SUN:WENW.0.2006-07-006
84. A. Jamieson, A. Carmagnini, J. Howard-McCombe, S. Doherty, A. Hirons, E. Dimopoulos, A. T. Lin, R. Allen, H. Anderson-Whymark, R. Barnett, Limited historical admixture between European wildcats and domestic cats. *Current Biology* **33**, 4751–4760 (2023). doi: 10.1016/j.cub.2023.08.031; Pmid: 37935117
85. A. F. Haruda, A. R. Ventresca Miller, J. L. A. Paijmans, A. Barlow, A. Tazhekeyev, S. Bilalov, Y. Hesse, M. Preick, T. King, R. Thomas, The earliest domestic cat on the Silk Road. *Scientific reports* **10**, 1–12 (2020). doi: 10.1038/s41598-020-67798-6; Pmid: 32647113
86. H. Yu, Y.-T. Xing, H. Meng, B. He, W.-J. Li, X.-Z. Qi, J.-Y. Zhao, Y. Zhuang, X. Xu, N. Yamaguchi, Genomic evidence for the Chinese mountain cat as a wildcat

conspecific (Felis silvestris bieti) and its introgression to domestic cats. *Science advances* **7**, eabg0221 (2021). doi: 10.1126/sciadv.abg0221; Pmid: 34162544

87. P. J. Reimer, W. E. Austin, E. Bard, A. Bayliss, P. G. Blackwell, C. B. Ramsey, M. Butzin, H. Cheng, R. L. Edwards, M. Friedrich, The IntCal20 Northern Hemisphere radiocarbon age calibration curve (0–55 cal kBP). *Radiocarbon* **62**, 725–757 (2020). doi: doi.org/10.1017/rdc.2020.41
88. J. Dabney, M. Knapp, I. Glocke, M.-T. Gansauge, A. Weihmann, B. Nickel, C. Valdiosera, N. García, S. Pääbo, J.-L. Arsuaga, Complete mitochondrial genome sequence of a Middle Pleistocene cave bear reconstructed from ultrashort DNA fragments. *Proceedings of the National Academy of Sciences* **110**, 15758–15763 (2013). doi: 10.1073/pnas.1314445110; Pmid: 24019490
89. P. B. Damgaard, A. Margaryan, H. Schroeder, L. Orlando, E. Willerslev, M. E. Allentoft, Improving access to endogenous DNA in ancient bones and teeth. *Scientific reports* **5**, 1–12 (2015). doi: 10.1038/srep11184; Pmid: 26081994
90. C. Carøe, S. Gopalakrishnan, L. Vinner, S. S. Mak, M. H. S. Sinding, J. A. Samaniego, N. Wales, T. Sicheritz-Pontén, M. T. P. Gilbert, Single-tube library preparation for degraded DNA. *Methods in Ecology and Evolution* **9**, 410–419 (2018). doi: 10.1111/2041-210x.12871
91. M. Kircher, S. Sawyer, M. Meyer, Double indexing overcomes inaccuracies in multiplex sequencing on the Illumina platform. *Nucleic acids research* **40**, e3–e3 (2012). doi: 10.1093/nar/gkr771; Pmid: 22021376
92. A. Modi, S. Vai, D. Caramelli, M. Lari, "The Illumina sequencing protocol and the NovaSeq 6000 system" in *Bacterial Pangenomics: Methods and Protocols* (Springer, 2021), pp. 15–42. doi: 10.1007/978-1-0716-1099-2_2; Pmid: 33961215
93. S. Kollias, M. Poortvliet, I. Smolina, G. Hoarau, Low cost sequencing of mitogenomes from museum samples using baits capture and Ion Torrent. *Conservation Genetics Resources* **7**, 345–348 (2015). doi: 10.1007/s12686-015-0433-7
94. J. Dabney, M. Meyer, S. Pääbo, Ancient DNA damage. *Cold Spring Harbor perspectives in biology* **5**, a012567 (2013). doi: 10.1101/cshperspect.a012567 Pmid: 23729639
95. M. Hofreiter, V. Jaenicke, D. Serre, A. von Haeseler, S. Pääbo, DNA sequences from multiple amplifications reveal artifacts induced by cytosine deamination in ancient DNA. *Nucleic acids research* **29**, 4793–4799 (2001). doi: 10.1093/nar/29.23.4793; Pmid: 11726688
96. M. Schubert, S. Lindgreen, L. Orlando, AdapterRemoval v2: rapid adapter trimming, identification, and read merging. *BMC research notes* **9**, 1–7 (2016). doi: 10.1186/s13104-016-1900-2; Pmid: 26868221
97. M. Martin, Cutadapt removes adapter sequences from high-throughput sequencing reads. *EMBnet. journal* **17**, 10–12 (2011). doi: 10.14806/ej.17.1.200
98. H. Li, R. Durbin, Fast and accurate short read alignment with Burrows–Wheeler transform. *bioinformatics* **25**, 1754–1760 (2009). doi: 10.1093/bioinformatics/btp324; Pmid: 19451168
99. P. Danecek, J. K. Bonfield, J. Liddle, J. Marshall, V. Ohan, M. O. Pollard, A. Whitwham, T. Keane, S. A. McCarthy, R. M. Davies, Twelve years of SAMtools

and BCFtools. *Gigascience* **10**, giab008 (2021). doi: 10.1093/gigascience/giab008; Pmid: 33590861
100. R. C. Edgar, Muscle5: High-accuracy alignment ensembles enable unbiased assessments of sequence homology and phylogeny. *Nature Communications* **13**, 6968 (2022). doi: 10.1038/s41467-022-34630-w; Pmid: 36379955
101. A. Ginolhac, M. Rasmussen, M. T. P. Gilbert, E. Willerslev, L. Orlando, mapDamage: testing for damage patterns in ancient DNA sequences. *Bioinformatics* **27**, 2153–2155 (2011). doi: 10.1093/bioinformatics/btr347; Pmid: 21659319
102. H. Jónsson, A. Ginolhac, M. Schubert, P. L. Johnson, L. Orlando, mapDamage2. 0: fast approximate Bayesian estimates of ancient DNA damage parameters. *Bioinformatics* **29**, 1682–1684 (2013). doi: 10.1093/bioinformatics/btt193; Pmid: 23613487
103. A. McKenna, M. Hanna, E. Banks, A. Sivachenko, K. Cibulskis, A. Kernytsky, K. Garimella, D. Altshuler, S. Gabriel, M. Daly, The Genome Analysis Toolkit: a MapReduce framework for analyzing next-generation DNA sequencing data. *Genome research* **20**, 1297–1303 (2010). doi: 10.1101/gr.107524.110; Pmid: 20644199
104. M. A. DePristo, E. Banks, R. Poplin, K. V. Garimella, J. R. Maguire, C. Hartl, A. A. Philippakis, G. Del Angel, M. A. Rivas, M. Hanna, A framework for variation discovery and genotyping using next-generation DNA sequencing data. *Nature genetics* **43**, 491–498 (2011). doi: 10.1038/ng.806; Pmid: 21478889
105. G. A. Van der Auwera, B. D. O'Connor, *Genomics in the Cloud: Using Docker, GATK, and WDL in Terra* (O'Reilly Media, 2020). ISBN: 9781491975190
106. S. Purcell, B. Neale, K. Todd-Brown, L. Thomas, M. A. Ferreira, D. Bender, J. Maller, P. Sklar, P. I. De Bakker, M. J. Daly, PLINK: a tool set for whole-genome association and population-based linkage analyses. *The American journal of human genetics* **81**, 559–575 (2007). doi: 10.1086/519795; Pmid: 17701901
107. A. R. Quinlan, I. M. Hall, BEDTools: a flexible suite of utilities for comparing genomic features. *Bioinformatics* **26**, 841–842 (2010). doi: 10.1093/bioinformatics/btq033; Pmid: 20110278
108. L.-T. Nguyen, H. A. Schmidt, A. Von Haeseler, B. Q. Minh, IQ-TREE: a fast and effective stochastic algorithm for estimating maximum-likelihood phylogenies. *Molecular biology and evolution* **32**, 268–274 (2015). doi: 10.1093/molbev/msu300; Pmid: 25371430
109. B. Q. Minh, H. A. Schmidt, O. Chernomor, D. Schrempf, M. D. Woodhams, A. Von Haeseler, R. Lanfear, IQ-TREE 2: new models and efficient methods for phylogenetic inference in the genomic era. *Molecular biology and evolution* **37**, 1530–1534 (2020). doi: 10.1093/molbev/msaa015; Pmid: 32011700
110. K. Tamura, M. Nei, Estimation of the number of nucleotide substitutions in the control region of mitochondrial DNA in humans and chimpanzees. *Molecular biology and evolution* **10**, 512–526 (1993). doi: 10.1093/oxfordjournals.molbev.a040023; Pmid: 8336541
111. I. Letunic, P. Bork, Interactive Tree Of Life (iTOL): an online tool for phylogenetic tree display and annotation. *Bioinformatics* **23**, 127–128 (2007). doi: 10.1093/bioinformatics/btl529; Pmid: 17050570

112. I. Letunic, P. Bork, Interactive Tree Of Life (iTOL) v5: an online tool for phylogenetic tree display and annotation. *Nucleic acids research* **49**, W293–W296 (2021). doi: 10.1093/nar/gkab301; Pmid: 33885785
113. L. D. Parker, M. T. R. Hawkins, M. Camacho-Sanchez, M. G. Campana, J. A. West-Roberts, T. R. Wilbert, H. C. Lim, L. L. Rockwood, J. A. Leonard, J. E. Maldonado, Little genetic structure in a Bornean endemic small mammal across a steep ecological gradient. *Molecular Ecology* **29**, 4074–4090 (2020). doi: 10.1111/mec.15626; Pmid: 32911576
114. A. L. Price, N. J. Patterson, R. M. Plenge, M. E. Weinblatt, N. A. Shadick, D. Reich, Principal components analysis corrects for stratification in genome-wide association studies. *Nature genetics* **38**, 904–909 (2006). doi: 10.1038/ng1847; Pmid: 16862161
115. N. Patterson, A. L. Price, D. Reich, Population structure and eigenanalysis. *PLoS genetics* **2**, e190 (2006). doi: 10.1371/journal.pgen.0020190; Pmid: 17194218
116. D. H. Alexander, J. Novembre, K. Lange, Fast model-based estimation of ancestry in unrelated individuals. *Genome research* **19**, 1655–1664 (2009). doi: 10.1101/gr.094052.109; Pmid: 19648217
117. N. Patterson, P. Moorjani, Y. Luo, S. Mallick, N. Rohland, Y. Zhan, T. Genschoreck, T. Webster, D. Reich, Ancient admixture in human history. *Genetics* **192**, 1065–1093 (2012). doi: 10.1534/genetics.112.145037; Pmid: 22960212
118. C. A. Driscoll, M. Menotti-Raymond, A. L. Roca, K. Hupe, W. E. Johnson, E. Geffen, E. H. Harley, M. Delibes, D. Pontier, A. C. Kitchener, The Near Eastern origin of cat domestication. *Science* **317**, 519–523 (2007). doi: 10.1126/science.1139518; Pmid: 17600185
119. I. Tammen, M. Mather, T. Leeb, F. W. Nicholas, Online Mendelian Inheritance in Animals (OMIA): a genetic resource for vertebrate animals. *Mamm Genome*, doi: 10.1007/s00335-024-10059-y (2024). doi: 10.1007/s00335-024-10059-y; Pmid: 39143381
120. H. Li, Aligning sequence reads, clone sequences and assembly contigs with BWA-MEM. *arXiv preprint arXiv:1303.3997* (2013). ArXiv ID: 1303.3997v2

Supplementary Figures

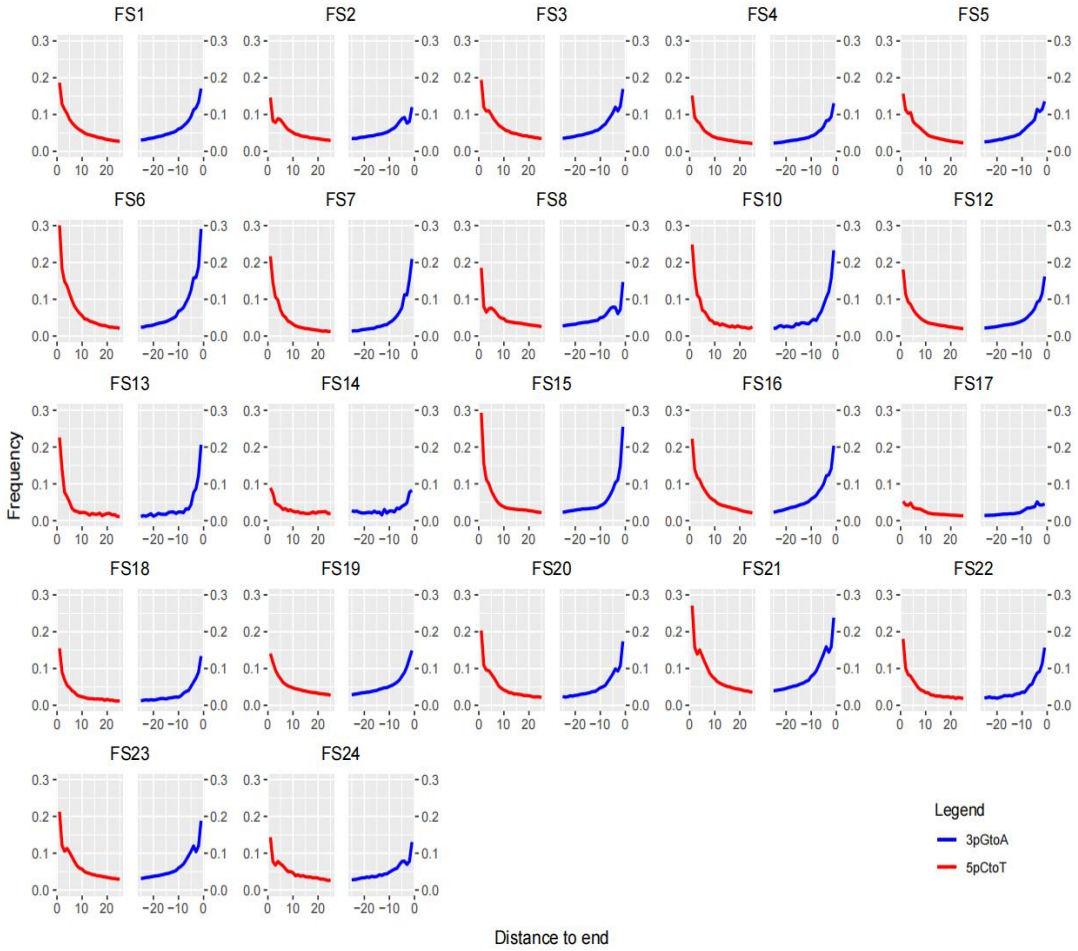

Fig. S1. Plots of mapDamage analysis showing damage patterns of 22 ancient Chinese cat specimens used in this study. The 5' and 3' ends of all samples exhibit a clear deamination pattern signature for ancient DNA.

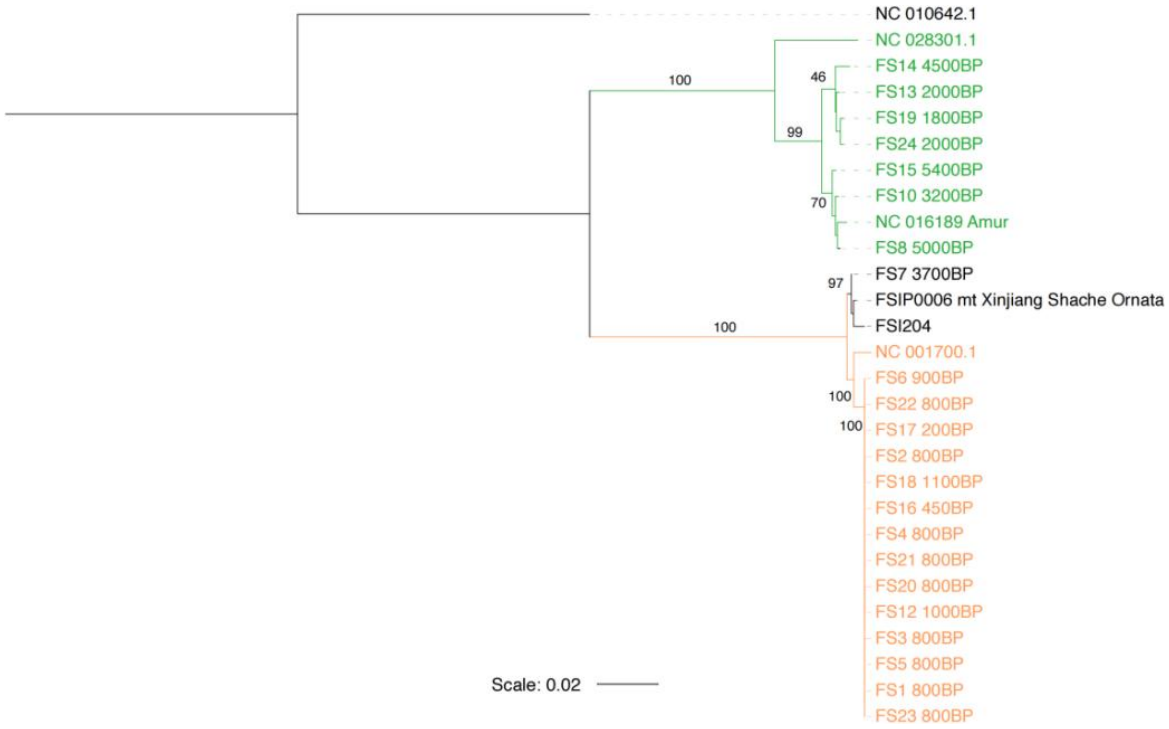

Fig. S2. A maximum likelihood (ML) phylogenetic tree constructed based on the mitochondrial genomes of 22 ancient felid samples collected from China. A TN93+I+G model is implemented with 1,000 bootstrap replicates and a tiger genome (NC_010642.1) is used as an outgroup. The numbers on branches represent the statistical support values based on 1,000 bootstrap replicates. A refined version of the tree is in Fig. 1B.

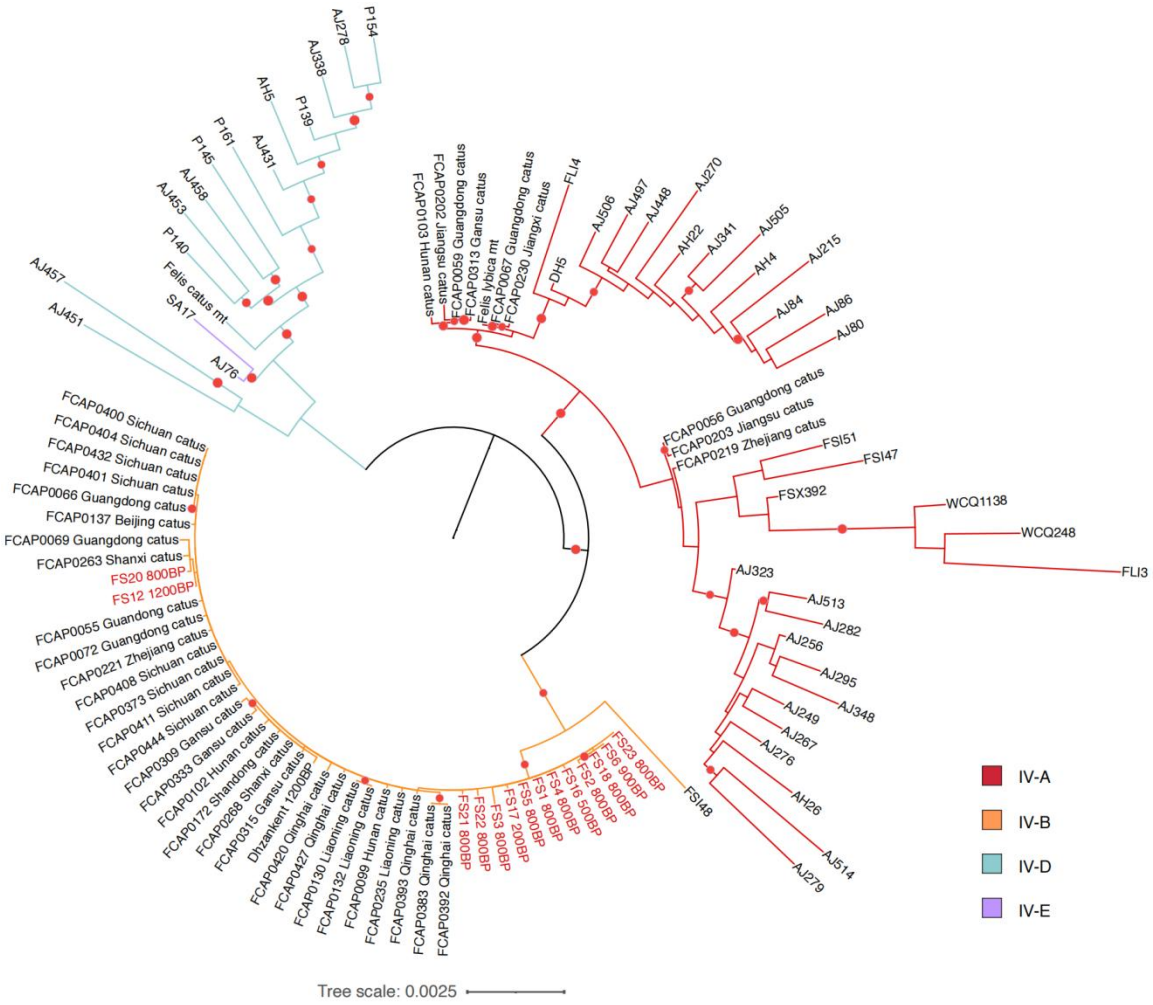

Fig. S3. A maximum likelihood (ML) phylogenetic tree based on mitogenomes of ancient and modern domestic cats worldwide, including 14 ancient domestic cats from China. A TN93+I+G model is implemented with 1,000 bootstrap replicates. The missing data rate for Chinese samples is less than 2% each and the sequencing depth is greater than 30×. The missing data rate for European or Central Asian samples is generally less than 10% and the sequencing depth is greater than 10×. Nodes with significant statistical support (≥ 70%) based on 1,000 bootstrap replicates are labeled with red dots.

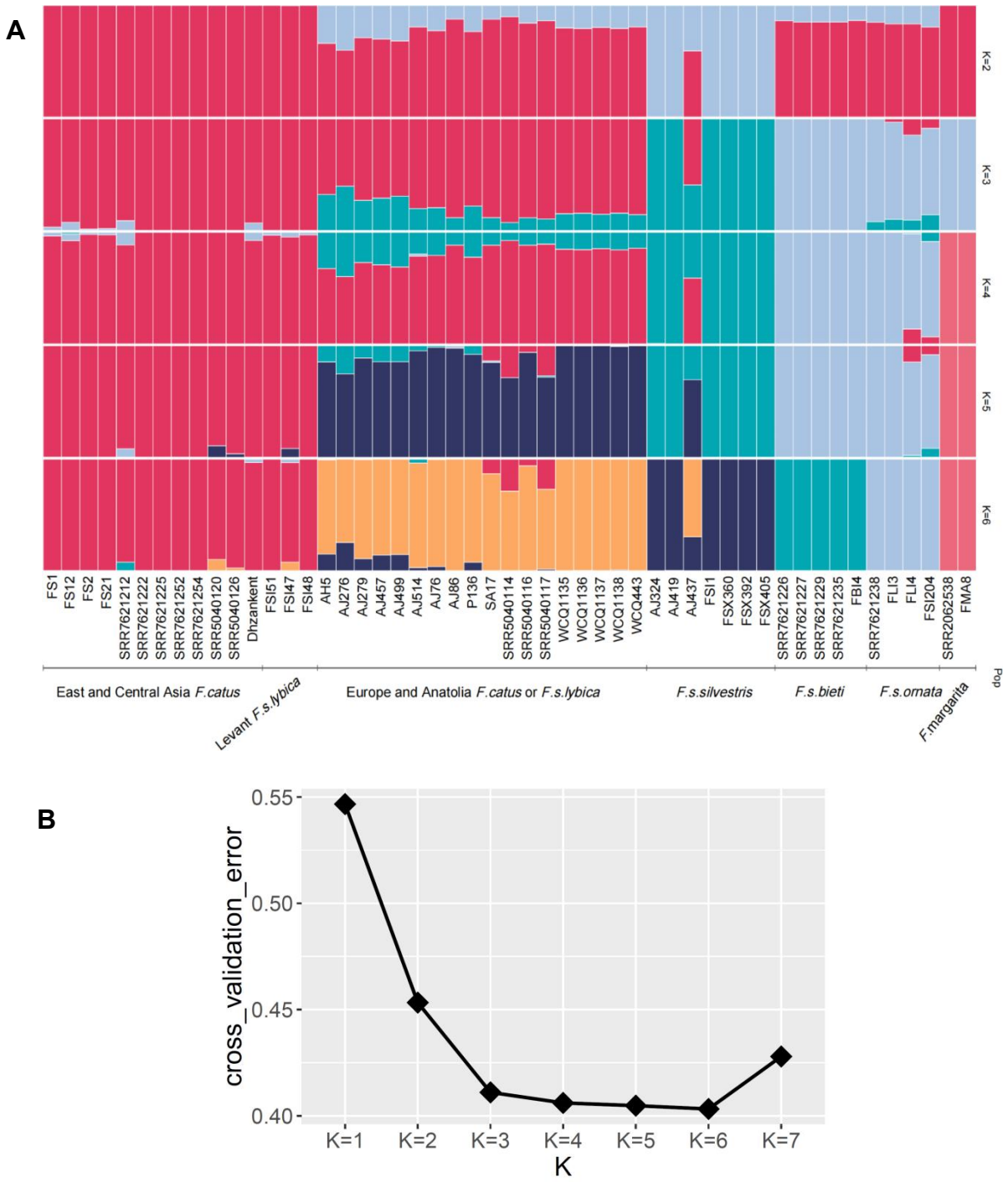

Fig. S4. ADMIXTURE analysis for ancient and modern domestic cats and wildcats from Eurasia. **(A)** ADMIXTURE clustering results based on the number of assumed ancestral populations (*K*) from 2 to 6. **(B)** Cross-validation (CV) errors for each number of assumed ancestral populations (*K*) from 1 to 7.

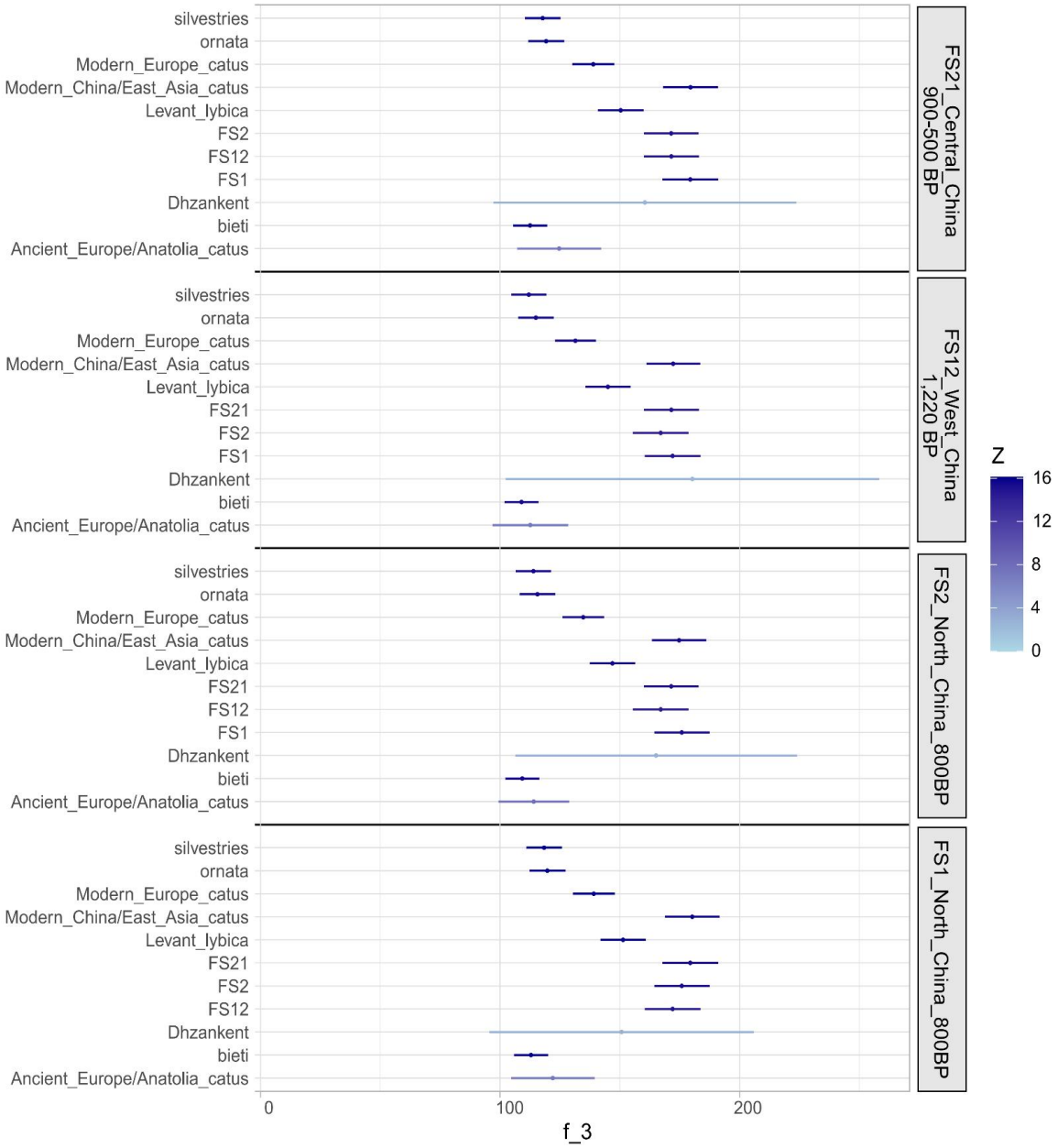

Fig. S5. The result of outgroup f_3-statistics illustrates the affinity between ancient domestic cats from China and other domestic cat populations. The error bars in the four stacked blocks, from bottom to top, correspond to the f3 values between FS1/FS2/FS12/FS21 and other cat populations (labeled on the right). The color gradient, ranging from light to dark blue, shows an increased magnitude of the absolute value of Z. This figure, compared to Fig. 3B, highlights the relationship between ancient domestic cats and modern domestic cats.

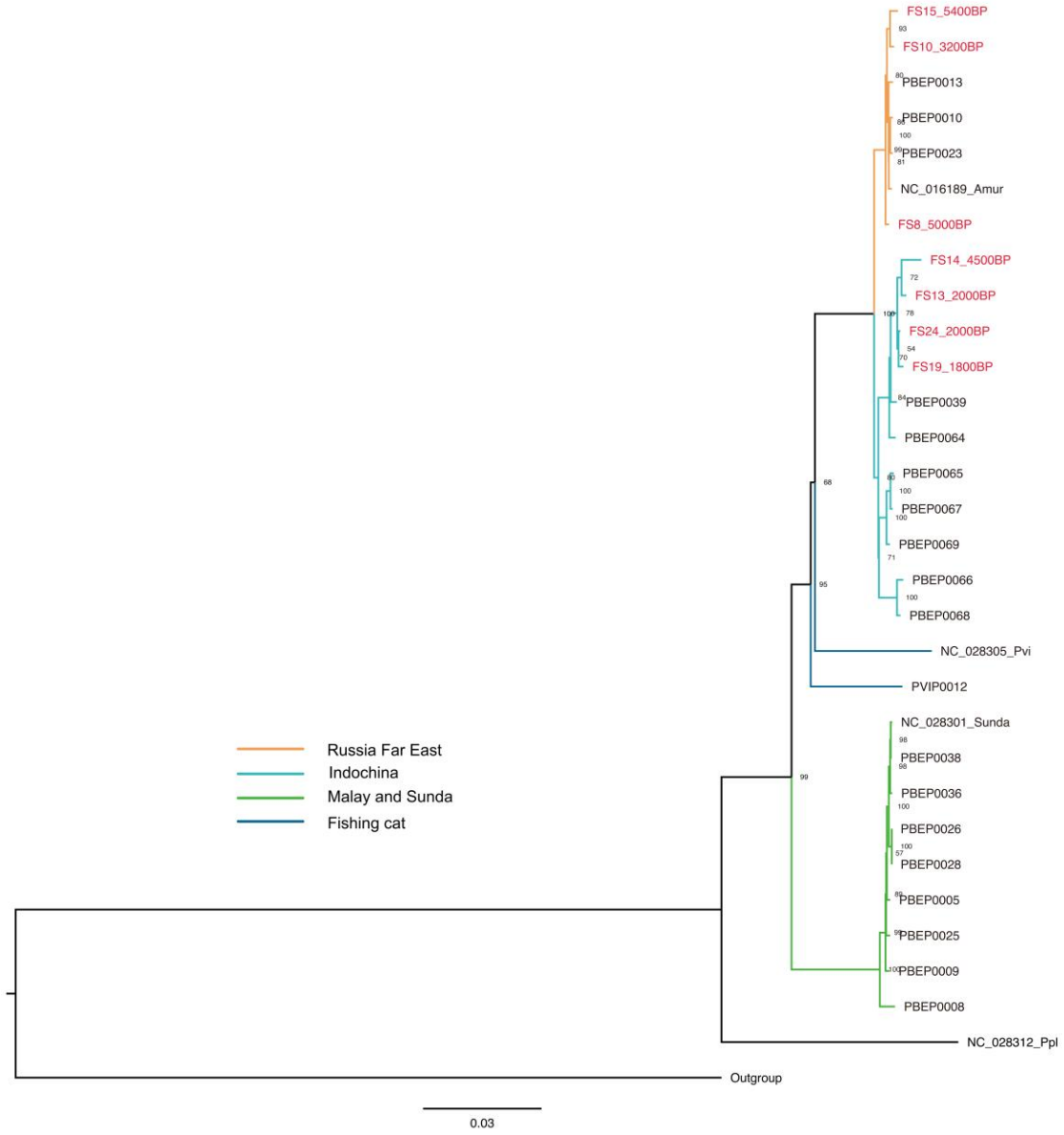

Fig. S6. A maximum likelihood (ML) phylogenetic tree based on leopard cat mitochondrial genomes. The tree is reconstructed based on ancient leopard cats from the middle Yellow River Basin of China (n=7) and modern leopard cats from the Russian Far East (n=4), Indochina (n=6), Malay Peninsula (n=6), and Sundaland (n=4). Two fishing cats (*P. viverrinus*) and a flat-headed cat (*P. planiceps*) are included in the analysis. The tiger reference genome (NC_010642.1) is used as an outgroup. The sample names of ancient leopard cats from the Yellow River Basin are marked in red.

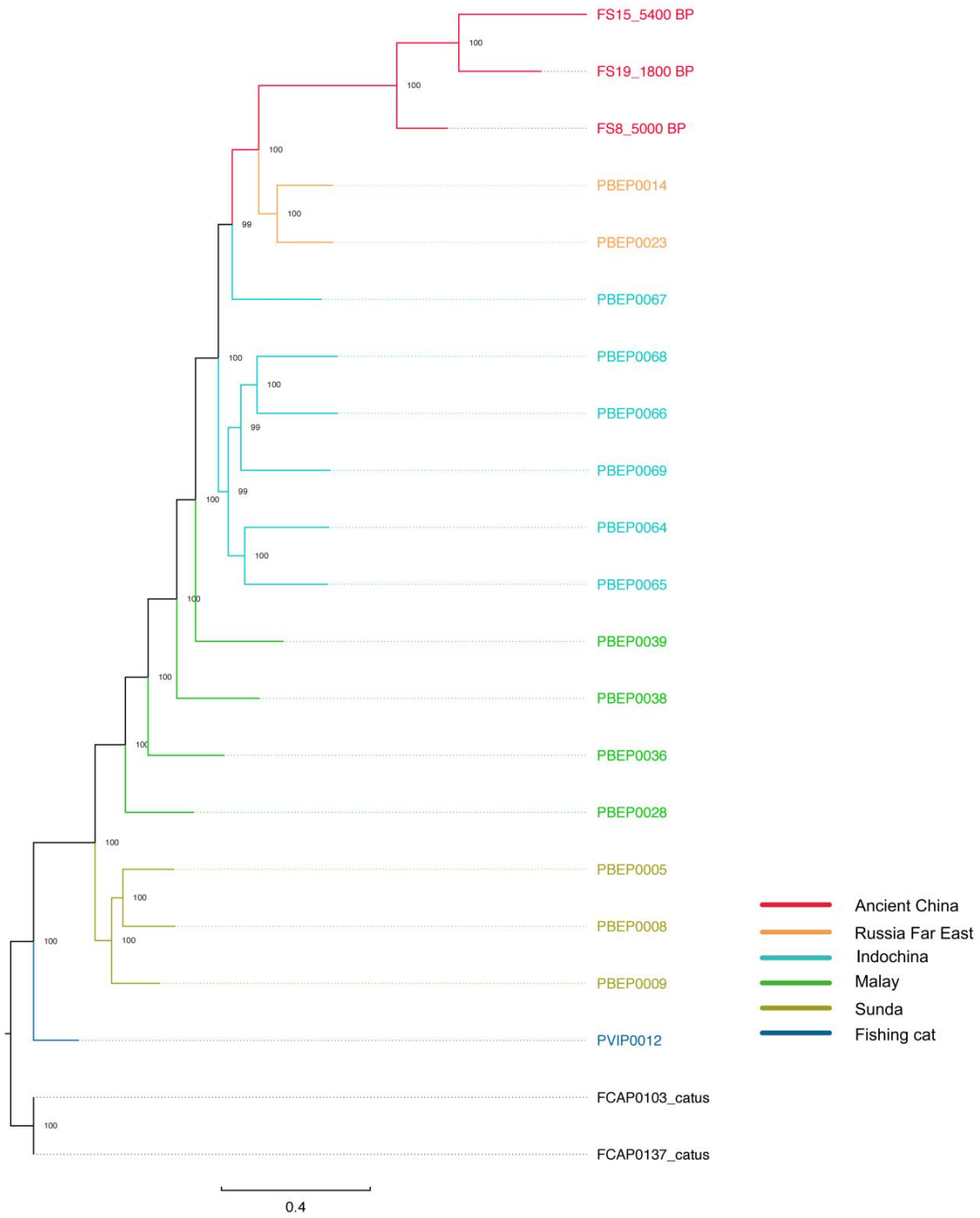

Fig. S7. A maximum likelihood (ML) phylogenetic tree based on ancient and modern leopard cats. The tree is reconstructed based on autosomal SNPs from ancient specimens from China (n=3) and modern samples from the Russian Far East (n=2), Indochina (n=6), Malay Peninsula (n=4), and Sunda (n=3). A fishing cat (*P. viverrinus*) is included in the analysis. Two domestic cats are used as outgroups. Numbers at each node represent the statistical support values based on 200 bootstrap replicates.

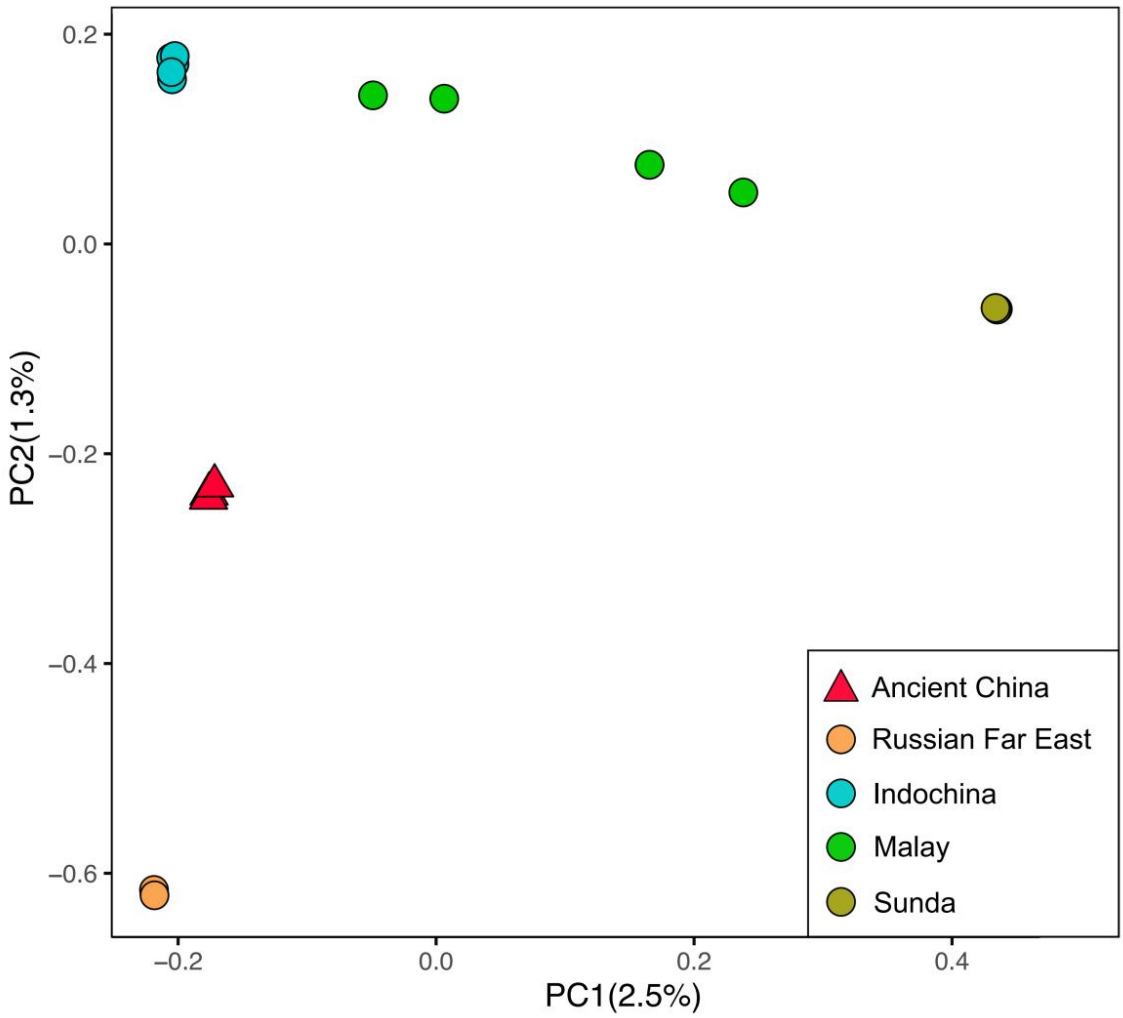

Fig. S8. Principal component analysis (PCA) of leopard cats. PCA is first conducted based on autosomal SNPs from high-quality genome data from modern leopard cats. Data from ancient leopard cats are then projected onto it. Three ancient leopard cats from China and 15 modern leopard cats from range wide, including the Russian Far East (n=2), Indochina (n=6), Malay Peninsula (n=4), and Sundaland (n=3), are included in the analysis.

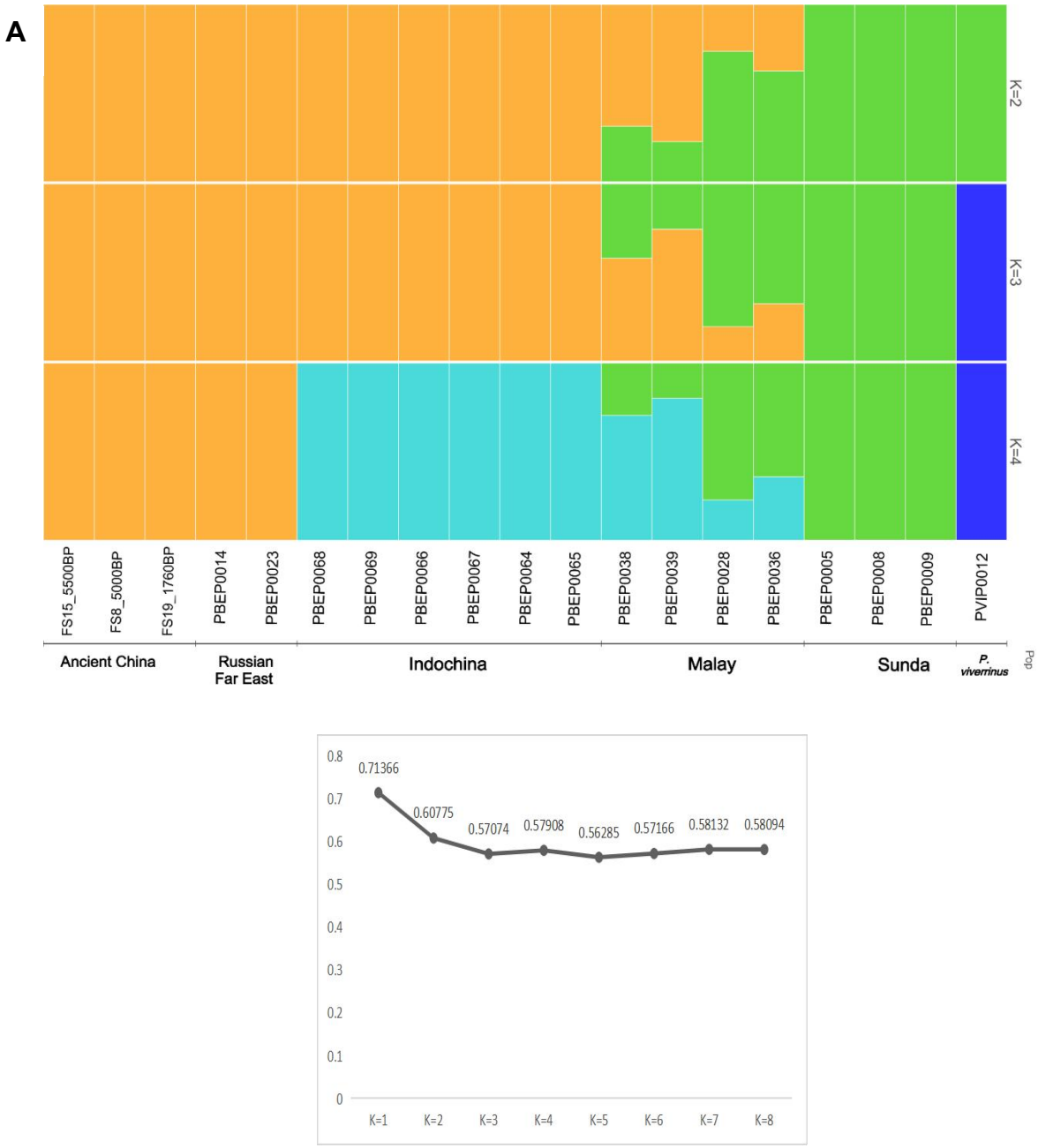

Fig. S9. ADMIXTURE analysis of leopard cats. (**A**) Clustering results based on the number of assumed ancestral populations (*K*) from 2 to 4. A total of 18 specimens are used in the analysis including ancient leopard cats from China (n=3) and modern leopard cats from the Russian Far East (n=2), Indochina (n=6), Malay (n=4), and Sundaland (n=3). A fishing cat was used as an outgroup. (**B**) Cross-validation (CV) errors for each number of assumed ancestral populations (*K*) from 1 to 8.

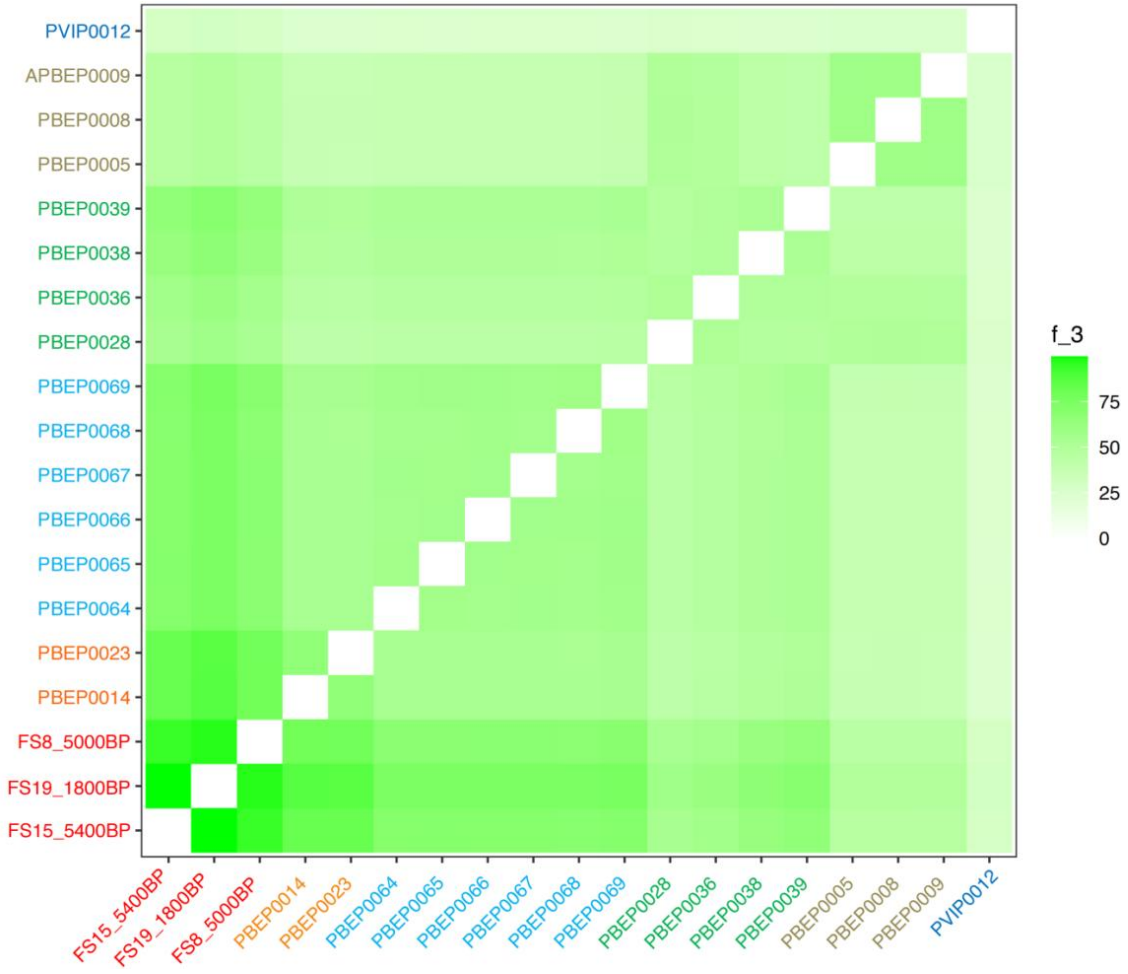

Fig. S10. Outgroup f_3-statistics analysis of leopard cats. A heatmap of the outgroup f_3-statistics analysis. Two domestic cats are used as outgroups. The shared drifts of different pairs of individuals of leopard cat or fishing cat are tested. The color gradient, ranging from light to dark green, shows the increased magnitude of f3 values. The sample names from different populations were labeled with different colors. Ancient Chinese leopard cats (n=2) were marked in red; Russian Far East (n=2) in orange; Indochina (n=6) in light blue; Malay (n=4) in green; Sunda (n=3) in brownish yellow; and fishing cat (n=1) in dark blue.

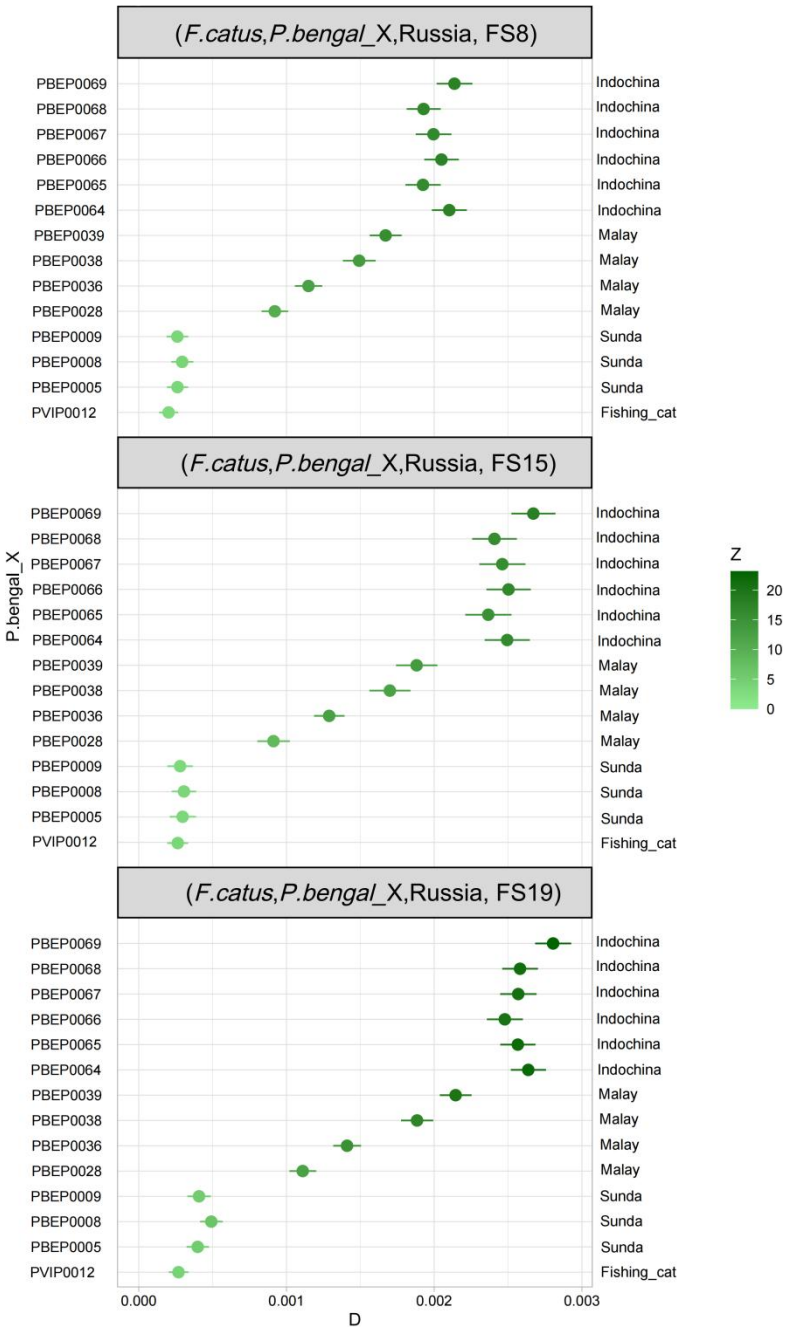

Fig. S11. *D*-statistics analysis of leopard cats. The population combinations were set as (Outgroup, *P. bengalensis*_X, Russian Far East, ancient China) (labeled on the top of each block). Two domestic cats were used as outgroups. Leopard cats from Indochina, Malay Peninsula, Sundaland, and a fishing cat are individually placed in P.bengal_X to evaluate the signals of gene flow between the target ancient Chinese leopard cat and a modern leopard cat from P.bengal_X, relative to a Russian Far East leopard cat. The vertical axis shows the ID of leopard cats in P.bengal_X (on the left) and their population assignments (on the right). The horizontal axis shows the *D* scores. The color gradient, ranging from light to dark green, indicates an increased magnitude of |Z| values.

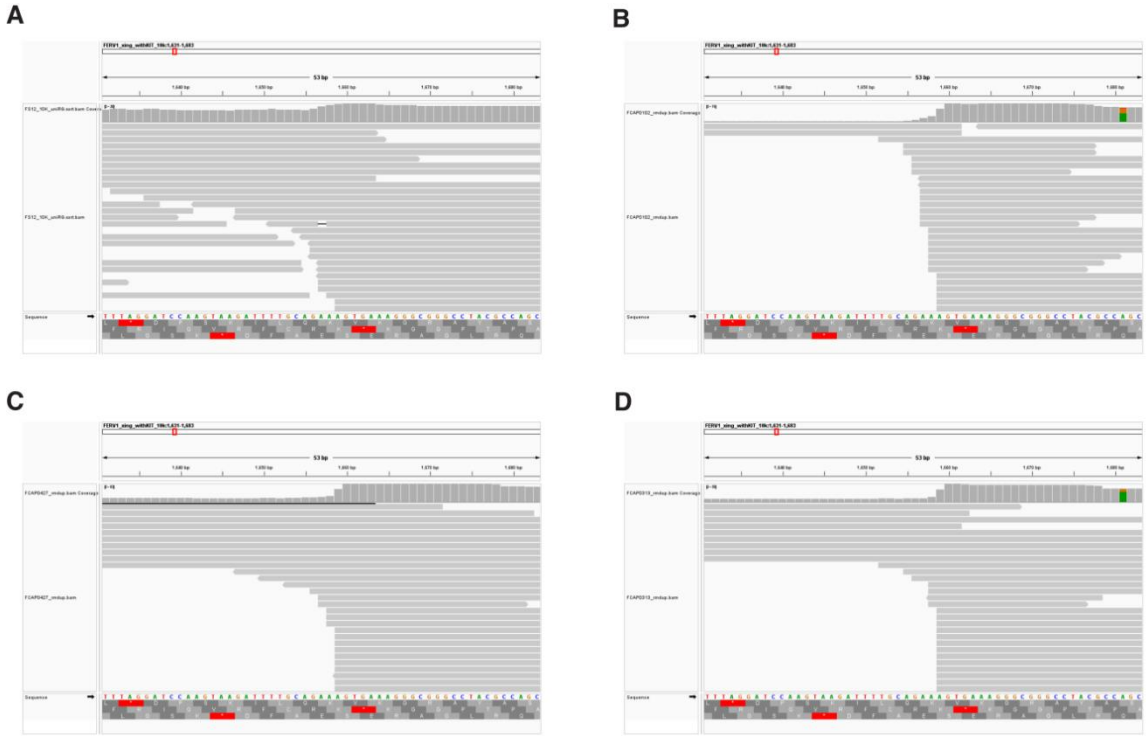

Fig. S12. Mapping patterns of the sequencing data to the domestic cat's *KIT* gene with *FERV1* insertion. (A) Alignment of FS12's *KIT* gene with *FERV1* insertion. **(B)** Alignment of a wild-type domestic cat *KIT* gene without *FERV1* insertion. **(C)** Alignment of a domestic cat homozygous of *FERV1* insertion. **(D)** Alignment of a domestic cat heterozygous of *FERV1* insertion.

Supplementary Tables

Table S1. (A) Information of the ancient samples from this study.

Sample ID	Site	City and Province	Geographical Unit	Country	Endogenous %	Num_reads (mt)	Length mt (bp)	Coverage (mt) %	Mean_depth (mt) x	Num_reads (Nuc)	Mean_depth (Nuc) x	SNPs_used (Nuc)	Date	MT_haplotype	Species
FS1	Xitucheng City	Zhangjiakou Hebei	North China	China	12.5	24336	16732	98.3789	86.5136	128005822	3.22737	95470	1,115-1,234 CE	IV-B	*F. catus*
FS2	Xitucheng City	Zhangjiakou Hebei	North China	China	13.82	21736	16865	99.158	82.8478	101903410	2.43784	99631	1,115-1,234 CE	IV-B	*F. catus*
FS3	Xitucheng City	Zhangjiakou Hebei	North China	China	11.4	11063	16473	96.8487	34.7035	N/A	N/A	N/A	1,115-1,234 CE	IV-B	*F. catus*
FS4	Xitucheng City	Zhangjiakou Hebei	North China	China	10.69	15936	16570	97.419	59.8712	N/A	N/A	N/A	1,115-1,234 CE	IV-B	*F. catus*
FS5	Xitucheng City	Zhangjiakou Hebei	North China	China	11.2	29916	16769	98.589	39.2182	N/A	N/A	N/A	1,115-1,234 CE	IV-B	*F. catus*
FS6	Xinxiang Song Tomb	Xinxiang Henan	Central China	China	0.34	15982	16961	99.7178	112.491	N/A	N/A	N/A	960-1,127 CE	IV-B	*F. catus*
FS7	Huoshiliang	Yulin Shaanxi	West China	China	0.91	17321	16730	99.53	16.9127	N/A	N/A	N/A	1,800 BCE	*Felis ornata*	*F. ornata*
FS8	Wuzhuangguoliang	Jingbian Shaanxi	West China	China	8.76	9870	16416	98.2935	47.3244	153959749	5.96269	17194519	3,000-221 BCE	PBE-RFE	*P. bengalensis*
FS10	Laoniupo	Xi'an Shaanxi	Cental China	China	0.45	24215	16338	97.8265	11.5208	N/A	N/A	N/A	1,200 BCE	PBE-RFE	*P. bengalensis*
FS12*	Tongwan City	Jingbian Shaanxi	West China	China	13.21	23207	16742	98.4377	78.8921	111504420	3.52959	107849	706-883 cal CE	IV-B	*F. catus*
FS13	Yangling	Xianyang Shaanxi	Cental China	China	0.06	4117	15792	94.5572	26.2551	N/A	N/A	N/A	168 - 48 cal BCE	PBE-Indochina	*P. bengalensis*
FS14	Xinjie	Lantian Shaanxi	Cental China	China	0.06	12377	15584	93.3118	20.1013	N/A	N/A	N/A	~3,500-1,800 BCE	PBE-Indochina	*P. bengalensis*
FS15	Quanhucun	Weinan Shaanxi	Cental China	China	2.3	2826	16114	96.4852	15.6682	162299570	3.32325	14322059	4,000-2,700 BCE	PBE-RFE	*P. bengalensis*
FS16	Zhengzhoushang City	Zhengzhou Henan	Cental China	China	4.04	6512	16991	99.8942	207.187	N/A	N/A	N/A	1,413 - 1,480 cal CE	IV-B	*F. catus*
FS17	Shaliangzi	Hohhot Inner Mongolia	North China	China	17.89	5274	16871	99.1887	45.9693	N/A	N/A	N/A	1,797 - 1,944 cal CE	IV-B	*F. catus*
FS18	Puyang Song Tomb	Puyang Henan	Cental China	China	0.05	4969	16975	99.8001	145.439	N/A	N/A	N/A	618-970 CE	IV-B	*F. catus*
FS19	Zheng and Han City	Xinzheng Henan	Cental China	China	6.48	27643	16518	98.9043	51.2599	175356056	4.70431	15747266	25-220 CE	PBE-Indochina	*P. bengalensis*
FS20	Zheng and Han City	Xinzheng Henan	Cental China	China	0.05	10271	16694	98.148	99.1598	N/A	N/A	N/A	960-1,368 CE	IV-B	*F. catus*
FS21	Zheng and Han City	Xinzheng Henan	Cental China	China	10.24	19562	16708	98.237	77.6107	115273634	3.23206	95137	960-1,368 CE	IV-B	*F. catus*
FS22	Zheng and Han City	Xinzheng Henan	Cental China	China	0.1	25761	16593	97.5542	59.5793	N/A	N/A	N/A	960-1,368 CE	IV-B	*F. catus*
FS23	Zheng and Han City	Xinzheng Henan	Cental China	China	3.42	13341	17009	100	304.291	N/A	N/A	N/A	960-1,368 CE	IV-B	*F. catus*
FS24	Han Chang'an City	Xi'an Shaanxi	Cental China	China	2.7	20836	16617	99.497	90.8493	N/A	N/A	N/A	44 cal BCE-76 cal CE	PBE-Indochina	*P. bengalensis*

* We conducted additional deep sequencing on the sample to reach a final genome sequencing depth of 15.97x.

Table S1. (B) Information of ancient samples from other studies.

Sample ID	Mean depth (Nuc)X	Mean depth (mt)X	Location	Geographical Unit	Country	Date	MT haplotype	Species	Source
AJ451	N/A	21.6	Snusgar	British Isles	UK	late 9th-10th century CE	IV-D	*F. catus*	Oxford
AJ457	0.4	20.3	Snusgar	British Isles	UK	late 9th-10th century CE	IV-D	*F. catus*	Oxford
AJ76	1.8	461.1	Lyminge	British Isles	UK	Anglo-Saxon	IV-E	*F. catus*	Oxford
SA17	0.8	44.5	Sagalassos	Near East	Turkey	Early Byzantine (end 500-1st half 600 CE)	IV-E	*F. catus*	Oxford
P140	N/A	17.2	Kongens Nytorv	North Europe	Denmark	1536-1670 CE	IV-D	*F. catus*	Oxford
AJ453	N/A	12.3	Snusgar	British Isles	UK	late 9th-10th century	IV-D	*F. catus*	Oxford
AJ458	N/A	10.5	Snusgar	British Isles	UK	late 9th-10th century	IV-D	*F. catus*	Oxford
P145	N/A	11.6	OvergCEe, Odense	North Europe	Denmark	1070 ± 100 CE	IV-D	*F. catus*	Oxford
P161	N/A	13	Læderstræd, Roskilde	North Europe	Denmark	1200-1400 CE	IV-D	*F. catus*	Oxford
AJ431	N/A	32.1	Jarlshof	British Isles	UK	Neolithic-Norse	IV-D	*F. catus*	Oxford
AH5	0.4	79.3	Lincoln Castle	British Isles	UK	Medieval	IV-D	*F. catus*	Oxford
P139	N/A	161.2	Kongens Nytorv	North Europe	Denmark	1536-1670 CE	IV-D	*F. catus*	Oxford
AJ338	N/A	82.1	Lincoln Castle	British Isles	UK	Medieval	IV-D	*F. catus*	Oxford
AJ278	N/A	27	Eyre Square, Galway	British Isles	Ireland	18th century CE	IV-D	*F. catus*	Oxford
P154	N/A	48.2	MøllegCEe, Svendborg	North Europe	Denmark	1200-1500 CE	IV-D	*F. catus*	Oxford
DH5	N/A	94.9	Daemircihöyük	Near East	Turkey	2500-2000 BCE	IV-A	*F. catus*	Oxford
AJ506	N/A	158	Hungate, York	British Isles	UK	13th- 14th century	IV-A	*F. catus*	Oxford
AJ497	N/A	38.4	Emanuel Point ship	North America	US	1559 CE	IV-A	*F. catus*	Oxford
AJ448	N/A	38.8	Lyminge	British Isles	UK	Anglo-Saxon	IV-A	*F. catus*	Oxford
AJ270	N/A	10	Guildford castle	British Isles	UK	Medieval	IV-A	*F. catus*	Oxford
AH22	N/A	53.4	Lyminge	British Isles	UK	Anglo-Saxon	IV-A	*F. catus*	Oxford
AJ341	N/A	35.8	Owslebury	British Isles	UK	Roman	IV-A	*F. catus*	Oxford
AJ505	N/A	11.4	Hungate, York	British Isles	UK	13th-14th century CE	IV-A	*F. catus*	Oxford
AH4	N/A	16.7	Lyminge	British Isles	UK	Anglo-Saxon	IV-A	*F. catus*	Oxford
AJ215	N/A	17.4	Guildford castle	British Isles	UK	Medieval	IV-A	*F. catus*	Oxford
AJ84	N/A	41.5	Lyminge	British Isles	UK	Anglo-Saxon	IV-A	*F. catus*	Oxford
AJ86	4.6	158	Fishbourne	British Isles	UK	Roman	IV-A	*F. catus*	Oxford
AJ80	N/A	28.3	Lyminge	British Isles	UK	Anglo-Saxon	IV-A	*F. catus*	Oxford
AJ323	N/A	70.6	Kilton Castle	British Isles	UK	Post- Medieval	IV-A	*F. catus*	Oxford
AJ513	N/A	58.3	Earls Bu	British Isles	UK	Late Norse	IV-A	*F. catus*	Oxford
AJ282	N/A	14.8	N/Avan	British Isles	Ireland	Early Medieval	IV-A	*F. catus*	Oxford
AJ256	N/A	68.8	Stalleen	British Isles	Ireland	Early Medieval	IV-A	*F. catus*	Oxford
AJ295	N/A	15	Kilton Castle	British Isles	UK	Post- Medieval	IV-A	*F. catus*	Oxford
AJ348	N/A	27.6	Bambrugh，Castle	British Isles	UK	Medieval	IV-A	*F. catus*	Oxford

Sample ID	Mean depth (Nuc)X	Mean depth (mt)X	Location	Geographical Unit	Country	Date	MT haplotype	Species	Source
AJ249	N/A	30.5	Ratoath	British Isles	Ireland	5th-8th century CE	IV-A	*F. catus*	Oxford
AJ267	N/A	42	Bective	British Isles	Ireland	Medieval	IV-A	*F. catus*	Oxford
AJ276	0.3	72.6	Eyre Square, Galway	British Isles	Ireland	Mid- 17th-18th century CE	IV-A	*F. catus*	Oxford
AH26	N/A	10.1	Caistor Roman，Town	British Isles	UK	Roman	IV-A	*F. catus*	Oxford
AJ514	0.1	12	Howe	British Isles	UK	Middle Iron	IV-A	*F. catus*	Oxford
AJ279	1.1	32.9	Timberyard	British Isles	Ireland	Post 1750 CE	IV-A	*F. catus*	Oxford
WCQ1138	14.99	N/A	Scotland	British Isles	UK	1895-1985 CE	IV-A	*F. catus*	Oxford
WCQ248	15.22	N/A	Scotland	British Isles	UK	1895-1985 CE	IV-A	*F. catus*	Oxford
Dhzankent	0.6	22.9	Dhzankent	Central Asia	Kazakhstan	1,225-1,060 BP	IV-B	*F. catus*	Haruda et al. 2020
AJ499	0.2	7.7	Hungate, York	British Isles	UK	1-4th century CE	N/A	*F. catus*	Oxford
AJ437	<0.1	24	Perwick Cave	British Isles	UK	Roman?	N/A	*F. silvestris*	Oxford
AJ419	0.2	34.23	An Corran	British Isles	UK	Mesolithic	N/A	*F. silvestris*	Oxford
AJ324	0.9	265.3	Kilton Castle	British Isles	UK	Post- Medieval	N/A	*F. silvestris*	Oxford
P136	0.3	9.6	Kongens Nytorv	North Europe	Denmark	1100- 1450 CE	N/A	*F. catus*	Oxford
WCQ1135	14.31	N/A	Scotland	British Isles	UK	1895-1985 CE	N/A	*F. catus*	Oxford
WCQ1136	14.84	N/A	Scotland	British Isles	UK	1895-1985 CE	N/A	*F, catus*	Oxford
WCQ1137	14.87	N/A	Scotland	British Isles	UK	1895-1985 CE	N/A	*F. catus*	Oxford
WCQ443	14.9	N/A	Scotland	British Isles	UK	1895-1985CE	N/A	*F. catus*	Oxford

Table S1. (C) Information of modern Felis samples from other resources.

Sample ID	Source	Mean depth (Nuc) X	Mean depth (mt) X	Location	Geographical Unit	Country	Date	Species	MT haplotype
FCAP0103	SRR7621222	14.65	1042.19	Hunan	South China	China	modern	*F. catus*	IV-A
FCAP0202	SRR7621253	N/A	2305.22	Jiangsu	East Coast of China	China	modern	*F. catus*	IV-A
FCAP0059	SRR7621259	N/A	355	Guangdong	South Coast of China	China	modern	*F. catus*	IV-A
FCAP0067	SRR7621233	N/A	803.31	Guangdong	South Coast of China	China	modern	*F. catus*	IV-A
FCAP0230	SRR7621256	N/A	823.40	Jiangxi	South China	China	modern	*F. catus*	IV-A
FLI4	SRR15116525	10.1	N/A	Tajikistan	Central Asia	Tajikistan	modern	*F. ornata*	IV-A
FCAP0056	SRR7621254	10.52	283.96	Guangdong	South Coast of China	China	modern	*F. catus*	IV-A
FCAP0203	SRR7621252	9.48	830.91	Jiangsu	East Coast of China	China	modern	*F. catus*	IV-A
FCAP0219	SRR7621250	N/A	898.11	Zhejiang	East Coast of China	China	modern	*F. catus*	IV-A
FCAP0128	SRR7621225	12.63	2231.54	Hebei	North China	China	modern	*F. catus*	N/A
FSI51	ERR10494336-ERR10494341	21.21	N/A	Israel	the Levant	Israel	modern	*F. lybica*	IV-A
FSI47	ERR10494332	11.17	N/A	Israel	the Levant	Israel	modern	*F. lybica*	IV-A
FSX392	ERR10494345	12.09	N/A	Scotland	British Isles	Scotland	modern	*F. silvestris*	IV-A
FLI3	SRR15116526	9.04	N/A	Tajikistan	Central Asia	Tajikistan	modern	*F. ornata*	IV-A
FSI48	ERR10494333-ERR10494335	18.76	N/A	Israel	the Levant	Israel	modern	*F. lybica*	IV-B
FCAP0400	SRR7621207	N/A	729.82	Sichuan	Southwest China	China	modern	*F. catus*	IV-B
FCAP0404	SRR7621243	N/A	704.08	Sichuan	Southwest China	China	modern	*F. catus*	IV-B
FCAP0432	SRR7621244	N/A	861.71	Sichuan	Southwest China	China	modern	*F. catus*	IV-B
FCAP0401	SRR7621206	N/A	510.36	Sichuan	Southwest China	China	modern	*F. catus*	IV-B
FCAP0066	SRR7621232	N/A	325.04	Guangdong	South Coast of China	China	modern	*F. catus*	IV-B
FCAP0137	SRR7621218	N/A	801.72	Beijing	North China	China	modern	*F. catus*	IV-B
FCAP0069	SRR7621230	N/A	436.44	Guangdong	South Coast of China	China	modern	*F. catus*	IV-B
FCAP0263	SRR7621223	N/A	790.72	Shannxi	North China	China	modern	*F. catus*	IV-B
FCAP0055	SRR7621255	N/A	376.78	Guangdong	South Coast of China	China	modern	*F. catus*	IV-B
FCAP0072	provided by PKU	N/A	756.09	Guangdong	South Coast of China	China	modern	*F. catus*	IV-B
FCAP0221	provided by PKU	N/A	N/A	Zhejiang	East Coast of China	China	modern	*F. catus*	IV-B
FCAP0408	SRR7621242	N/A	585.48	Sichuan	Southwest China	China	modern	*F. catus*	IV-B
FCAP0373	SRR7621246	N/A	796.02	Sichuan	Southwest China	China	modern	*F. catus*	IV-B
FCAP0411	SRR7621245	N/A	620.53	Sichuan	Southwest China	China	modern	*F. catus*	IV-B
FCAP0444	SRR7621247	N/A	1125.63	Sichuan	Southwest China	China	modern	*F. catus*	IV-B
FCAP0309	SRR7621211	N/A	1053.49	Gansu	West China	China	modern	*F. catus*	IV-B
FCAP0333	SRR7621248	N/A	681.41	Gansu	West China	China	modern	*F. catus*	IV-B
FCAP0102	SRR7621240	N/A	669.54	Hunan	South China	China	modern	*F. catus*	IV-B
FCAP0172	SRR7621217	N/A	1040.97	Shandong	Central China	China	modern	*F. catus*	IV-B
FCAP0268	SRR7621224	N/A	1091.05	Shannxi	North China	China	modern	*F. catus*	IV-B
FCAP0315	SRR7621209	N/A	1084.61	Gansu	West China	China	modern	*F. catus*	IV-B
FCAP0420	SRR7621208	N/A	615.50	Qinghai	West China	China	modern	*F. catus*	IV-B
FCAP0427	SRR7621215	N/A	1132.00	Qinghai	West China	China	modern	*F. catus*	IV-B
FCAP0130	SRR7621219	N/A	600.37	Liaoning	North China	China	modern	*F. catus*	IV-B

Sample ID	Source	Mean depth (Nuc) X	Mean depth (mt) X	Location	Geographical Unit	Country	Date	Species	MT haplotype
FCAP0132	SRR7621220	N/A	984.46	Liaoning	North China	China	modern	*F. catus*	IV-B
FCAP0099	SRR7621241	N/A	408.39	Hunan	South China	China	modern	*F. catus*	IV-B
FCAP0235	SRR7621216	N/A	933.45	Liaoning	North China	China	modern	*F. catus*	IV-B
FCAP0393	SRR7621212	15.46	832.63	Qinghai	West China	China	modern	*F. catus*	IV-B
FCAP0383	SRR7621214	N/A	539.14	Qinghai	West China	China	modern	*F. catus*	IV-B
FCAP0392	SRR7621213	N/A	1589.83	Qinghai	West China	China	modern	*F. catus*	IV-B
SRR5040120	SRR5040120	14.67	N/A	Thailand	East Asia	Thailand	modern	*F. catus*	N/A
SRR5040126	SRR5040126	14.58	N/A	South Korea	East Asia	South Korea	modern	*F. catus*	N/A
SRR5040114	SRR5040114	9.95	N/A	Portugal	Mainland Europe	Portugal	modern	*F. catus*	N/A
SRR5040114	SRR5040114	9.95	N/A	Portugal	Mainland Europe	Portugal	modern	*F. catus*	N/A
SRR5040117	SRR5040117	13.04	N/A	Italy	Mainland Europe	Italy	modern	*F. catus*	N/A
FSI1	SRR8401848	16.78	N/A	Azerbaijan	Central Asia	Azerbaijan	modern	*F. silvestris*	N/A
FSX360	ERR10494342-ERR10494344	17.35	N/A	Portugal	Mainland Europe	Portugal	modern	*F. silvestris*	N/A
FSX405	ERR10494347 -ERR10494349	15.3	N/A	Scotland	British Isles	Scotland	modern	*F. silvestris*	N/A
FBIP0004	SRR7621226	13.20	911.04	Gansu	West China	China	modern	*F. bieti*	N/A
FBIP0008	SRR7621227	11.48	929.99	Sichuan	Southwest China	China	modern	*F. bieti*	N/A
FBIP0003	SRR7621229	11.90	871.06	Qinghai	West China	China	modern	*F. bieti*	N/A
FSIP0006	SRR7621238	11.08	4789.78	Xinjiang	West China	China	modern	*F. ornata*	N/A
FBIP0026	SRR7621235	11.87	642.33	Gansu	West China	China	modern	*F. bieti*	N/A
FSI204	ERR10494331	10.74	N/A	Kazakhstan	Central Asia	Kazakhstan	modern	*F. ornata*	N/A
SRR2062538	SRR2062538	N/A	N/A	N/A	N/A	N/A	modern	*F. margarita*	N/A
FMA8	ERR10494328-ERR10494330	22.74	N/A	N/A	N/A	N/A	modern	*F. margarita*	N/A

Table S1. (D) Information of Leopard cat and fishing cat samples from other studies.

ID	Source	location	Mean_depth (Nuc)X	Mean_depth (mt)X	Date	MT_haplotype
PBEP0014	SRR4426166	Russian Far East	12.17	1719	modern	PBE-RFE
PBEP0023	SRR4426167	Russian Far East	11.1209	621	modern	PBE-RFE
PBEP0010	SRR4426164	Russian Far East	N/A	747	modern	PBE-RFE
PVIP0012	SRR4426169	N/A	13.9554	612	modern	PVI
PBEP0005	SRR4426170	Sunda	11.3489	530	modern	PBE-Sunda
PBEP0008	SRR4426171	Sunda	11.7308	1415	modern	PBE-Sunda
PBEP0009	SRR4426172	Sunda	11.0208	1094	modern	PBE-Sunda
PBEP0068	SRR4426173	Indochina	13.1926	1800	modern	PBE-Indochina
PBEP0069	SRR4426174	Indochina	11.9837	948	modern	PBE-Indochina
PBEP0066	SRR4426175	Indochina	11.4505	579	modern	PBE-Indochina
PBEP0067	SRR4426176	Indochina	11.6046	1216	modern	PBE-Indochina
PBEP0064	SRR4426177	Indochina	11.3286	911	modern	PBE-Indochina
PBEP0065	SRR4426178	Indochina	11.4206	1302	modern	PBE-Indochina
PBEP0038	SRR4426179	Malay	13.0935	1320	modern	PBE-Sunda
PBEP0039	SRR4426180	Malay	12.8588	840	modern	PBE-Indochina
PBEP0028	SRR4426181	Malay	12.7609	1209	modern	PBE-Sunda
PBEP0036	SRR4426182	Malay	11.7445	2397	modern	PBE-Sunda
PBEP0026	SRR4426163	Malay	N/A	1324	modern	PBE-Sunda
PBEP0025	SRR4426162	Malay	N/A	1290	modern	PBE-Sunda
NC_016189.1	N/A	N/A	N/A	N/A	modern	PBE-RFE
NC_028301.1	N/A	N/A	N/A	N/A	modern	PBE-Sunda

Table S2. Radiocarbon dating of small cat specimens from archeological sites of China.

ID	Site	Location	Context date	Uncalibrated date (BP)	Date cal. BCE/CE (95.4%, overall range IntCal 20)
FS12	Tongwan City	Western China	Song Dynasty	1,220+/-20	706-728 cal CE (7.5%) (1,244 -1,222 cal BP) 772 - 883 cal CE (88.0%) (1,178 -1,067 cal BP)
FS13	Yangling Tomb	Central China	Han Dynasty	2,095+/-20	168 - 48 cal BCE (95.4%) (2,118 - 1,998 cal BP)
FS16	Zhengzhou Shang City	Central China	Tang Dynasty	450+/-30	1,413 - 1,480 cal CE (95.4%) (537 - 470 cal BP)
FS17	Shanliangzi	Northern China	Han Dynasty	140+/-30	1,797 - 1,944 cal CE (153 - 6 cal BP) (58.2%); 1,671 - 1,779 cal CE (37.2%) (279 - 171 cal BP)
FS19	Zheng and Han City	Central China	Han Dynasty	1,760+/-30	200 - 380 cal CE (95.4%) (1,750 - 1,570 cal BP)
FS24	Han Chang'an City	Central China	Han Dynasty	1,995+/-20	44 cal BCE - 76 cal CE (95.4%) (1,994 -1,874 cal BP)

Notes: Six samples were submitted for accelerator mass spectrometry (AMS) dating. Three samples (FS16, FS17, and FS19) were dated at Beta Analytic in the United States, while the remaining samples (FS12, FS13, and FS24) were processed at the School of Archaeology, Peking University, China. All radiocarbon dates reported were calibrated using the INTCAL20 calibration curve (Reimer et al., 2020).

Table S3. Pairwise outgroup f3-statistics of ancient and modern leopard cats (Data of Fig. S10)

Pop1	Pop2	Outgroup	f_3	std.err	Z	SNPs
FS15	FS15	*Felis catus*	0	-1	0	-1
FS15	FS8	*Felis catus*	94.479252	3.161095	29.888	703660
FS15	FS19	*Felis catus*	99.536262	3.275273	30.39	642087
FS15	PBEP0014	*Felis catus*	82.320955	2.499533	32.935	785997
FS15	PBEP0023	*Felis catus*	82.094914	2.511656	32.686	780733
FS15	PVIP0012	*Felis catus*	28.737047	0.917571	31.319	700068
FS15	PBEP0005	*Felis catus*	46.123892	1.4261	32.343	858528
FS15	PBEP0008	*Felis catus*	46.164718	1.428339	32.321	857682
FS15	PBEP0009	*Felis catus*	45.917531	1.403135	32.725	858237
FS15	PBEP0068	*Felis catus*	69.950411	2.10229	33.273	894240
FS15	PBEP0069	*Felis catus*	71.417436	2.211924	32.287	882128
FS15	PBEP0066	*Felis catus*	70.576964	2.153776	32.769	884207
FS15	PBEP0067	*Felis catus*	70.503829	2.15352	32.739	851996
FS15	PBEP0064	*Felis catus*	70.628207	2.143967	32.943	885700
FS15	PBEP0065	*Felis catus*	70.682337	2.159481	32.731	887683
FS15	PBEP0038	*Felis catus*	62.92979	1.919277	32.788	915250
FS15	PBEP0039	*Felis catus*	65.392363	1.992234	32.824	907600
FS15	PBEP0028	*Felis catus*	54.652416	1.671718	32.692	911959
FS15	PBEP0036	*Felis catus*	57.967153	1.790102	32.382	907314
FS8	FS8	*Felis catus*	0	-1	0	-1
FS8	FS15	*Felis catus*	94.479252	3.161095	29.888	703660
FS8	FS19	*Felis catus*	96.856843	3.252197	29.782	760198
FS8	PBEP0014	*Felis catus*	79.309033	2.459222	32.25	974613
FS8	PBEP0023	*Felis catus*	78.955336	2.462822	32.059	969790
FS8	PVIP0012	*Felis catus*	28.183928	0.906908	31.077	888823
FS8	PBEP0005	*Felis catus*	45.603351	1.436178	31.753	1074427
FS8	PBEP0008	*Felis catus*	45.538826	1.439044	31.645	1072055
FS8	PBEP0009	*Felis catus*	45.358966	1.405665	32.269	1073212
FS8	PBEP0068	*Felis catus*	68.206189	2.100244	32.475	1107559
FS8	PBEP0069	*Felis catus*	69.39284	2.205899	31.458	1090504
FS8	PBEP0066	*Felis catus*	68.65733	2.146608	31.984	1094816
FS8	PBEP0067	*Felis catus*	68.672333	2.137885	32.122	1055827
FS8	PBEP0064	*Felis catus*	68.828178	2.138988	32.178	1095339
FS8	PBEP0065	*Felis catus*	68.826358	2.144858	32.089	1098540
FS8	PBEP0038	*Felis catus*	61.557468	1.923598	32.001	1135282
FS8	PBEP0039	*Felis catus*	64.069036	1.998685	32.056	1123996
FS8	PBEP0028	*Felis catus*	53.800577	1.676275	32.095	1134106
FS8	PBEP0036	*Felis catus*	56.795691	1.798561	31.578	1126856
FS19	FS19	*Felis catus*	0	-1	0	-1
FS19	FS15	*Felis catus*	99.536262	3.275273	30.39	642087
FS19	FS8	*Felis catus*	96.856843	3.252197	29.782	760198
FS19	PBEP0014	*Felis catus*	87.648307	2.650553	33.068	852906
FS19	PBEP0023	*Felis catus*	87.220844	2.666313	32.712	847048
FS19	PVIP0012	*Felis catus*	30.388756	0.97351	31.216	766663
FS19	PBEP0005	*Felis catus*	49.332079	1.51644	32.532	940866
FS19	PBEP0008	*Felis catus*	49.320579	1.528168	32.274	939748
FS19	PBEP0009	*Felis catus*	49.121241	1.508188	32.57	940176
FS19	PBEP0068	*Felis catus*	75.043667	2.265701	33.122	974334
FS19	PBEP0069	*Felis catus*	75.997938	2.354484	32.278	962071
FS19	PBEP0066	*Felis catus*	75.1633	2.299679	32.684	964114
FS19	PBEP0067	*Felis catus*	75.071234	2.287896	32.812	928363
FS19	PBEP0064	*Felis catus*	75.280656	2.28575	32.935	965174
FS19	PBEP0065	*Felis catus*	75.449196	2.293242	32.901	966873
FS19	PBEP0038	*Felis catus*	67.478661	2.06905	32.613	998387

Pop1	Pop2	Outgroup	f_3	std.err	Z	SNPs
FS19	PBEP0039	*Felis catus*	69.956229	2.136028	32.751	990065
FS19	PBEP0028	*Felis catus*	58.522595	1.79248	32.649	997491
FS19	PBEP0036	*Felis catus*	61.711387	1.896681	32.537	992332
PBEP0014	PBEP0014	*Felis catus*	0	-1	0	-1
PBEP0014	FS15	*Felis catus*	82.320955	2.499533	32.935	785997
PBEP0014	FS8	*Felis catus*	79.309033	2.459222	32.25	974613
PBEP0014	FS19	*Felis catus*	87.648307	2.650553	33.068	852906
PBEP0014	PBEP0023	*Felis catus*	66.197117	2.082669	31.785	1190087
PBEP0014	PVIP0012	*Felis catus*	23.948674	0.758141	31.589	1186896
PBEP0014	PBEP0005	*Felis catus*	37.477295	1.185413	31.615	1377780
PBEP0014	PBEP0008	*Felis catus*	37.671307	1.204158	31.284	1371085
PBEP0014	PBEP0009	*Felis catus*	37.416043	1.177416	31.778	1376009
PBEP0014	PBEP0068	*Felis catus*	53.490127	1.666208	32.103	1419107
PBEP0014	PBEP0069	*Felis catus*	54.881495	1.770938	30.99	1379219
PBEP0014	PBEP0066	*Felis catus*	54.002324	1.700729	31.752	1394879
PBEP0014	PBEP0067	*Felis catus*	53.889496	1.691444	31.86	1349399
PBEP0014	PBEP0064	*Felis catus*	54.118805	1.708585	31.675	1393811
PBEP0014	PBEP0065	*Felis catus*	54.12236	1.701883	31.801	1399547
PBEP0014	PBEP0038	*Felis catus*	48.951724	1.532748	31.937	1449191
PBEP0014	PBEP0039	*Felis catus*	50.68284	1.589837	31.879	1429287
PBEP0014	PBEP0028	*Felis catus*	43.426948	1.377289	31.531	1445233
PBEP0014	PBEP0036	*Felis catus*	45.649228	1.458796	31.292	1430275
PBEP0023	PBEP0023	*Felis catus*	0	-1	0	-1
PBEP0023	FS15	*Felis catus*	82.094914	2.511656	32.686	780733
PBEP0023	FS8	*Felis catus*	78.955336	2.462822	32.059	969790
PBEP0023	FS19	*Felis catus*	87.220844	2.666313	32.712	847048
PBEP0023	PBEP0014	*Felis catus*	66.197117	2.082669	31.785	1190087
PBEP0023	PVIP0012	*Felis catus*	23.837789	0.760999	31.324	1174225
PBEP0023	PBEP0005	*Felis catus*	37.35184	1.195286	31.249	1366269
PBEP0023	PBEP0008	*Felis catus*	37.504124	1.215381	30.858	1359709
PBEP0023	PBEP0009	*Felis catus*	37.248091	1.187525	31.366	1364656
PBEP0023	PBEP0068	*Felis catus*	53.251322	1.677011	31.754	1410661
PBEP0023	PBEP0069	*Felis catus*	54.652481	1.789079	30.548	1370795
PBEP0023	PBEP0066	*Felis catus*	53.74023	1.716968	31.299	1386675
PBEP0023	PBEP0067	*Felis catus*	53.715082	1.708844	31.434	1340270
PBEP0023	PBEP0064	*Felis catus*	53.891182	1.714463	31.433	1385607
PBEP0023	PBEP0065	*Felis catus*	53.891158	1.713174	31.457	1391553
PBEP0023	PBEP0038	*Felis catus*	48.685729	1.54992	31.412	1441364
PBEP0023	PBEP0039	*Felis catus*	50.451412	1.603709	31.459	1420513
PBEP0023	PBEP0028	*Felis catus*	43.196526	1.382828	31.238	1435808
PBEP0023	PBEP0036	*Felis catus*	45.449093	1.469906	30.92	1420822
PVIP0012	PVIP0012	*Felis catus*	0	-1	0	-1
PVIP0012	FS15	*Felis catus*	28.737047	0.917571	31.319	700068
PVIP0012	FS8	*Felis catus*	28.183928	0.906908	31.077	888823
PVIP0012	FS19	*Felis catus*	30.388756	0.97351	31.216	766663
PVIP0012	PBEP0014	*Felis catus*	23.948674	0.758141	31.589	1186896
PVIP0012	PBEP0023	*Felis catus*	23.837789	0.760999	31.324	1174225
PVIP0012	PBEP0005	*Felis catus*	25.634429	0.832234	30.802	1039423
PVIP0012	PBEP0008	*Felis catus*	25.673187	0.844428	30.403	1032625
PVIP0012	PBEP0009	*Felis catus*	25.638723	0.825598	31.055	1037937
PVIP0012	PBEP0068	*Felis catus*	24.329028	0.767674	31.692	1298418
PVIP0012	PBEP0069	*Felis catus*	24.554984	0.814497	30.147	1244679
PVIP0012	PBEP0066	*Felis catus*	24.290088	0.777031	31.26	1265061
PVIP0012	PBEP0067	*Felis catus*	24.293093	0.780768	31.114	1200500
PVIP0012	PBEP0064	*Felis catus*	24.218761	0.776431	31.192	1265322

Pop1	Pop2	Outgroup	f_3	std.err	Z	SNPs
PVIP0012	PBEP0065	*Felis catus*	24.356293	0.783999	31.067	1272804
PVIP0012	PBEP0038	*Felis catus*	24.560739	0.782955	31.369	1278932
PVIP0012	PBEP0039	*Felis catus*	24.501967	0.786403	31.157	1269500
PVIP0012	PBEP0028	*Felis catus*	25.061814	0.803433	31.193	1202629
PVIP0012	PBEP0036	*Felis catus*	24.969234	0.808118	30.898	1209863
PBEP0005	PBEP0005	*Felis catus*	0	-1	0	-1
PBEP0005	FS15	*Felis catus*	46.123892	1.4261	32.343	858528
PBEP0005	FS8	*Felis catus*	45.603351	1.436178	31.753	1074427
PBEP0005	FS19	*Felis catus*	49.332079	1.51644	32.532	940866
PBEP0005	PBEP0014	*Felis catus*	37.477295	1.185413	31.615	1377780
PBEP0005	PBEP0023	*Felis catus*	37.35184	1.195286	31.249	1366269
PBEP0005	PVIP0012	*Felis catus*	25.634429	0.832234	30.802	1039423
PBEP0005	PBEP0008	*Felis catus*	59.109367	1.954609	30.241	1046564
PBEP0005	PBEP0009	*Felis catus*	58.574828	1.900872	30.815	1052285
PBEP0005	PBEP0068	*Felis catus*	38.187278	1.224464	31.187	1466928
PBEP0005	PBEP0069	*Felis catus*	38.972885	1.292857	30.145	1424331
PBEP0005	PBEP0066	*Felis catus*	38.377598	1.235497	31.062	1441564
PBEP0005	PBEP0067	*Felis catus*	38.422704	1.239383	31.001	1384954
PBEP0005	PBEP0064	*Felis catus*	38.320087	1.237798	30.958	1442591
PBEP0005	PBEP0065	*Felis catus*	38.46402	1.24436	30.911	1448224
PBEP0005	PBEP0038	*Felis catus*	43.72363	1.403629	31.15	1392550
PBEP0005	PBEP0039	*Felis catus*	42.41455	1.37545	30.837	1402302
PBEP0005	PBEP0028	*Felis catus*	50.648952	1.643772	30.813	1261340
PBEP0005	PBEP0036	*Felis catus*	48.824514	1.58665	30.772	1290000
PBEP0008	PBEP0008	*Felis catus*	0	-1	0	-1
PBEP0008	FS15	*Felis catus*	46.164718	1.428339	32.321	857682
PBEP0008	FS8	*Felis catus*	45.538826	1.439044	31.645	1072055
PBEP0008	FS19	*Felis catus*	49.320579	1.528168	32.274	939748
PBEP0008	PBEP0014	*Felis catus*	37.671307	1.204158	31.284	1371085
PBEP0008	PBEP0023	*Felis catus*	37.504124	1.215381	30.858	1359709
PBEP0008	PVIP0012	*Felis catus*	25.673187	0.844428	30.403	1032625
PBEP0008	PBEP0005	*Felis catus*	59.109367	1.954609	30.241	1046564
PBEP0008	PBEP0009	*Felis catus*	58.850098	1.936179	30.395	1046302
PBEP0008	PBEP0068	*Felis catus*	38.376315	1.24739	30.765	1458998
PBEP0008	PBEP0069	*Felis catus*	39.171144	1.314889	29.79	1419140
PBEP0008	PBEP0066	*Felis catus*	38.564098	1.259783	30.612	1434541
PBEP0008	PBEP0067	*Felis catus*	38.617735	1.261538	30.612	1378483
PBEP0008	PBEP0064	*Felis catus*	38.535139	1.25923	30.602	1436094
PBEP0008	PBEP0065	*Felis catus*	38.647117	1.265993	30.527	1441722
PBEP0008	PBEP0038	*Felis catus*	43.885647	1.430986	30.668	1385733
PBEP0008	PBEP0039	*Felis catus*	42.62025	1.396354	30.523	1396048
PBEP0008	PBEP0028	*Felis catus*	50.883481	1.662097	30.614	1255154
PBEP0008	PBEP0036	*Felis catus*	49.032855	1.617148	30.321	1285300
PBEP0009	PBEP0009	*Felis catus*	0	-1	0	-1
PBEP0009	FS15	*Felis catus*	45.917531	1.403135	32.725	858237
PBEP0009	FS8	*Felis catus*	45.358966	1.405665	32.269	1073212
PBEP0009	FS19	*Felis catus*	49.121241	1.508188	32.57	940176
PBEP0009	PBEP0014	*Felis catus*	37.416043	1.177416	31.778	1376009
PBEP0009	PBEP0023	*Felis catus*	37.248091	1.187525	31.366	1364656
PBEP0009	PVIP0012	*Felis catus*	25.638723	0.825598	31.055	1037937
PBEP0009	PBEP0005	*Felis catus*	58.574828	1.900872	30.815	1052285
PBEP0009	PBEP0008	*Felis catus*	58.850098	1.936179	30.395	1046302
PBEP0009	PBEP0068	*Felis catus*	38.118426	1.216623	31.331	1465594
PBEP0009	PBEP0069	*Felis catus*	38.861658	1.284087	30.264	1422781
PBEP0009	PBEP0066	*Felis catus*	38.251629	1.225227	31.22	1440249

Pop1	Pop2	Outgroup	f_3	std.err	Z	SNPs
PBEP0009	PBEP0067	*Felis catus*	38.330881	1.235669	31.02	1383051
PBEP0009	PBEP0064	*Felis catus*	38.248548	1.229581	31.107	1440539
PBEP0009	PBEP0065	*Felis catus*	38.352801	1.237209	30.999	1446463
PBEP0009	PBEP0038	*Felis catus*	43.641591	1.394671	31.292	1391361
PBEP0009	PBEP0039	*Felis catus*	42.336655	1.367342	30.963	1400471
PBEP0009	PBEP0028	*Felis catus*	50.585553	1.634403	30.95	1259817
PBEP0009	PBEP0036	*Felis catus*	48.71554	1.581173	30.81	1288682
PBEP0068	PBEP0068	*Felis catus*	0	-1	0	-1
PBEP0068	FS15	*Felis catus*	69.950411	2.10229	33.273	894240
PBEP0068	FS8	*Felis catus*	68.206189	2.100244	32.475	1107559
PBEP0068	FS19	*Felis catus*	75.043667	2.265701	33.122	974334
PBEP0068	PBEP0014	*Felis catus*	53.490127	1.666208	32.103	1419107
PBEP0068	PBEP0023	*Felis catus*	53.251322	1.677011	31.754	1410661
PBEP0068	PVIP0012	*Felis catus*	24.329028	0.767674	31.692	1298418
PBEP0068	PBEP0005	*Felis catus*	38.187278	1.224464	31.187	1466928
PBEP0068	PBEP0008	*Felis catus*	38.376315	1.24739	30.765	1458998
PBEP0068	PBEP0009	*Felis catus*	38.118426	1.216623	31.331	1465594
PBEP0068	PBEP0069	*Felis catus*	58.441624	1.913531	30.541	1411327
PBEP0068	PBEP0066	*Felis catus*	57.58135	1.824227	31.565	1426744
PBEP0068	PBEP0067	*Felis catus*	56.680701	1.803141	31.434	1398764
PBEP0068	PBEP0064	*Felis catus*	56.393183	1.796036	31.399	1443298
PBEP0068	PBEP0065	*Felis catus*	56.737073	1.812383	31.305	1446165
PBEP0068	PBEP0038	*Felis catus*	50.571	1.608067	31.448	1511299
PBEP0068	PBEP0039	*Felis catus*	52.322734	1.654707	31.621	1487696
PBEP0068	PBEP0028	*Felis catus*	44.533386	1.423341	31.288	1518078
PBEP0068	PBEP0036	*Felis catus*	46.901036	1.520153	30.853	1498384
PBEP0069	PBEP0069	*Felis catus*	0	-1	0	-1
PBEP0069	FS15	*Felis catus*	71.417436	2.211924	32.287	882128
PBEP0069	FS8	*Felis catus*	69.39284	2.205899	31.458	1090504
PBEP0069	FS19	*Felis catus*	75.997938	2.354484	32.278	962071
PBEP0069	PBEP0014	*Felis catus*	54.881495	1.770938	30.99	1379219
PBEP0069	PBEP0023	*Felis catus*	54.652481	1.789079	30.548	1370795
PBEP0069	PVIP0012	*Felis catus*	24.554984	0.814497	30.147	1244679
PBEP0069	PBEP0005	*Felis catus*	38.972885	1.292857	30.145	1424331
PBEP0069	PBEP0008	*Felis catus*	39.171144	1.314889	29.79	1419140
PBEP0069	PBEP0009	*Felis catus*	38.861658	1.284087	30.264	1422781
PBEP0069	PBEP0068	*Felis catus*	58.441624	1.913531	30.541	1411327
PBEP0069	PBEP0066	*Felis catus*	58.552373	1.922908	30.45	1395854
PBEP0069	PBEP0067	*Felis catus*	57.836758	1.902992	30.393	1363949
PBEP0069	PBEP0064	*Felis catus*	57.746294	1.89774	30.429	1407299
PBEP0069	PBEP0065	*Felis catus*	58.039258	1.919653	30.234	1410521
PBEP0069	PBEP0038	*Felis catus*	51.890591	1.71557	30.247	1468425
PBEP0069	PBEP0039	*Felis catus*	53.71418	1.762043	30.484	1450464
PBEP0069	PBEP0028	*Felis catus*	45.55532	1.507132	30.226	1477220
PBEP0069	PBEP0036	*Felis catus*	47.900895	1.604823	29.848	1461155
PBEP0066	PBEP0066	*Felis catus*	0	-1	0	-1
PBEP0066	FS15	*Felis catus*	70.576964	2.153776	32.769	884207
PBEP0066	FS8	*Felis catus*	68.65733	2.146608	31.984	1094816
PBEP0066	FS19	*Felis catus*	75.1633	2.299679	32.684	964114
PBEP0066	PBEP0014	*Felis catus*	54.002324	1.700729	31.752	1394879
PBEP0066	PBEP0023	*Felis catus*	53.74023	1.716968	31.299	1386675
PBEP0066	PVIP0012	*Felis catus*	24.290088	0.777031	31.26	1265061
PBEP0066	PBEP0005	*Felis catus*	38.377598	1.235497	31.062	1441564
PBEP0066	PBEP0008	*Felis catus*	38.564098	1.259783	30.612	1434541
PBEP0066	PBEP0009	*Felis catus*	38.251629	1.225227	31.22	1440249

Pop1	Pop2	Outgroup	f_3	std.err	Z	SNPs
PBEP0066	PBEP0068	*Felis catus*	57.58135	1.824227	31.565	1426744
PBEP0066	PBEP0069	*Felis catus*	58.552373	1.922908	30.45	1395854
PBEP0066	PBEP0067	*Felis catus*	57.043378	1.830176	31.168	1377887
PBEP0066	PBEP0064	*Felis catus*	56.830802	1.8231	31.173	1421893
PBEP0066	PBEP0065	*Felis catus*	57.080744	1.832016	31.157	1425738
PBEP0066	PBEP0038	*Felis catus*	50.912261	1.634442	31.15	1487144
PBEP0066	PBEP0039	*Felis catus*	52.786739	1.686925	31.292	1465598
PBEP0066	PBEP0028	*Felis catus*	44.785824	1.435889	31.19	1493950
PBEP0066	PBEP0036	*Felis catus*	47.165809	1.535822	30.71	1476621
PBEP0067	PBEP0067	*Felis catus*	0	-1	0	-1
PBEP0067	FS15	*Felis catus*	70.503829	2.15352	32.739	851996
PBEP0067	FS8	*Felis catus*	68.672333	2.137885	32.122	1055827
PBEP0067	FS19	*Felis catus*	75.071234	2.287896	32.812	928363
PBEP0067	PBEP0014	*Felis catus*	53.889496	1.691444	31.86	1349399
PBEP0067	PBEP0023	*Felis catus*	53.715082	1.708844	31.434	1340270
PBEP0067	PVIP0012	*Felis catus*	24.293093	0.780768	31.114	1200500
PBEP0067	PBEP0005	*Felis catus*	38.422704	1.239383	31.001	1384954
PBEP0067	PBEP0008	*Felis catus*	38.617735	1.261538	30.612	1378483
PBEP0067	PBEP0009	*Felis catus*	38.330881	1.235669	31.02	1383051
PBEP0067	PBEP0068	*Felis catus*	56.680701	1.803141	31.434	1398764
PBEP0067	PBEP0069	*Felis catus*	57.836758	1.902992	30.393	1363949
PBEP0067	PBEP0066	*Felis catus*	57.043378	1.830176	31.168	1377887
PBEP0067	PBEP0064	*Felis catus*	57.033927	1.826729	31.222	1378841
PBEP0067	PBEP0065	*Felis catus*	57.425261	1.845202	31.121	1380255
PBEP0067	PBEP0038	*Felis catus*	50.865001	1.628588	31.233	1444001
PBEP0067	PBEP0039	*Felis catus*	52.606408	1.68338	31.25	1424429
PBEP0067	PBEP0028	*Felis catus*	44.835111	1.441555	31.102	1445197
PBEP0067	PBEP0036	*Felis catus*	47.149441	1.536355	30.689	1429407
PBEP0064	PBEP0064	*Felis catus*	0	-1	0	-1
PBEP0064	FS15	*Felis catus*	70.628207	2.143967	32.943	885700
PBEP0064	FS8	*Felis catus*	68.828178	2.138988	32.178	1095339
PBEP0064	FS19	*Felis catus*	75.280656	2.28575	32.935	965174
PBEP0064	PBEP0014	*Felis catus*	54.118805	1.708585	31.675	1393811
PBEP0064	PBEP0023	*Felis catus*	53.891182	1.714463	31.433	1385607
PBEP0064	PVIP0012	*Felis catus*	24.218761	0.776431	31.192	1265322
PBEP0064	PBEP0005	*Felis catus*	38.320087	1.237798	30.958	1442591
PBEP0064	PBEP0008	*Felis catus*	38.535139	1.25923	30.602	1436094
PBEP0064	PBEP0009	*Felis catus*	38.248548	1.229581	31.107	1440539
PBEP0064	PBEP0068	*Felis catus*	56.393183	1.796036	31.399	1443298
PBEP0064	PBEP0069	*Felis catus*	57.746294	1.89774	30.429	1407299
PBEP0064	PBEP0066	*Felis catus*	56.830802	1.8231	31.173	1421893
PBEP0064	PBEP0067	*Felis catus*	57.033927	1.826729	31.222	1378841
PBEP0064	PBEP0065	*Felis catus*	57.47477	1.844152	31.166	1420493
PBEP0064	PBEP0038	*Felis catus*	50.949881	1.634895	31.164	1487328
PBEP0064	PBEP0039	*Felis catus*	52.791184	1.687717	31.28	1466847
PBEP0064	PBEP0028	*Felis catus*	44.772867	1.436449	31.169	1494998
PBEP0064	PBEP0036	*Felis catus*	47.143791	1.536757	30.677	1477374
PBEP0065	PBEP0065	*Felis catus*	0	-1	0	-1
PBEP0065	FS15	*Felis catus*	70.682337	2.159481	32.731	887683
PBEP0065	FS8	*Felis catus*	68.826358	2.144858	32.089	1098540
PBEP0065	FS19	*Felis catus*	75.449196	2.293242	32.901	966873
PBEP0065	PBEP0014	*Felis catus*	54.12236	1.701883	31.801	1399547
PBEP0065	PBEP0023	*Felis catus*	53.891158	1.713174	31.457	1391553
PBEP0065	PVIP0012	*Felis catus*	24.356293	0.783999	31.067	1272804
PBEP0065	PBEP0005	*Felis catus*	38.46402	1.24436	30.911	1448224

Pop1	Pop2	Outgroup	f_3	std.err	Z	SNPs
PBEP0065	PBEP0008	*Felis catus*	38.647117	1.265993	30.527	1441722
PBEP0065	PBEP0009	*Felis catus*	38.352801	1.237209	30.999	1446463
PBEP0065	PBEP0068	*Felis catus*	56.737073	1.812383	31.305	1446165
PBEP0065	PBEP0069	*Felis catus*	58.039258	1.919653	30.234	1410521
PBEP0065	PBEP0066	*Felis catus*	57.080744	1.832016	31.157	1425738
PBEP0065	PBEP0067	*Felis catus*	57.425261	1.845202	31.121	1380255
PBEP0065	PBEP0064	*Felis catus*	57.47477	1.844152	31.166	1420493
PBEP0065	PBEP0038	*Felis catus*	51.049324	1.641499	31.099	1493130
PBEP0065	PBEP0039	*Felis catus*	52.893594	1.693741	31.229	1471647
PBEP0065	PBEP0028	*Felis catus*	44.908315	1.455199	30.861	1499890
PBEP0065	PBEP0036	*Felis catus*	47.319543	1.547917	30.57	1482257
PBEP0038	PBEP0038	*Felis catus*	0	-1	0	-1
PBEP0038	FS15	*Felis catus*	62.92979	1.919277	32.788	915250
PBEP0038	FS8	*Felis catus*	61.557468	1.923598	32.001	1135282
PBEP0038	FS19	*Felis catus*	67.478661	2.06905	32.613	998387
PBEP0038	PBEP0014	*Felis catus*	48.951724	1.532748	31.937	1449191
PBEP0038	PBEP0023	*Felis catus*	48.685729	1.54992	31.412	1441364
PBEP0038	PVIP0012	*Felis catus*	24.560739	0.782955	31.369	1278932
PBEP0038	PBEP0005	*Felis catus*	43.72363	1.403629	31.15	1392550
PBEP0038	PBEP0008	*Felis catus*	43.885647	1.430986	30.668	1385733
PBEP0038	PBEP0009	*Felis catus*	43.641591	1.394671	31.292	1391361
PBEP0038	PBEP0068	*Felis catus*	50.571	1.608067	31.448	1511299
PBEP0038	PBEP0069	*Felis catus*	51.890591	1.71557	30.247	1468425
PBEP0038	PBEP0066	*Felis catus*	50.912261	1.634442	31.15	1487144
PBEP0038	PBEP0067	*Felis catus*	50.865001	1.628588	31.233	1444001
PBEP0038	PBEP0064	*Felis catus*	50.949881	1.634895	31.164	1487328
PBEP0038	PBEP0065	*Felis catus*	51.049324	1.641499	31.099	1493130
PBEP0038	PBEP0039	*Felis catus*	52.325796	1.674354	31.251	1462386
PBEP0038	PBEP0028	*Felis catus*	48.251508	1.536723	31.399	1453227
PBEP0038	PBEP0036	*Felis catus*	49.911117	1.611623	30.969	1441111
PBEP0039	PBEP0039	*Felis catus*	0	-1	0	-1
PBEP0039	FS15	*Felis catus*	65.392363	1.992234	32.824	907600
PBEP0039	FS8	*Felis catus*	64.069036	1.998685	32.056	1123996
PBEP0039	FS19	*Felis catus*	69.956229	2.136028	32.751	990065
PBEP0039	PBEP0014	*Felis catus*	50.68284	1.589837	31.879	1429287
PBEP0039	PBEP0023	*Felis catus*	50.451412	1.603709	31.459	1420513
PBEP0039	PVIP0012	*Felis catus*	24.501967	0.786403	31.157	1269500
PBEP0039	PBEP0005	*Felis catus*	42.41455	1.37545	30.837	1402302
PBEP0039	PBEP0008	*Felis catus*	42.62025	1.396354	30.523	1396048
PBEP0039	PBEP0009	*Felis catus*	42.336655	1.367342	30.963	1400471
PBEP0039	PBEP0068	*Felis catus*	52.322734	1.654707	31.621	1487696
PBEP0039	PBEP0069	*Felis catus*	53.71418	1.762043	30.484	1450464
PBEP0039	PBEP0066	*Felis catus*	52.786739	1.686925	31.292	1465598
PBEP0039	PBEP0067	*Felis catus*	52.606408	1.68338	31.25	1424429
PBEP0039	PBEP0064	*Felis catus*	52.791184	1.687717	31.28	1466847
PBEP0039	PBEP0065	*Felis catus*	52.893594	1.693741	31.229	1471647
PBEP0039	PBEP0038	*Felis catus*	52.325796	1.674354	31.251	1462386
PBEP0039	PBEP0028	*Felis catus*	47.650117	1.532367	31.096	1459517
PBEP0039	PBEP0036	*Felis catus*	49.743939	1.61294	30.841	1444072
PBEP0028	PBEP0028	*Felis catus*	0	-1	0	-1
PBEP0028	FS15	*Felis catus*	54.652416	1.671718	32.692	911959
PBEP0028	FS8	*Felis catus*	53.800577	1.676275	32.095	1134106
PBEP0028	FS19	*Felis catus*	58.522595	1.79248	32.649	997491
PBEP0028	PBEP0014	*Felis catus*	43.426948	1.377289	31.531	1445233
PBEP0028	PBEP0023	*Felis catus*	43.196526	1.382828	31.238	1435808

Pop1	Pop2	Outgroup	f_3	std.err	Z	SNPs
PBEP0028	PVIP0012	*Felis catus*	25.061814	0.803433	31.193	1202629
PBEP0028	PBEP0005	*Felis catus*	50.648952	1.643772	30.813	1261340
PBEP0028	PBEP0008	*Felis catus*	50.883481	1.662097	30.614	1255154
PBEP0028	PBEP0009	*Felis catus*	50.585553	1.634403	30.95	1259817
PBEP0028	PBEP0068	*Felis catus*	44.533386	1.423341	31.288	1518078
PBEP0028	PBEP0069	*Felis catus*	45.55532	1.507132	30.226	1477220
PBEP0028	PBEP0066	*Felis catus*	44.785824	1.435889	31.19	1493950
PBEP0028	PBEP0067	*Felis catus*	44.835111	1.441555	31.102	1445197
PBEP0028	PBEP0064	*Felis catus*	44.772867	1.436449	31.169	1494998
PBEP0028	PBEP0065	*Felis catus*	44.908315	1.455199	30.861	1499890
PBEP0028	PBEP0038	*Felis catus*	48.251508	1.536723	31.399	1453227
PBEP0028	PBEP0039	*Felis catus*	47.650117	1.532367	31.096	1459517
PBEP0028	PBEP0036	*Felis catus*	51.988861	1.676199	31.016	1360165
PBEP0036	PBEP0036	*Felis catus*	0	-1	0	-1
PBEP0036	FS15	*Felis catus*	57.967153	1.790102	32.382	907314
PBEP0036	FS8	*Felis catus*	56.795691	1.798561	31.578	1126856
PBEP0036	FS19	*Felis catus*	61.711387	1.896681	32.537	992332
PBEP0036	PBEP0014	*Felis catus*	45.649228	1.458796	31.292	1430275
PBEP0036	PBEP0023	*Felis catus*	45.449093	1.469906	30.92	1420822
PBEP0036	PVIP0012	*Felis catus*	24.969234	0.808118	30.898	1209863
PBEP0036	PBEP0005	*Felis catus*	48.824514	1.58665	30.772	1290000
PBEP0036	PBEP0008	*Felis catus*	49.032855	1.617148	30.321	1285300
PBEP0036	PBEP0009	*Felis catus*	48.71554	1.581173	30.81	1288682
PBEP0036	PBEP0068	*Felis catus*	46.901036	1.520153	30.853	1498384
PBEP0036	PBEP0069	*Felis catus*	47.900895	1.604823	29.848	1461155
PBEP0036	PBEP0066	*Felis catus*	47.165809	1.535822	30.71	1476621
PBEP0036	PBEP0067	*Felis catus*	47.149441	1.536355	30.689	1429407
PBEP0036	PBEP0064	*Felis catus*	47.143791	1.536757	30.677	1477374
PBEP0036	PBEP0065	*Felis catus*	47.319543	1.547917	30.57	1482257
PBEP0036	PBEP0038	*Felis catus*	49.911117	1.611623	30.969	1441111
PBEP0036	PBEP0039	*Felis catus*	49.743939	1.61294	30.841	1444072
PBEP0036	PBEP0028	*Felis catus*	51.988861	1.676199	31.016	1360165

Table S4. D-statistics of leopard cats from modern Asia and ancient China (Data of Fig. S11).

Outgroup	Pop1	Pop2	Pop3	D	std.err	Z	SNPs
Felis catus	PBEP0068	Russian Far East	FS8	0.001928	0.000114	16.92	2089721
Felis catus	PBEP0069	Russian Far East	FS8	0.002137	0.00012	17.775	2086193
Felis catus	PBEP0066	Russian Far East	FS8	0.002049	0.000116	17.679	2082559
Felis catus	PBEP0067	Russian Far East	FS8	0.001995	0.00012	16.601	2087328
Felis catus	PBEP0064	Russian Far East	FS8	0.002102	0.000117	17.903	2095996
Felis catus	PBEP0065	Russian Far East	FS8	0.001924	0.000118	16.301	2081063
Felis catus	PBEP0038	Russian Far East	FS8	0.001492	0.00011	13.516	2090739
Felis catus	PBEP0039	Russian Far East	FS8	0.001671	0.000107	15.668	2089949
Felis catus	PBEP0028	Russian Far East	FS8	0.000921	0.000089	10.387	2089592
Felis catus	PBEP0036	Russian Far East	FS8	0.001149	0.000092	12.492	2090655
Felis catus	PBEP0005	Russian Far East	FS8	0.000262	0.000071	3.703	2096009
Felis catus	PBEP0008	Russian Far East	FS8	0.000294	0.000074	3.954	2090335
Felis catus	PBEP0009	Russian Far East	FS8	0.000261	0.000073	3.573	2090861
Felis catus	PVIP0012	Russian Far East	FS8	0.000202	0.000064	3.173	2085955
Felis catus	PBEP0068	Russian Far East	FS15	0.002408	0.00015	16.032	2335310
Felis catus	PBEP0069	Russian Far East	FS15	0.002671	0.000148	18.103	2331886
Felis catus	PBEP0066	Russian Far East	FS15	0.002503	0.000149	16.786	2328008
Felis catus	PBEP0067	Russian Far East	FS15	0.002461	0.000155	15.885	2333039
Felis catus	PBEP0064	Russian Far East	FS15	0.002494	0.000152	16.439	2341941
Felis catus	PBEP0065	Russian Far East	FS15	0.002366	0.000155	15.312	2326744
Felis catus	PBEP0038	Russian Far East	FS15	0.0017	0.000138	12.338	2336410
Felis catus	PBEP0039	Russian Far East	FS15	0.001881	0.000139	13.565	2335622
Felis catus	PBEP0028	Russian Far East	FS15	0.000912	0.000109	8.337	2335303
Felis catus	PBEP0036	Russian Far East	FS15	0.001289	0.000102	12.622	2336387
Felis catus	PBEP0005	Russian Far East	FS15	0.000297	0.000087	3.432	2342306
Felis catus	PBEP0008	Russian Far East	FS15	0.000306	0.000083	3.709	2336127
Felis catus	PBEP0009	Russian Far East	FS15	0.00028	0.000086	3.264	2336820
Felis catus	PVIP0012	Russian Far East	FS15	0.000264	0.000071	3.728	2331636
Felis catus	PBEP0068	Russian Far East	FS19	0.002581	0.00012	21.513	2613447
Felis catus	PBEP0069	Russian Far East	FS19	0.002805	0.000121	23.159	2608527
Felis catus	PBEP0066	Russian Far East	FS19	0.002478	0.000121	20.545	2603553
Felis catus	PBEP0067	Russian Far East	FS19	0.002569	0.000122	21.055	2609780
Felis catus	PBEP0064	Russian Far East	FS19	0.002637	0.000118	22.31	2621480
Felis catus	PBEP0065	Russian Far East	FS19	0.002566	0.000118	21.719	2600836
Felis catus	PBEP0038	Russian Far East	FS19	0.001884	0.000108	17.379	2614086
Felis catus	PBEP0039	Russian Far East	FS19	0.002145	0.000107	20.029	2612845
Felis catus	PBEP0028	Russian Far East	FS19	0.00111	0.00009	12.295	2612407
Felis catus	PBEP0036	Russian Far East	FS19	0.00141	0.000093	15.156	2614254
Felis catus	PBEP0005	Russian Far East	FS19	0.000399	0.000075	5.324	2621116
Felis catus	PBEP0008	Russian Far East	FS19	0.000491	0.000076	6.437	2613456
Felis catus	PBEP0009	Russian Far East	FS19	0.000408	0.000078	5.198	2614325
Felis catus	PVIP0012	Russian Far East	FS19	0.000269	0.000066	4.061	2607464

Table S5. Pairwise f3-statistics of the genetic relationships between various populations of ancient or modern Felis species (Data of Fig. 3B).

Pop1	Pop2	Outgroup	f_3	std.err	Z	SNPs
FS1	Modern_China/East_Asia_catus	*Felis margarita*	180.21786	11.322142	15.92	81007
FS1	FS21	*Felis margarita*	179.38697	11.588262	15.48	50863
FS1	FS2	*Felis margarita*	175.83828	11.48101	15.32	53082
FS1	FS12	*Felis margarita*	172.01661	11.573873	14.86	58323
FS1	Levant lybica	*Felis margarita*	151.32251	9.438672	16.03	77866
FS1	Dhzankent	*Felis margarita*	150.71702	55.144777	2.733	1878
FS1	modern_European_catus	*Felis margarita*	139.11256	8.677047	16.03	81937
FS1	Ancient_European/Anatolia_catus	*Felis margarita*	122.01078	17.430569	7	8738
FS1	ornata	*Felis margarita*	119.73996	7.444453	16.08	66125
FS1	silvestries	*Felis margarita*	118.399	7.344451	16.09	70271
FS1	bieti	*Felis margarita*	112.93601	7.047862	16.02	60043
FS2	FS1	*Felis margarita*	175.83828	11.48101	15.32	53082
FS2	Modern_China/East_Asia_catus	*Felis margarita*	174.72111	11.255582	15.52	84297
FS2	FS21	*Felis margarita*	171.42282	11.359815	15.09	53303
FS2	FS12	*Felis margarita*	167.05408	11.598646	14.4	60457
FS2	Dhzankent	*Felis margarita*	165.10907	58.683773	2.814	1966
FS2	Levant lybica	*Felis margarita*	146.89282	9.435001	15.57	81263
FS2	modern_European_catus	*Felis margarita*	134.72156	8.629847	15.61	85434
FS2	ornata	*Felis margarita*	115.6054	7.403732	15.61	69362
FS2	Ancient_European/Anatolia_catus	*Felis margarita*	114.05922	14.730644	7.743	9158
FS2	silvestries	*Felis margarita*	113.90879	7.306579	15.59	73504
FS2	bieti	*Felis margarita*	109.28301	7.022039	15.56	63007
FS12	Dhzankent	*Felis margarita*	180.25164	77.922663	2.313	2125
FS12	Modern_China/East_Asia_catus	*Felis margarita*	172.25718	11.165351	15.43	91443
FS12	FS1	*Felis margarita*	172.01661	11.573873	14.86	58323
FS12	FS21	*Felis margarita*	171.49798	11.460161	14.97	57531
FS12	FS2	*Felis margarita*	167.05408	11.598646	14.4	60457
FS12	Levant lybica	*Felis margarita*	145.00226	9.403209	15.42	88355
FS12	modern_European_catus	*Felis margarita*	131.4479	8.489932	15.48	93524
FS12	ornata	*Felis margarita*	114.95499	7.393877	15.55	75907
FS12	Ancient_European/Anatolia_catus	*Felis margarita*	112.61497	15.776276	7.138	10099

Pop1	Pop2	Outgroup	f_3	std.err	Z	SNPs
FS12	silvestries	*Felis margarita*	111.98298	7.232932	15.48	80847
FS12	bieti	*Felis margarita*	108.95904	7.022332	15.52	69196
FS21	Modern_China/East_Asia_catus	*Felis margarita*	179.48462	11.363918	15.79	80396
FS21	FS1	*Felis margarita*	179.38697	11.588262	15.48	50863
FS21	FS12	*Felis margarita*	171.49798	11.460161	14.97	57531
FS21	FS2	*Felis margarita*	171.42282	11.359815	15.09	53303
FS21	Dhzankent	*Felis margarita*	160.43269	63.095555	2.543	1855
FS21	Levant lybica	*Felis margarita*	150.35494	9.507685	15.81	77340
FS21	modern_European_catus	*Felis margarita*	138.90525	8.728777	15.91	81089
FS21	Ancient_European/Anatolia_catus	*Felis margarita*	124.68283	17.452172	7.144	8715
FS21	ornata	*Felis margarita*	119.25503	7.460807	15.98	65445
FS21	silvestries	*Felis margarita*	117.79287	7.376722	15.97	69232
FS21	bieti	*Felis margarita*	112.53383	7.053864	15.95	59429
FS21	FS21	*Felis margarita*	0	-1	0	-1
Dhzankent	FS1	*Felis margarita*	150.71702	55.144777	2.733	1878
Dhzankent	FS2	*Felis margarita*	165.10907	58.683773	2.814	1966
Dhzankent	FS12	*Felis margarita*	180.25164	77.922663	2.313	2125
Dhzankent	FS21	*Felis margarita*	160.43269	63.095555	2.543	1855
Dhzankent	Dhzankent	*Felis margarita*	0	-1	0	-1
Dhzankent	Ancient_European/Anatolia_catus	*Felis margarita*	116.97977	23.262014	5.029	5356
Dhzankent	Modern_China/East_Asia_catus	*Felis margarita*	120.93274	23.63015	5.118	7215
Dhzankent	modern_European_catus	*Felis margarita*	109.55539	21.377054	5.125	8111
Dhzankent	Levant lybica	*Felis margarita*	113.87666	22.249337	5.118	6969
Dhzankent	silvestries	*Felis margarita*	97.587149	19.052361	5.122	6541
Dhzankent	ornata	*Felis margarita*	96.563797	18.809416	5.134	5567
Dhzankent	bieti	*Felis margarita*	91.958451	17.888265	5.141	4915
Modern China/E Asia_cat	FS1	*Felis margarita*	180.21786	11.322142	15.92	81007
Modern China/E Asia_cat	FS2	*Felis margarita*	174.72111	11.255582	15.52	84297
Modern China/E Asia_cat	FS12	*Felis margarita*	172.25718	11.165351	15.43	91443
Modern China/E Asia_cat	FS21	*Felis margarita*	179.48462	11.363918	15.79	80396
Modern China/E Asia_cat	Dhzankent	*Felis margarita*	120.93274	23.63015	5.118	7215
Modern China/E Asia_cat	Ancient_European/Anatolia_catus	*Felis margarita*	85.16037	6.992342	12.18	30964

Pop1	Pop2	Outgroup	f_3	std.err	Z	SNPs
Modern China/E Asia_cat	Modern_China/East_Asia_catus	*Felis margarita*	0	-1	0	-1
Modern China/E Asia_cat	modern_European_catus	*Felis margarita*	98.470755	2.751153	35.79	350175
Modern China/E Asia_cat	Levant lybica	*Felis margarita*	99.70676	2.790807	35.73	342163
Modern China/E Asia_cat	silvestries	*Felis margarita*	91.460678	2.55638	35.78	350244
Modern China/E Asia_cat	ornata	*Felis margarita*	89.930103	2.514533	35.76	338484
Modern China/E Asia_cat	bieti	*Felis margarita*	87.520902	2.442639	35.83	334647

Table S6. D-statistics test for gene flow between ancient Chinese domestic cats (FS1, FS2, FS12, FS21) and wildcats (F. lybica, F. silvestris, F. bieti, F. ornata) with the analysis set up as D(Outgroup, wildcatsX, Pop2, ancient_China) (Data of Fig. 3D).

Outgroup	Pop1	Pop2	Pop3	D	Z	SNPs
Felis margarita	Levantine Felis lybica	Dhzankent	FS1	0.003013	0.734	3796
Felis margarita	Levantine*Felis lybica*	Ancient_Europe/Anatolia_catus	FS1	0.003676	1.734	14083
Felis margarita	Levantine*Felis lybica*	Modern_China_catus	FS1	0.002478	3.119	91803
Felis margarita	Levantine*Felis lybica*	Modern_Europe_catus	FS1	0.012225	11.399	91803
Felis margarita	Levantine*Felis lybica*	Dhzankent	FS2	0.009122	2.288	3967
Felis margarita	Levantine*Felis lybica*	Ancient_Europe/Anatolia_catus	FS2	0.004266	2.039	14776
Felis margarita	Levantine*Felis lybica*	Modern_China_catus	FS2	0.002518	3.35	95851
Felis margarita	Levantine*Felis lybica*	Modern_Europe_catus	FS2	0.01215	12.056	95851
Felis margarita	Levantine*Felis lybica*	Dhzankent	FS12	0.003034	0.851	4367
Felis margarita	Levantine*Felis lybica*	Ancient_Europe/Anatolia_catus	FS12	0.002854	1.436	16257
Felis margarita	Levantine*Felis lybica*	Modern_China_catus	FS12	0.000346	0.424	103613
Felis margarita	Levantine*Felis lybica*	Modern_Europe_catus	FS12	0.009908	8.888	103613
Felis margarita	Levantine*Felis lybica*	Dhzankent	FS21	0.005496	1.441	3730
Felis margarita	Levantine*Felis lybica*	Ancient_Europe/Anatolia_catus	FS21	0.004433	1.971	13978
Felis margarita	Levantine*Felis lybica*	Modern_China_catus	FS21	0.001583	1.998	91356
Felis margarita	Levantine*Felis lybica*	Modern_Europe_catus	FS21	0.01114	10.838	91356
Felis margarita	*Felis silvestries*	Dhzankent	FS1	-0.00152	-0.389	3796
Felis margarita	*Felis silvestries*	Ancient_Europe/Anatolia_catus	FS1	-0.0191	-9.084	14083
Felis margarita	*Felis silvestries*	Modern_China_catus	FS1	-0.00212	-2.925	91803
Felis margarita	*Felis silvestries*	Modern_Europe_catus	FS1	-0.02942	-26.87	91803
Felis margarita	*Felis silvestries*	Levantine*Felis lybica*	FS1	-0.01017	-11.27	91803
Felis margarita	*Felis silvestries*	Dhzankent	FS2	0.006861	1.816	3967
Felis margarita	*Felis silvestries*	Ancient_Europe/Anatolia_catus	FS2	-0.01812	-8.02	14776
Felis margarita	*Felis silvestries*	Modern_China_catus	FS2	-0.003	-4.514	95851
Felis margarita	*Felis silvestries*	Modern_Europe_catus	FS2	-0.03066	-27.56	95851
Felis margarita	*Felis silvestries*	Levantine*Felis lybica*	FS2	-0.01134	-13.37	95851
Felis margarita	*Felis silvestries*	Dhzankent	FS12	-0.00028	-0.079	4367
Felis margarita	*Felis silvestries*	Ancient_Europe/Anatolia_catus	FS12	-0.01843	-8.896	16257
Felis margarita	*Felis silvestries*	Modern_China_catus	FS12	-0.00502	-7.21	103613
Felis margarita	*Felis silvestries*	Modern_Europe_catus	FS12	-0.03322	-29.27	103613
Felis margarita	*Felis silvestries*	Levantine*Felis lybica*	FS12	-0.01324	-15.27	103613
Felis margarita	*Felis silvestries*	Dhzankent	FS21	0.000822	0.21	3730
Felis margarita	*Felis silvestries*	Ancient_Europe/Anatolia_catus	FS21	-0.01945	-8.598	13978
Felis margarita	*Felis silvestries*	Modern_China_catus	FS21	-0.00251	-3.659	91356
Felis margarita	*Felis silvestries*	Modern_Europe_catus	FS21	-0.02978	-27.23	91356
Felis margarita	*Felis silvestries*	Levantine*Felis lybica*	FS21	-0.01059	-12.4	91356
Felis margarita	*Felis ornata*	Dhzankent	FS1	0.001663	0.417	3796
Felis margarita	*Felis ornata*	Ancient_Europe/Anatolia_catus	FS1	-6.1E-05	-0.029	14083
Felis margarita	*Felis ornata*	Modern_China_catus	FS1	0.001762	2.171	91803
Felis margarita	*Felis ornata*	Modern_Europe_catus	FS1	-0.00324	-2.875	91803
Felis margarita	*Felis ornata*	Levantine*Felis lybica*	FS1	-0.00525	-4.877	91803

Outgroup	Pop1	Pop2	Pop3	D	Z	SNPs
Felis margarita	*Felis ornata*	Dhzankent	FS2	0.006649	1.73	3967
Felis margarita	*Felis ornata*	Ancient_Europe/Anatolia_catus	FS2	-0.00155	-0.743	14776
Felis margarita	*Felis ornata*	Modern_China_catus	FS2	0.000982	1.315	95851
Felis margarita	*Felis ornata*	Modern_Europe_catus	FS2	-0.00433	-4.39	95851
Felis margarita	*Felis ornata*	Levantine*Felis lybica*	FS2	-0.00656	-7.014	95851
Felis margarita	*Felis ornata*	Dhzankent	FS12	0.002548	0.678	4367
Felis margarita	*Felis ornata*	Ancient_Europe/Anatolia_catus	FS12	-0.00215	-1.069	16257
Felis margarita	*Felis ornata*	Modern_China_catus	FS12	0.000507	0.58	103613
Felis margarita	*Felis ornata*	Modern_Europe_catus	FS12	-0.0047	-4.285	103613
Felis margarita	*Felis ornata*	Levantine*Felis lybica*	FS12	-0.00662	-6.313	103613
Felis margarita	*Felis ornata*	Dhzankent	FS21	0.004172	1.036	3730
Felis margarita	*Felis ornata*	Ancient_Europe/Anatolia_catus	FS21	-0.00097	-0.44	13978
Felis margarita	*Felis ornata*	Modern_China_catus	FS21	0.000976	1.348	91356
Felis margarita	*Felis ornata*	Modern_Europe_catus	FS21	-0.00413	-4.075	91356
Felis margarita	*Felis ornata*	Levantine*Felis lybica*	FS21	-0.00629	-6.395	91356
Felis margarita	*Felis bieti*	Dhzankent	FS1	0.002792	0.71	3796
Felis margarita	*Felis bieti*	Ancient_Europe/Anatolia_catus	FS1	-0.00136	-0.643	14083
Felis margarita	*Felis bieti*	Modern_China_catus	FS1	0.001245	1.636	91803
Felis margarita	*Felis bieti*	Modern_Europe_catus	FS1	-0.00561	-5.536	91803
Felis margarita	*Felis bieti*	Levantine*Felis lybica*	FS1	-0.0037	-3.901	91803
Felis margarita	*Felis bieti*	Dhzankent	FS2	0.010978	2.852	3967
Felis margarita	*Felis bieti*	Ancient_Europe/Anatolia_catus	FS2	-0.00239	-1.124	14776
Felis margarita	*Felis bieti*	Modern_China_catus	FS2	0.000737	1.032	95851
Felis margarita	*Felis bieti*	Modern_Europe_catus	FS2	-0.00628	-6.65	95851
Felis margarita	*Felis bieti*	Levantine*Felis lybica*	FS2	-0.00459	-4.967	95851
Felis margarita	*Felis bieti*	Dhzankent	FS12	0.007259	1.925	4367
Felis margarita	*Felis bieti*	Ancient_Europe/Anatolia_catus	FS12	-0.00272	-1.316	16257
Felis margarita	*Felis bieti*	Modern_China_catus	FS12	0.000648	0.737	103613
Felis margarita	*Felis bieti*	Modern_Europe_catus	FS12	-0.00654	-5.991	103613
Felis margarita	*Felis bieti*	Levantine*Felis lybica*	FS12	-0.00417	-4.071	103613
Felis margarita	*Felis bieti*	Dhzankent	FS21	0.005241	1.249	3730
Felis margarita	*Felis bieti*	Ancient_Europe/Anatolia_catus	FS21	-0.00279	-1.263	13978
Felis margarita	*Felis bieti*	Modern_China_catus	FS21	0.000583	0.833	91356
Felis margarita	*Felis bieti*	Modern_Europe_catus	FS21	-0.00674	-7.382	91356
Felis margarita	*Felis bieti*	Levantine*Felis lybica*	FS21	-0.00462	-5.343	91356
Felis margarita	*Felis bieti*	Dhzankent	FS1	0.002792	0.71	3796
Felis margarita	*Felis bieti*	Dhzankent	FS2	0.010978	2.852	3967
Felis margarita	*Felis bieti*	Dhzankent	FS12	0.007259	1.925	4367
Felis margarita	Felis bieti	Dhzankent	FS21	0.005241	1.249	3730

Table S7. (A) Genotypes and inferred phenotypes of FS12 associated with coat colors.

Coat color	Gene	Ref genome	Chr	Position	mutation	If FS12 carries the allele	Reference
Black	*ASIP*	catus_9.0	A3	25086566-25086567	Deletion	No	(Eizirik et al., 2003)
Amber	*MC1R*	catus_9.0	E2	63829934	G>A	No	(Peterschmitt et al., 2009)
Russet	*MC1R*	catus_9.0	E2	63830124-63830126	Deletion	No	(Gustafson et al., 2017)
Copal	*MC1R*	catus_9.0	E2	63830324-63830353	Deletion	No	(Abitbol & Gache, 2019)
Dilution	*MLPH*	catus_9.0	C1	219396820	Deletion	NA	(Ishida et al., 2006)
Siamese coat colour pattern	*TYR*	catus_9.0	D1	45898803	C>T	No	(Lyons, Imes, et al., 2005)
Burmese coat colour pattern	*TYR*	catus_9.0	D1	45907839	C>A	No	(Lyons, Imes, et al., 2005)
Complete albinism	*TYR*	catus_9.0	D1	45898772	Deletion	No	(Imes et al., 2006)
Albinism	*TYR*	catus_9.0	D1	45812806	G>A	No	(Abitbol et al., 2017)
Mocha	*TYR*	catus_9.0	D1	45898609-45898771	Duplication	NA	(Y. Yu et al., 2019)
Cinnamon	*TYRP1*	catus_9.0	D4	40069161	C>T	No	(Lyons, Foe, et al., 2005)
Chocolate	*TYRP1*	catus_9.0	D4	40081229	G>A	No	(Lyons, Foe, et al., 2005)
White spotting	*KIT*	catus_9.0	B1	164038110-164038111	Insertion	Yes	(David et al., 2014)

Table S7. (B) Genotypes and inferred phenotypes of FS12 associated with coat patterns.

Pigmentation pattern	Gene	Ref genome	Chr	Position	mutation	If FS12 carries the allele	Reference
Ticked	*DKK4*	catus_9.0	B1	42620835	C>T	No	(Lyons et al., 2021)
Ticked	*DKK4*	catus_9.0	B1	42621481	G>A	No	(Lyons et al., 2021)
Blotched tabby	*LVRN*	catus_9.0	A1	96753652	C>A	No	(Kaelin et al., 2012)
Blotched tabby	*LVRN*	catus_9.0	A1	96754158	G>A	No	(Kaelin et al., 2012)
Blotched tabby	*LVRN*	catus_9.0	A1	96813484	G>A	No	(Kaelin et al., 2012)

Table S7. (C) Genotypes and inferred phenotypes of FS12 associated hair morphology.

Hair type	Gene	Ref genome	Chr	Position	mutation	If FS12 carries the allele	Reference
Long hair	*FGF5*	catus_9.0	B1	142165952	T>G	No	(Drögemüller et al., 2007)
Long hair	*FGF5*	catus_9.0	B1	142165953	Deletion	No	(Drögemüller et al., 2007)
Long hair	*FGF5*	catus_9.0	B1	142177919	G>A	No	(Kehler et al., 2007)
Long hair	*FGF5*	catus_9.0	B1	142185646-142185647	Insertion A	No	(Kehler et al., 2007)
Long hair	*FGF5*	catus_9.0	B1	142165850	C>T	No	(Shaffer et al., 2021)
Lykoi	*HR*	catus_9.0	B1	36040784-36040785	dup	NA	(Buckley, Gandolfi, et al., 2020)
Lykoi	*HR*	catus_9.0	B1	36040933	Indel CAG	No	(Buckley, Gandolfi, et al., 2020)
Lykoi	*HR*	catus_9.0	B1	36045776	G>A	No	(Buckley, Gandolfi, et al., 2020)
Lykoi	*HR*	catus_9.0	B1	36047047	C>T	No	(Buckley, Gandolfi, et al., 2020)
Lykoi	*HR*	catus_9.0	B1	36047518	C>T	No	(Buckley, Gandolfi, et al., 2020)
Lykoi	*HR*	catus_9.0	B1	36051555-36051556	Insertion GACA	NA	(Buckley, Gandolfi, et al., 2020)
Sphynx hairless	*KRT71*	catus_9.0	B4	81048680	C>T	No	(Gandolfi et al., 2010)
Curly	*KRT71*	catus_9.0	B4	81046358-81046359	Insertion A	No	(Gandolfi et al., 2010)
Curly	*LPAR6*	catus_9.0	A1	22919307_22919310	Deletion	No	(Gandolfi, Alhaddad, Affolter, et al., 2013)
Curly	*LIPH*	catus_9.0	C2	84136341_84136347	Indel	No	(Manakhov et al., 2020)
Curly	*KRT71*	catus_9.0	B4	81050264	C>G	No	(Gandolfi, Alhaddad, Joslin, et al., 2013)

Table S7. (D) Genotypes and inferred phenotypes of FS12 associated with tail length and morphology.

Tail length	Gene	Ref genome	Chr	Position	mutation	If FS12 carries the allele	Reference
Short tail	*HES7*	catus_9.0	E1	2918735	A>G	No	(Xu et al., 2016)
Short tail	*T*	catus_9.0	B2	152019395	Deletion	No	(Buckingham et al., 2013)
Short tail	*T*	catus_9.0	B2	152019424	Deletion	No	(Buckingham et al., 2013)
Short tail	*T*	catus_9.0	B2	152021360-152021362	Deletion	No	(Buckingham et al., 2013)
Short tail	*T*	catus_9.0	B2	152021363-152021379	Duplication	N/A	(Buckingham et al., 2013)

Table S7. (E) Genotypes and inferred phenotypes of FS12 associated with genetic diseases.

Disease	Gene	Chr	Ref genome	Position	Mutation	If FS12 carries the genotype	Reference
Factor XII Deficiency (Variant 1)	*F12*	A1	catus_9.0	175381113-175381114	Deletion	No	(Bender et al., 2015)
Factor XII Deficiency (Variant 2)	*F12*	A1	catus_9.0	175382065	Deletion	No	(Maruyama et al., 2017)
Hypertrophic Cardiomyopathy	*MYBPC*	D1	catus_9.0	101329646	C>T	No	(Meurs et al., 2007)
Hypertrophic Cardiomyopathy	*MYBPC*	D1	catus_9.0	1340772	C>G	No	(Meurs et al., 2005)
Polycystic Kidney Disease (PKD)	*PKD1*	E3	catus_9.0	42858112	C>A	No	(Lyons et al., 2004)
Polycystic Kidney Disease (PKD)	*PKD1*	E3	catus_9.0	42848725	Deletion	No	(Shitamori et al., 2023)
Polycystic Kidney Disease (PKD)	*PKD1*	E3	catus_9.0	42850283	C>T	No	(Shitamori et al., 2023)
Mucopolysaccharidosis Type VI Modifier	*ARSB*	A1	catus_9.0	145138738	G>A	No	(Crawley et al., 1998)
Mucopolysaccharidosis Type VI Modifier	*ARSB*	A1	catus_9.0	145138869	A>G	No	(Yogalingam et al., 1996)
Acute Intermittent Porphyria (Variant 1)	*HMBS*	D1	catus_9.0	16540928-16540931	Deletion	No	(Clavero et al., 2013)
Acute Intermittent Porphyria (Variant 2)	*HMBS*	D1	catus_9.0	16544575	G>A	No	(Clavero et al., 2013)
Acute Intermittent Porphyria (Variant 3)	*HMBS*	D1	catus_9.0	16541469	Insertion	No	(Clavero et al., 2013)
Acute Intermittent Porphyria (Variant 4)	*HMBS*	D1	catus_9.0	16544592-16544594	Deletion	No	(Clavero et al., 2013)
Acute Intermittent Porphyria (Variant 5)	*HMBS*	D1	catus_9.0	16541613	G>A	No	(Clavero et al., 2013)
Autoimmune Lymphoproliferative Syndrome	*FASL*	F1	catus_9.0	16871911	Insertion	No	(Aberdein et al., 2017)
Burmese Head Defect	*ALX1*	B4	catus_9.0	110088245-110088254	Deletion	No	(Lyons, Erdman, et al., 2016)
Chediak-Higashi Syndrome	*LYST*	D2	catus_9.0	13289499-13308862	Insertion	N/A	(Buckley, Grahn, et al., 2020)
Congenital Adrenal Hyperplasia	*CYP11B1*	F2	catus_9.0	84247412	G>A	No	(Owens et al., 2012)
Congenital Erythropoietic Porphyria	*UROS*	D2	catus_9.0	83467845	C>T	No	(Clavero et al., 2010)
Congenital Myasthenic Syndrome	*COLQ*	C2	catus_9.0	135068287	G>A	No	(Abitbol, Hitte, et al., 2015)
Cystinuria Type 1A	*SCL3A1*	A3	catus_9.0	66539609	C>T	No	(Mizukami et al., 2015)
Cystinuria Type B (Variant 1)	*SCL7A9*	E2	catus_9.0	20228722	C>T	No	(Mizukami et al., 2016)
Cystinuria Type B (Variant 2)	*SCL7A9*	E2	catus_9.0	20218196	G>A	No	(Mizukami et al., 2016)
Cystinuria Type B (Variant 3)	*SCL7A9*	E2	catus_9.0	20219555	T>A	No	(Mizukami et al., 2016)
Dihydropyrimidinase Deficiency	*DPYS*	F2	catus_9.0	52064442	G>A	No	(Chang et al., 2012)
Earfold and Osteochondrodysplasia	*TRPV4*	D3	catus_9.0	18884250	G>T	No	(Gandolfi et al., 2016)
Familial Episodic Hypokalemic Polymyopathy	*WNK4*	E1	catus_9.0	43304422	C>T	No	(Gandolfi et al., 2012)
Glutaric Aciduria Type II	*ETFDH*	B1	catus_9.0	71374289	T>G	No	(Wakitani et al., 2014)
Glycogen Storage Disease	*GBE1*	C2	catus_9.0	34744477-34781895	Insertion	N/A	(Fyfe et al., 2007)
GM1 Gangliosidosis	*GLB1*	C2	catus_9.0	158932167	C>G	No	(D. R. Martin et al., 2008)
GM2 Gangliosidosis	*GM2A*	A1	catus_9.0	198114664-198114667	Deletion	No	(D. R. Martin et al., 2005)
GM2 Gangliosidosis Type II	*HEXB*	A1	catus_9.0	141571788-141571812	Inversion	N/A	(D. R. Martin et al., 2004)
GM2 Gangliosidosis Type II	*HEXB*	A1	catus_9.0	141565348	C>T	No	(Kanae et al., 2007)
Hemophilia B (Variant 1)	*F9*	X	catus_9.0	117111577	C>T	No	(Goree et al., 2005)
Hemophilia B (Variant 2)	*F9*	X	catus_9.0	117091961	G>A	No	(Goree et al., 2005)
Hypertrophic Cardiomyopathy	*MYBPC*	D1	catus_9.0	101340772	G>C	No	(Meurs et al., 2005)
Hypertrophic Cardiomyopathy	*MYBPC*	D1	catus_9.0	101329646	G>A	No	(Meurs et al., 2007)
Hypotrichosis	*FONXN1*	E1	catus_9.0	18255880-18255883	Deletion	No	(Abitbol, Bossé, et al., 2015)
Lipoprotein Lipase Deficiency	*LPL*	B1	catus_9.0	38078551	G>A	No	(Ginzinger et al., 1996)
MDR1 Medication Sensitivity	*ABCB1*	A2	catus_9.0	93144356-93144357	Deletion	No	(Mealey & Burke, 2015)
Mucopolysaccharidosis Type I	*IDUA*	B1	catus_9.0	207800585- 207800587	Deletion	No	(X. He et al., 1999)
Mucopolysaccharidosis Type VI	*ARSB*	A1	catus_9.0	145138869	A>G	No	(Yogalingam et al., 1996)
Mucopolysaccharidosis Type VI	*ARSB*	A1	catus_9.0	145138738	C>T	N/A	(Crawley et al., 1998)
Mucopolysaccharidosis Type VII (Variant 1)	*GUSB*	E3	catus_9.0	16120173	G>A	No	(Fyfe et al., 1999)
Mucopolysaccharidosis Type VII (Variant 2)	*GUSB*	E3	catus_9.0	16123229/16123232	T>G/C>T	No	(Wang et al., 2015)
Myotonia Congenita	*CLCN1*	A2	catus_9.0	158986498	G>T	No	(Gandolfi et al., 2014)
Progressive Retinal Atrophy	*CEP290*	B4	catus_9.0	112522818	A>C	No	(Menotti-Raymond et al., 2007)
Progressive Retinal Atrophy	*KIF3B*	A3	catus_9.0	26784019	G>A	No	(Cogné et al., 2020)
Progressive Retinal Atrophy	*AIPL1*	E1	catus_9.0	940445	C>T	No	(Lyons, Creighton, et al., 2016)
Pyruvate Kinase Deficiency	*PKLR*	F1	catus_9.0	70310110	G>A	No	(Grahn, Grahn, et al., 2012)
Sphingomyelinosis (Variant 1)	*NPC1*	D3	catus_9.0	48234217	C>G	No	(Somers et al., 2003)
Sphingomyelinosis (Variant 1)	*NPC1*	D3	catus_9.0	48250290	T>G	N/A	(Mauler et al., 2017)
Sphingomyelinosis (Variant 2)	*NPC2*	B3	catus_9.0	121872988	C>T	No	(Zampieri et al., 2014)
Spinal Muscular Atrophy	*LIX1*	A1	catus_9.0	161036890-161176706	Deletion	No	(Fyfe et al., 2006)
Vitamin D-Dependent Rickets	*CYP27B1*	B4	catus_9.0	86180281	Deletion	N/A	(Geisen et al., 2009)
Vitamin D-Dependent Rickets	*CYP27B1*	B4	catus_9.0	86180375	C>A	No	(Grahn, Ellis, et al., 2012)
Polydactyly	*LMBR1*	A2	catus_9.0	169532842	T>A	No	(Lettice et al., 2008)
Polydactyly	*LMBR1*	A2	catus_9.0	169532844	T>C	No	(Lettice et al., 2008)
Polydactyly	*SHH*	A2	catus_9.0	169533066	C>G	No	(Lettice et al., 2008)

Table S8. Information of ancient artwork related to cats in China between 827 CE and 1930 CE within the time frame of this research.

Theme	Date	Period	Type	Black	White	Unclear	Number of individuals	Collector/Source
M126 of the Tombs of the Tang and Song Dynasties at Liujiazhuang Locus North in Anyang City, Henan	827 CE	Tang	Tomb mural	1	1	2	3	The excavation report f the Tombs of the Tang and Song Dynasties at Liujiazhuang Locus North in Anyang City, Henan
Tang Dynasty Mural Tomb at Beiguan, Anyang City, Henan	835-907 CE	Tang	Tomb mural	1	1	0	1	Preliminary Report on the Excavation of Tang Dynasty Mural Tombs at Beiguan, Anyang City, Henan
Anyang Xiaonanhai Mural	960-1,127 CE	Song	Tomb mural	1	0	0	1	Zhaoling's Painted Brick Chamber from the Tang Dynasty
Dengfeng Heishangou Song Tomb	11th -12th centuries CE	Song	Tomb mural	1	1	0	1	Research on Images from Song Dynasty Tomb in Dengfeng's Heishan Gou by Yi Qing
Xu Congbin's Tomb	982 CE	Song	Tomb mural	1	1	0	1	Newly Added Fort's Liao Dynasty Tomb of Xu Congyuan
Chen Shu's Cat and butterfly Painting	17th -18th centuries CE	Qing	Legacy painting	1	2	0	2	The Palace Museum in Beijing
Cheng Zhang's Two Cats Peering at Fish	1930 CE	modern times	Legacy painting	2	2	0	2	The Palace Museum in Beijing
Qiu Ying's Portrait of a Lady	16th century CE	Ming	Legacy painting	2	3	0	3	The Palace Museum in Beijing
Li Di's Winter Play with Infant	10th - 11th centuries CE	Song	Legacy painting	1	1	0	1	National Palace Museum in Taipei
Wealthy FloralCat Painting	12th -13th centuries CE	Song	Legacy painting	1	1	0	1	National Palace Museum in Taipei
Siblings in Unity Painting	13th - 14th centuries CE	Yuan	Legacy painting	1	1	0	1	National Palace Museum in Taipei
Yi Yuanji's Cat and Monkey	11th century CE	Song	Legacy painting	2	2	0	2	National Palace Museum in Taipei
Wealth in the Pot Painting	15th century CE	Ming	Legacy painting	1	1	0	1	National Palace Museum in Taipei
Cat Under the Banana Shade	14th-17th centuries CE	Min	Legacy painting	4	4	0	4	The Metropolitan Museum of Art
Xuanzong's Scroll of FiveCats	15th century CE	Min	Legacy painting	4	5	0	5	The Metropolitan Museum of Art
Tao Cheng'sCat in Fragrant Grass	15th century CE	Min	Legacy painting	6	5	0	14	National Palace Museum in Taipei
Li Di'sCat and Dragonfly	10th - 11th centuries CE	Song	Legacy painting	1	1	0	1	Collection of Osaka City Museum of Fine Arts, Japan
Cat Painting	10th - 11th centuries CE	Song	Legacy painting	1	1	0	1	National Palace Museum in Taipei
LittleCat Shadow	10th - 11th centuries CE	Song	Legacy painting	0	1	0	1	National Palace Museum in Taipei
Cat and Infant Play Painting	10th - 13th centuries CE	Song	Legacy painting	2	2	0	2	Museum of Fine Arts, Boston
Song Huizong's Cat and butterfly Painting (Signature)	12th centuries CE	Song	Legacy painting	1	1	0	1	National Palace Museum in Taipei
Li Di's Okra Mountain and Rock	13th century CE	Southern Song	Legacy painting	1	1	0	1	National Palace Museum in Taipei
Shen Zhenlin's Cat and butterfly in Spring Album, WisteriaCat	19th century CE	Qing	Legacy painting	10	15	0	15	National Palace Museum in Taipei
Shang Xi's Playful Cat Scroll	15th century CE	Ming	Legacy painting	1	2	0	2	National Palace Museum in Taipei
Five Cats Painting	12th -13th centuries CE	Song	Legacy painting	4	4	0	5	Private Collection
Shen Zhenlin's Cat and Bamboo	19th century CE	Qing	Legacy painting	1	3	0	3	National Palace Museum in Taipei
Zhou Wenju's Portrait of a Lady	10th century CE	Five Dynasties	Legacy painting	1	1	0	1	National Palace Museum in Taipei
Liangkai's Scroll of Leisurely Delights of the cats	12th century CE	Song	Legacy painting	2	5	0	5	Nara Yamato Bunkakan in Japan
Luo Zonggui's Hibiscus Cat Play Fan Painting	10th - 13th centuries CE	Song	Legacy painting	1	2	0	2	N/A
Mao Yi's Sichuan Hibiscus and Wandering Cat	13th century CE	Southern Song	Legacy painting	3	3	0	4	Nara Yamato Bunkakan in Japan
Jin Qing's Twin Cats	10th - 13th centuries CE	Song	Legacy painting	1	2	0	2	N/A
Wang Weilie's Cat and Rock	17th century CE	Qing	Legacy painting	1	1	0	1	National Art Museum of China
Wang Guxiang's Cat and butterfly Painting	16th century CE	Ming	Legacy painting	1	1	0	1	N/A
				62	77	2	91	
				68%	85%			

Notes: In a painting where an individual has both black and white fur, the color statistics would be recorded once under both the black ("Black" in table title) and white ("White" in table title) categories. The final proportion of colors is calculated as the count of records for black or white divided by the total number of observed individuals ("Number of individuals" in table title).